Annual Report of Naka Fusion Research Establishment
from April 1, 1998 to March 31, 1999

Naka Fusion Research Establishment

Japan Atomic Energy Research Institute
Naka-machi, Naka-gun, Ibaraki-ken

(Received August 18, 1999)

This report provides an overview of research and development activities at the Naka Fusion Research Establishment, JAERI, during the period from April 1, 1998 to March 31, 1999. The activities in the Naka Fusion Research Establishment are highlighted by high temperature plasma research in JT-60 and JFT-2M as well as DIII-D (US-Japan collaboration), and progress in ITER EDA, including ITER technology R&D.

The objectives of the JT-60 project are to contribute to the ITER physics R&D and to establish the physics basis for a steady state tokamak fusion reactor like SSTR.

The W-shaped divertor was modified to open the outside divertor slot and improve the divertor pumping in the high-triangularity (δ) configuration from November through December 1998 when JT-60 operation was halted. After the integrated tests of a 110 GHz ECH/ECCD system newly introduced in January 1999, the Electron Cyclotron (EC) waves were firstly launched into JT-60 in February 1999.

Highlights of the plasma performance in JT-60 are as follows: (1) the production of a high performance reversed shear plasma with the equivalent fusion amplification factor Q_{DT}^{eq} of 1.25 in a deuterium discharge and (2) the sustainment of reversed shear plasma with internal transport barriers in a steady-state for 6 s by the current profile control with lower hybrid waves. High β_p H-mode in a high triangularity configuration was sustained for about 4.5 s at Q_{DT}^{eq} of ~0.16 with a large non-inductive current drive fraction of 60-70 % of the plasma current. It should be emphasized that a high normalized beta β_N ~ 2.6-2.7 was sustained in a quasi-steady state in a low-q (q_{95} ~ 3) regime comparable with ITER due to improved edge stability by high triangularity. The power threshold for L-H transition was reduced by approximately 30 % in the W-shaped divertor compared with the open divertor. Ar gas puffing into an ELMy H-mode

---

Editors: Nagashima, T., Kurita, G., Masaki, K., Nemoto, S., Shoji, T., Shu, W.

plasma increased H-factor up to 1.5 at $n_e/n^{Gr} = 0.7$. L-H transition with 350 keV negative ion-based NBI (N-NBI) was first observed in JT-60. With N-NBI, a relatively large driven current of 0.6 MA was demonstrated at the current drive efficiency of 0.6×10^{19} A/W/m^2.

JFT-2M carries out advanced and basic researches for the development of high-performance plasmas for nuclear fusion and contribution to the physics R&D for ITER, taking full advantage of flexibility of a medium-size device.

A fast change of the electric potential distribution at the L-H transition was measured directly for the first time with a Heavy Ion Beam Probe in collaboration with National Institute for Fusion Science (NIFS). EC current drive was confirmed and it appeared that no difference in the suppression of the tearing mode between the co-direction and the counter direction current drive. The closed divertor maintained low temperature and high density divertor plasma, and high confinement performance. Fuelling by the compact toroid (CT) injection to a central part of the high power NBI-heated plasma (H-mode) was demonstrated for the first time in collaboration with the Himeji Institute of Technology. Optimized design for the ripple reduction by the ferritic board installation outside the vacuum vessel was established.

The primary objective of theoretical and analytical studies is to improve the physical understanding of the magnetically confined tokamak plasma. Remarkable progress was made on physical understanding of transport phenomena such as the internal barrier in JT-60 in connection with radial electric field. Progress was also made on the study of stability such as the neoclassical tearing mode and the double tearing. As for divertor plasma, the importance of thermoelectric instability was shown by using the five point model for the scrape-off layer and divertor plasmas.

The main focus of the NEXT (Numerical EXperiment of Tokamak) project is to research complex physical processes in core plasmas and divertor plasma by using recently advanced computer resources. The role of shear rotation and weak/reversed magnetic shear on these semi-global toroidal modes was studied by employing our toroidal simulation code together with a non-local theory.

R&D of fusion reactor technology has focused on the ITER EDA-related areas. Major highlights in FY1998 are as follows:

(1) The high precision assembly and electric joint connection of eight layers of solenoid coils to produce the Outer Module of the CS Model Coil have been successfully completed. Successful heat treatment of the CS Insert Coil for activation of Nb_3Sn was completed in collaboration with U.S.A.

(2) Fabrication of the full-scale vacuum vessel sector was completed as well as the arrival of the port structure from Russia and remote assembly test plan was in progress. As for seismic isolation development the sub-scaled rubber bearings with diameters from 0.2 m to 0.7 m were tested and basic performance test was completed. Regarding the development of ITER divertor,

full-scale mock-ups were fabricated. 5 MW/m^2 steady state and 20 MW/m^2 transient heat load tests were also conducted successfully with the 1-m long ion source at JAERI. The divertor mock-ups were shown to withstand the lifetime worthy of 3 years. Full-scale mock-up test for blanket remote replacement based on the rail-mounted vehicle type manipulator system was operated at an automatic control mode. The mock-up weighing 4 tons was fixed in position within accuracy of ±2 mm. A small-scale (300 mm^w x 200 mm^d) first wall/blanket model made of a reduced activation ferritic steel F82H for DEMO breeding blanket was successfully fabricated by Hot Isostatic Pressing (HIP).

(3) Negative H-ions with high current density of 15 mA/cm^2 were extracted from 9 apertures of the ITER concept source, called KAMABOKO source, and converged to produce 200 mA negative ion-beam at 700 keV for 1 s. Development of a gyrotron has progressed to deliver maximum energy of 450 kW for 8 s (3.6 MJ) at 170 GHz with a diamond disk window. Tritium gas behavior in the caisson (called CATS) of 12 m^3 was tested under various conditions to develop the codes.

In the fusion reactor design, the conceptual study of the commercial DREAM reactor with very high aspect ratio configuration and SiC/SiC composite material has been continued relating specially to the safety aspect. In the area of safety research, In-vessel Loss Of Coolant Accident (LOCA) has been evaluated as a representative accident scenario.

The ITER Council formally accepted in June 1998 the Final Design Report (FDR). In November 1998 the Fusion Council of Japan confirmed: Japan should continue to promote actively the ITER project because of its most importance in the fusion research and development in Japan by national endeavor and it is possible to continue and complete the EDA by three Parties (EU, RF, and JA) except US for another three years. In December the Japan Atomic Energy Commission endorsed this report by the Fusion Council. Joint Central Team (JCT) and three Home Teams have been jointly working on the design of Reduced Technical Objective and Reduced Cost ITER following the guidelines (performance and testing requirements and design requirements) reported by Special Working Group (SWG). A JCT/Home Team Task Force was endorsed to pursue convergence of views as required by the Parties, with the objective of making an Outline Design Report available to the Parties by the end of 1999.

Keywords: Fusion Research, JAERI, JT-60, JFT-2M, DIII-D, Plasma Physics, Fusion Reactor Engineering, ITER, EDA, Fusion Reactor Design, Annual Report

Contents

I. JT-60 PROGRAM

Objectives of the JT-60 project are to contribute the design of International Thermonuclear Experimental Reactor (ITER) and to establish the physics basis for a steady state tokamak fusion reactor like SSTR. In the fiscal year 1998, JT-60 experiments were devoted to high performance reversed shear, long sustainment of high β_p H-mode, divertor physics, heating and current drive with a negative ion-based neutral beam injection (N-NBI), energetic particle physics and disruption study.

Highlights in plasma performance are the production of a high performance reversed shear plasma with the equivalent fusion amplification factor Q_{DT}^{eq} of 1.25 in a deuterium discharge, and the sustainment of reversed shear with internal transport barriers in a steady-state (6 s) by the current profile control with lower hybrid waves. High β_p H-mode in a high triangularity (δ) configuration was sustained for about 4.5 s at Q_{DT}^{eq} of ~0.16 with a large non-inductive current drive fraction of 60-70 % of the plasma current. It should be emphasized that a high normalized beta β_N ~ 2.6-2.7 was sustained in a quasi-steady state in a low-q (q_{95} ~ 3) regime comparable with ITER due to improved edge stability by high triangularity. Divertor experiments with the W-shaped pumped divertor demonstrated an impurity reduction by gas puff and pump technique, a suppression of chemical sputtering and a reduction of neutral back-flow. The power threshold for L-H transition was reduced by approximately 30 % in the W-shaped divertor, compared with the open divertor. Ar gas puffing into an ELMy H-mode plasma increased H-factor up to 1.5 at n_e/n^{Gr} = 0.7. L-H transition with 350-keV negative ion-based NBI (N-NBI) was first observed in JT-60. In the ELMy H-mode phase, H factor of 1.64 and $T_e(0)$ = 1.4 $T_i(0)$ were obtained in the electron heating with N-NBI. With N-NBI, a relatively large driven current of 0.6 MA was demonstrated at the current drive efficiency of 0.6×10^{19} A/W/m^2. Furthermore, understandings on energetic particle behavior and disruption have been steadily progressed especially on Alfvén eigenmodes, runaway electrons and halo current.

The W-shaped divertor was modified to open the outside divertor slot and improve the divertor pumping in high-δ configuration in November through December 1998 when JT-60 operation was halted. After the integrated tests of a 110 GHz ECH/ECCD system newly introduced in January 1999, the EC waves were first launched into JT-60 in February 1999. The central ECH at 0.6 MW for 0.3 s led to a distinctive electron temperature rise of 2 keV. The system is expected to use to suppress neoclassical tearing modes and to reach higher β_N in steady state in coming years.

1. Operation and Machine Improvements

1.1 Tokamak Machine

Operation and maintenance of the toroidal magnetic field coil of JT-60 has been carefully executed since cooling water leak due to birth of cracks on the cooling pipes was found in 1992. In every annual maintenance period from November to December, the status of the cooling pipes with cracks are inspected with a fiberscope with CCD camera and airtightness of the other healthy cooling pipes are checked with highly pressurized air. The total discharge number after the previous inspection was 2383, where the number of high toroidal magnetic field discharges of 3.5 – 4 T was 506 and the number of disruptions was 326. For these operations, it was confirmed in this inspection that no extension of the existing cracks was recognized and no new air leak was found for eight coils sampled as representatives for this test.

Modification of the vacuum pumping system for JT-60 to oil-free vacuum pumping one, which started in 1994, was completed in December 1998. Twelve turbo molecular pumps with oil bearing and four oil sealed rotary vacuum pumps had been replaced to magnetic suspended turbo molecular pumps and dry vacuum pumps step by step since 1994. This modification aimed not only to renew the vacuum pumping system that had been operated for 15 years, but also to reduce the maintenance works. Owing to this modification, the amount of radioactive waste vacuum oil contaminated by tritium, which was exchanged in the maintenance work, was reduced to about 1/5. Also, the consumption of liquid nitrogen was reduced to about 1/3.

A new piezoelectric valve (PEV) for supplying working gas has been developed to renew the present PEV that has been deteriorated by 15 years use. The present PEV uses a bimorph type piezoelectric element that acts as a sheet valve. This valve sometimes causes sheet leak due to deterioration of the piezoelectric element. The new PEV has been developed using a combination of a metal sheet valve and a stack type piezoelectric element filled in the metal case as an actuator. In the new PEV, pushing force of the piezoelectric element to the metal sheet valve is adjustable to suppress sheet leak. This work can be done without opening the PEV. Therefore, sheet leak can be easily repaired even if it occurs. Gas flow range of the new PEV is < 5 Pam^3/s for L-type PEV and <50 Pam^3/s for H-type PEV. The new PEV's are to be installed in the maintenance period of next year.

In December 1998, the pumping scheme of the W-shaped divertor was modified from inner pumping only to both sides pumping to study pumping location effects. Fig.I.1.1-1 shows the structure of the W-shaped divertor with both sides-pumping slots between dome and inner/outer divertor tiles. The outer-pumping slot was added only by removing gas seals between dome and outer divertor and by replacing dome tiles to smaller ones. To carry out this modification work easily, the above structures were taken into the design of the W-shaped divertor at the beginning.

Compared with the previous inner pumping only, which relies on strong in-out asymmetry of divertor neutral pressure [1.1-1], the both sides pumping is expected to have good pumping performance in detached divertor states and highly triangular-shaped configurations in the following reasons. In detached divertor states, neutral pressure in the divertor is almost in-out symmetric or rather strong at the outer region. In highly triangular-shaped configurations of JT-60, the inner strike point is kept away from the entrance of the inner-pumping slot as shown in Fig.I.1.1-1, resulting in inefficient pumping. Consequently the outer pumping slot is necessary. According to the initial experiment with an optimized configuration for the both sides pumping, the pumping speed of $16 m^3/s$ was found, which was improved by 30% compared with the inner pumping only.

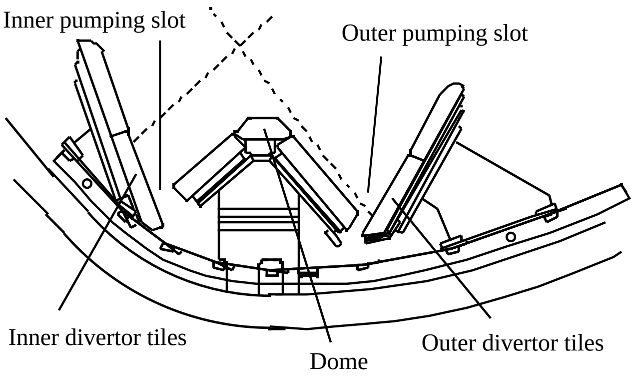

Fig. I.1.1-1 W-shaped divertor with both sides pumping slots. Separatrii of a highly triangular-shaped configuration are shown by dashed lines.

Inner and outer dome tiles, where relatively low heat flux was expected, were isotropic graphite tiles. To allow a variety of plasma configurations, the outer dome tiles were replaced with CFC tiles, since high heat flux up to 10 MW/m^2 is expected on the outer dome tiles, for example, in highly triangular-shaped configurations.

References

[1.1-1] Hosogane N., "Operational performance of JT-60U W-shaped divertor", Proc. of 13 th Int. Conf. on Plasma Surface Interactions (PSI) in Contr. Devices. p.296, San Diego, USA, May 18-22, 1998.

1.2 Control System

The control system works in the JT-60 experiments according to the required schedule. The following developments were newly performed in this fiscal year to improve plasma control performances and operational efficiency.

(a) New precise long-time digital integrator

The newly developed integrators (also applicable to the 2000-s pulse discharge in ITER) has started in operation for JT-60 magnetic measurements (75 channels).

(b) New advanced real-time plasma control system for particle supply and heating

This new system has been installed in JT-60. The computational time was greatly reduced to a hundredth of that for the former system. The reflective memory network has been employed for newly developed real-time communication. (Refer to 1.2.1)

(c) New shape real-time reproduction method based on the Cauchy-condition surface

Plasma shape reproduction methods having been applied to JT-60 are the following problems: (i) The FBI (fast plasma boundary identification) method stands on the weak theoretical basis. (ii) Hence, the FBI produces essentially inaccurate shape independently of the increase in number of sensors. (iii) The entire execution time of full equilibrium analysis is too long to be applied to real-time calculation. It has been clarified that a newly developed method based on the Cauchy-condition surface can solve those problems, and reproduce the shape precisely. (Refer to 1.2.2)

(d) Development of a new discharge control system

Since it has been becoming difficult to satisfy increasing requirements in recent years, remodeling of the overall discharge control system is necessary to improve operational efficiency. Hence, the old system is superseded by a combined system composed of UNIX workstations, VME-bus, and Ethernet network. In this fiscal year, a prototype of the system has been completed. (Refer to 1.2.3)

(e) New plasma real-time feedback (FB) control algorithms

The following control algorithms are newly developed for improvement of plasma performance: (i) Poloidal beta value FB control by NBI. (ii) Electron temperature (at the center of a plasma) FB control by NBI. (iii) Electron temperature gradient FB control by NBI. (iv) Plasma-launcher distance FB control by the poloidal field coil. (v) ECH (electron cyclotron heating) On/Off control.

(f) Development of plasma picture database with "sound" of the magnetic fluctuation

A plasma picture has been considered one of the most important results in the plasma experiment, because it is very efficient to know the overall performance of a plasma. Hence, two pictures of real-time visualized plasma shape movie and plasma visible camera picture are combined by the video multi-viewer. The stereo sound channels input the amplified magnetic pick-up coil signals, that measure poloidal magnetic field fluctuation (Mirnov oscillation). As the cut-off frequency of the pick-up coil is approximately up to 20 kHz, we can hear the change of plasma bunch toroidal/poloidal rotation. After the combined movie is compressed into a tenth of the original volume through the MJPEG (Motion JPEG) reduction procedure, the plasma picture data (30-40 Mbyte/shot) is stored in the network server, and can be download to all personal computers on site.

For the maintenance of the control system, annual inspections were made for the computer system, control boards, and the signal processing system for plasma control in the shut-down period of November and December.

1.2.1 New Advanced Real-time Plasma Control System for Particle Supply and Heating [1.2-1]

Since requirements of modification for advanced plasma control and efficient discharge control has been increasing, a new control system was started to be developed. Concerning this new system, we chose an Alpha-288 VME board (made by DEC. Ltd.) for main processors, and built a VME-bus system together with the I/O boards and a reflective memory module as shown in Fig.I.1.2-1. As a result from its performance test, this system can execute the real-time program within 0.1 ms. This period is approximately 100 times faster than that for the old mini-computer (10 ms). However, slow communication (1.4 ms) with the existing old subsystems through CAMAC highway is an obstacle for minimization of the total execution time.

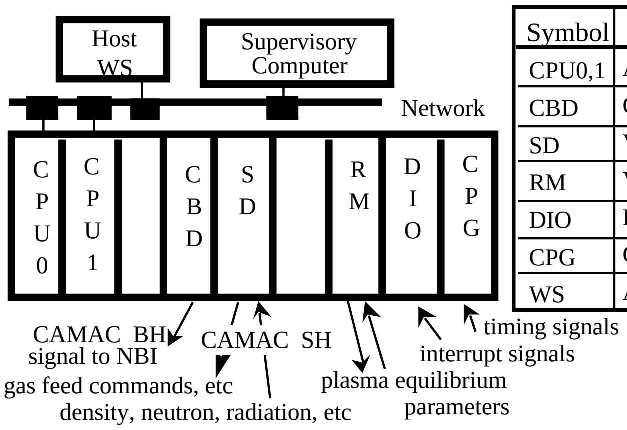

Symbol	Type	Function /Manufacturer
CPU0,1	AXPvme280	DEC 21066A, 288MHz, 64MB/ DEC
CBD	CBD8210	CAMAC Branch Driver / CES
SD	VSHD2992	CAMAC Serial Driver / HYTEC
RM	VMIVME5576	Reflective Memory (256kB) / VMIC
DIO	DSP8230	Digital Input (32 ch) / MTT
CPG	CPG241	Clock Pulse Generator / MTT
WS	Alpha WS 255	UNIX-WS alpha 255MHz / DEC

BH: Branch Highway SH: Serial Highway

Fig. I.1.2-1 Configuration of the plasma real-time control system for particle supply and heating.

This system has started in JT-60 operation since May 1998, after several integration tests with the other subsystems. At the same time of the installation, "reflective memory" network is employed for real-time communications in which the VME module "VMIVME 5576 (VMIC Co.)" is plugged in all the VME-bus systems in Fig.I.1.2-2.

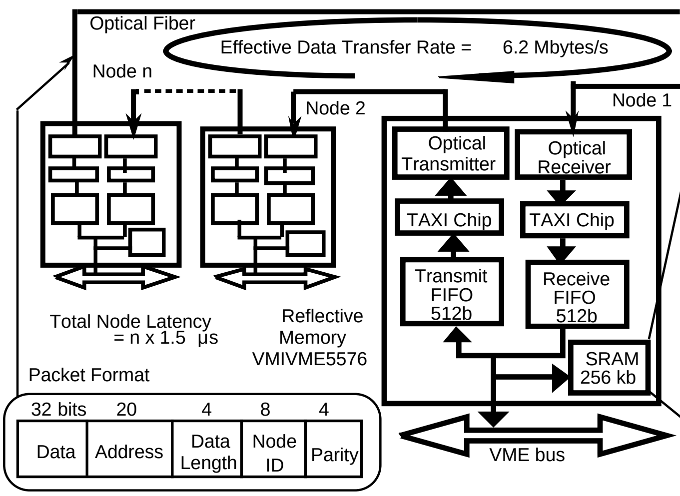

Contents	ch	Update cycle
Commands		
PFC voltage	5	0.25/0.5 ms
Gas flow rate	4	10 ms
NBI On/Off #	14	10 ms
RF On/Off	4	10 ms
Actuator status		
NBI ready/not	14	10 ms
NBI On/Off	14	10 ms
RF ready/not	4	10 ms
Raw measured data		
Magnetics	50	1 ms
Coil current	6	1 ms
Plasma position	4	1 ms
Diagnostics *	10	10 ms
Processed data	volume	
Plasma shape	1 kW	1 ms
Electron temp. profile, Current profile, etc.	15 kW /profile	?
Counter (Clock)	1 ms/10 ms	

: Timing pulses are used at present.
* : neutron production rate, radiation power, gas pressure, etc.

Fig.I.1.2-2 The reflective memory network linking the JT-60 controllers through optical fibers.

1.2.2 A New Shape Reproduction Method Based on the Cauchy-condition Surface for Real-time Tokamak Reactor Control [1.2-2]

Shape reproduction in a tokamak has been considered one of the key issues for control of reactor-relevant plasmas. Necessary conditions of the sensors for shape reproduction have been analytically clarified on the basis of the exact solution [1.2-3]. At the same time, a new method had been expected to reproduce shape even under insufficient sensor conditions.

Hence, such a practical method has been developed on the basis of the following analytical exact solution of the static Maxwell equation in toroidal axisymmetric region:

$$\sigma\,\phi(\mathbf{x}) + \int_{\partial\Omega_p} \left[G(\mathbf{x},\mathbf{y})\,\mathrm{grad}\,\phi(\mathbf{y}) - \phi(\mathbf{y})\,\mathrm{grad}\,G(\mathbf{x},\mathbf{y}) \right] \frac{dS(\mathbf{y})}{r_y^2} = \int_{\Omega_p} \mu_0\, j_c(\mathbf{y})\, G(\mathbf{x},\mathbf{y}) \frac{dV(\mathbf{y})}{r_y} \qquad (1.2.2\text{-}1)$$

where φ is the poloidal flux function ($\equiv r\cdot A$, $A$is a toroidal component of the vector potential), G is the Green's function, Ω is the entire region containing the known current sources (i.e., poloidal field coils), $\partial\Omega$ is the boundary surface of Ω enclosed by a plasma, j is the current density, and s is a constant (e.g., $4\pi^2$ for $\mathbf{x}$ on $\partial\Omega$). $x\equiv(r, z)$, $y\equiv(r, z)$.

In the second term of the left-hand side, Cauchy condition (i.e., $\phi(\mathbf{y})$ and grad$\phi(\mathbf{y})$) on the boundary surface $\partial\Omega$ is unknown quantity. Then, this Cauchy condition should be identified by the method of least-squares using adequate number of magnetic sensors.

This method for shape reproduction has been tested using various actual plasmas in JT-60. It has been confirmed the identified shapes agree with the results from the full equilibrium analysis. It should be noted that this new shape reproduction method has all the following features: (a) Preferably the method stands on the theoretical basis. (b) Various types of sensors can be involved in the numerical procedures. (c) Reproduction precision can be improved corresponding to the increase in number of sensors. (d) The real-time calculation is possible.

1.2.3 Development of A New Discharge Control System

Concerning a new discharge control system, we have built a prototype system to test software and hardware. According to the current design, this system is composed of two parts: A supervisor for compilation of discharge condition files and acquisition of result data from all the subsystems (DC/RD-SV), and a supervisor for discharge sequential control (SQ-SV).

DC/RD-SV, as a master for discharge condition files before discharge, distributes the appropriate conditions to the corresponding subsystems after compilation procedures. After discharge, DC/RD-SV works as a master for result data acquisition. This receives result data from all subsystems, and builds an intermediate file before transferring it to the JT-60 database production server. SQ-SV manages all the actions and events occurred in the JT-60 systems according to the discharge sequence by sending the command messages and receiving the replies. This part will be composed of VME modules due to the required fast on-line communications. DC/RD and SQ-SV's will be expected to come into operation in 2000. The new system configuration is shown in Fig.I.1.2-3.

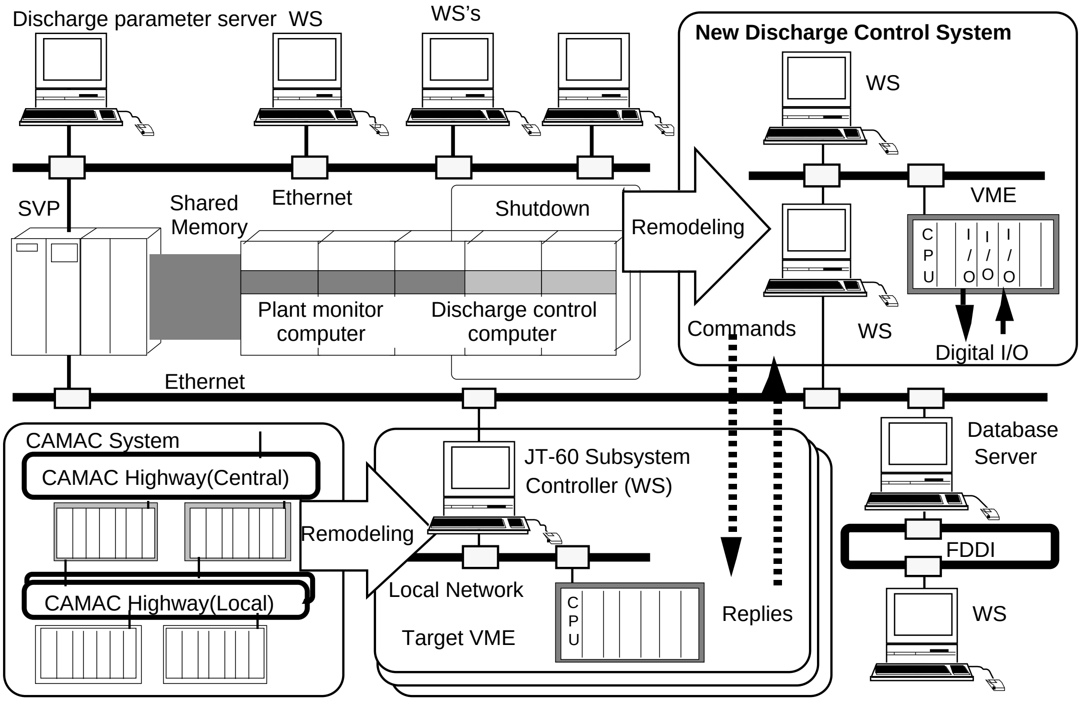

Fig.I.1.2-3 Configuration of JT-60 new discharge control system.

References

[1.2-1] Kurihara, K., Kawamata, Y., Akiba, K., et al., " Plasma Real-Time Control System for Advanced Tokamak Operation Scenarios in JT-60," to be published in Proceedings of IEEE/NPSS Real-Time Conference 99, (Santa Fe, 1999).

[1.2-2] Kurihara, K., "A new shape reproduction method based on the Cauchy-condition surface for real-time tokamak reactor control " to be published in Proceedings of 5th Symposium on Fusion Nuclear Technology (Rome, 1999).

[1.2-3] Kurihara, K., " Tokamak plasma shape identification on the basis of boundary integral equations," Nuclear Fusion 33, 399-412 (1993).

[1.2-4] Yonekawa, I., Totsuka, T., Akasaka, H., et al., "Remodeling of JT-60 discharge control system," to be published in Proceedings of IAEA TCM on control, data acquisition and remote participation on fusion research, (Lisbon , 1999).

1.3 Power Supply System

Except for the toroidal field coil power supply (TFPS), the JT-60 power supplies continued to run satisfactorily throughout the year with regular access for preventive maintenance and fault correction. In the poloidal field power supply (PFPS), the workstation for the direct digital controller (DDC) was replaced with a new one and the CAMAC-based test system was remodelled to a VME-based one. Design work was also carried out for rejuvenation of the TFPS control system. Development of an IGBT current-driven PWM converter and a current interrupter with a capability of carrying a large current in steady state was continued from the previous year.

1.3.1 Burnout of a Filter Capacitor in the TFPS and its Replacement

The toroidal field power supply (TFPS) is composed of six diode rectifier banks and a moter-generator (MG) with a large flywheel. The TFPS is divided into two subsystems. One is called the commercial line (CL) subsystem, where four banks of the rectifiers are directly connected to a commercial power grid. The other is the MG subsystem, where the rest of the banks are powered from the MG.

One of the capacitors in the harmonic filters of the TFPS CL subsystem burnt out in June 1998. In parallel with the investigation of the capacitor fault cause, the system integrity of the JT-60 power supplies including those for the NBI and RF heating systems were checked. After that, the JT-60 operation up to a toroidal magnetic field of 2.1 T (a half of the maximum rating) with the MG subsystem alone was restarted early in July.

The cause of the fault was carefully investigated by break-up of the capacitor and observation of its inside. Then, it was concluded that the fault had been caused by aged deterioration of the insulation performance of the capacitor, and that the repeated application of a transient high voltage to the capacitor in the case of its connection to the circuit had accelerated the deterioration. In fact, the TFPS had continued to run over 14 years and the capacitor was connected and disconnected over twenty thousands times in total.

For deciding the technical specifications of a new capacitor, the latest information on a power capacitor was collected from its specialists and industries. Then, the new capacitor with a dielectric strength 25 % larger than that of the original one was fabricated and installed by the end of August 1998. Moreover, an electrical fault detector using the zero-phase-sequence voltage of capacitor, which can respond even in the case of a single capacitor element fault, was also introduced in conjunction with the exiting mechanical fault detector. Thus, the JT-60 operation at a toroidal magnetic field of 4 T (the maximum rating) was restarted at the beginning of September 1998. Hence, although the JT-60 operation schedule was changed a little owing to the capacitor fault, the experimental programs were almost executed according to the annual plan by rearrangement of the programs.

From the viewpoint of the assurance of safety and system integrity, it is most important how to prevent the similar fault. Hence, replacement of all of the power capacitors in the JT-60 power supplies equipped for harmonic filtering and var compensation was decided as preventive maintenance. The rest three capacitors of the harmonic filters in the TFPS CL subsystem were replaced in the middle of October 1998. Seven new capacitors of the var compensators in the TFPS, the PFPS and the MG system for the NBI and RF heating (H-MG) were installed from November 1998 through January 1999. The filter capacitors in the TFPS MG subsystem, the PFPS and the H-MG were replaced in May 1999.

1.3.2 Development of an IGBT Current-driven PWM Converter

Development of the insulated gate bipolar transistor (IGBT) current-driven pulse width modulation (PWM) converter was continued from last year. A new PWM pulse generation method applicable to superconducting magnet power supplies was developed [1.3-1, 2]. This method has the following features.

(i) It is possible to realize the operation with a power factor of unity.

(ii) When a zero DC output voltage is required, this method can completely suppressed the output voltage of an IGBT converter to zero and not in the average.

(iii) Switching frequency can be reduced to three-fourth of that of a conventional method.

(iv) The proposed method has a good compatibility with a computer control system.

1.3.3 Development of a Forced Air-cooled VCB

Much effort was made to develop the water-cooled VCB for a superconducting magnet power supply [1.3-3] until the previous fiscal year. However, some difficulties of water-cooled VCB arose from the viewpoint of quality assurance in manufacturing. For example, the flexible water pipe is required for the movable rod cooling, but the possibility of water leak can not be completely removed from the experiences so far. Then we decided to develop a forced air-cooled VCB with a current rating of 12 kA.

In the development of the air-cooled VCB, it is a key issue how to maximize the capability of heat removal from the electrodes as in the development of the water-cooled VCB. Then, the design work was focused onto the VCB itself at first, and the design of mechanical structure was postponed. The electrodes of the VCB were designed to be as thick as possible so as to minimize the electric resistance and to maximize the heat removal capability at the same time. The newly designed VCB was fabricated and the basic test was performed. The measured electric resistance well agreed with the expected value. For the confirmation of the current carrying capability of the air-cooled VCB, the power test is planned in next fiscal year.

References

[1.3-1] Miura Y. M., Matsukawa M., Hirotami N., “A New Method of Switching Pulses Generation in Three-Phase PWM Current Source Type Converter”(in Japanese), T.IEE Japan, Vol.119-D, No.7, p.1022, 1999.

[1.3-2] Miura Y. M., Matsukawa M., Hirotami N., “A New PWM Pattern Generation Method for a PWM Converter applied to a superconducting magnet”, to be presented in 18th SOFE, Albuquerque, NM, 1999.

[1.3-3] Matsukawa M., Miura Y. M., Kimura T., et al., “Design and Model Test of a Water-cooled VCB for Superconducting Magnet Power Supplies”, Fusion Technology, Vol. 34, p.684, 1998.

1.4 Neutral Beam Injection System

1.4.1 Positive-ion Based NBI System

For evacuating the W-shape divertor section in the JT-60 vacuum vessel, the cryopumps for three beamlines out of 14 beamlines have been used exclusively as a pumping of deuterium gas or deuterium/helium mixture gas since 1998. The pumping speed of the cryopump is 1000 m^3/s for deuterium gas and $700m^3/s$ for deuterium/helium mixture gas. However the pumping speed at the divertor section decreased to around 15 m^3/s in total because of the small conductance between the divertor and beamline tank. The rest of beamlines, eleven units, are being injected the neutral beams into JT-60 for plasma heating and NB current drive experiments, and the beam power injected into the plasma was 25 MW at around 90 keV for 9 s at maximum.

A new data acquisition / calculation system of the infra-red camera signal monitored at the NBI armor plate in the JT-60 vacuum vessel has been developed for easy evaluation of a beam shine through in plasma. The new system has made it possible a time evolution of the beam shine through to evaluate just after plasma shot.

1.4.2 Negative-ion Based NBI System

The development to extend the beam duration time in the ion source operation has been conducted by optimizing arc discharge. In negative ion source with cesium seeding, a time constant of arc discharge has been found to be longer than that in the conventional positive ion source because of a contamination of cesium atoms during arc discharge from the arc chamber wall. To stabilize the arc discharge even in a cesium contamination into plasma, a pre-arc discharge duration time before beam acceleration has been extended for more than 1.5 s. The beam duration time in the neutral beam injection, under the longer pre-arc discharge time, has reached near 2 s at 4 MW without breakdown, as shown in Fig.I.1.4-1.

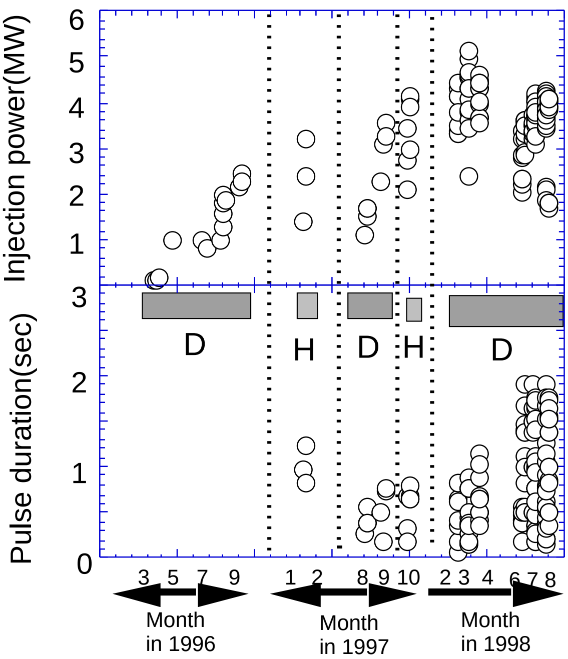

Fig.I.1.4-1 Time evolution of injection power and beam duration time

Unfortunately, the beam operation toward a higher beam power could not be conducted because of water leakage of an ion source and a malfunction of the insulating transformer for the negative ion generator power supply. The first trouble of the water leakage in the ion source broke out at a current-feed-through for a filament current in the arc chamber. Its cause had been found that two malfunctions happened simultaneously. One is an abnormal discharge broke out between the filament feed through and arc chamber wall at the moment of an ion source breakdown, and the other is a failure of cut-off in the abnormal discharge current with the GTO switching in the arc power supply. The two malfunctions happened simultaneously had destroyed the feed through, and made the water leakage from a pin hole in the cooling water tube.

A surge absorber component has been added in the filament circuit as the countermeasure against the abnormal discharge, and a double cut-off system of the conventional GTO switching and a newly added thyristor switching has adopted against the failure of the cut-off. The second trouble, the malfunction of the insulating transformer, was found by detecting about 20 ppm of acetylene gas in the insulation oil when we inspected contamination gas in the oil. The acetylene gas in the transformer oil, usually, is produced only when a discharge or a high temperature hot spot break out in the transformer. After opened the transformer, we found a melting down section in a part of the coils caused by a discharge between coil turns. The cause of the discharge was that an insulating sheet of the coil was worn out by overlapping of two adjacent coils through an imperfect manufacturing. Four months were needed for refurbishing the transformer.

1.5 Radio-Frequency Heating System

1.5.1 ICRF System

The ion cyclotron range of frequencies (ICRF) system for JT-60 was operated well at 102 MHz in FY 1998. RF power of 3-4 MW was coupled to JT-60 plasma for the experiments of "TAE mode investigation using reflectometer" and "Combined heating with negative ion based NBI". Some trials were performed to prove ideas of advanced methods to enhance the antenna coupling performance. One of the ideas is an active control of SOL plasma by gas-puffing. Increase in SOL density may improve antenna coupling with large antenna-separatrix distance. However, the gas-puffing just before and during an ICRF pulse tends to reduce the break-down voltage of the antenna, and strong gas-puffing may degrade plasma performance. Thus optimization of the position, the pressure and the pulse width of gas-puffing are important. As a result of this trial, it is found that the coupling was improved with H_2 gas-puffing near antenna (FC-18 at P-11), as shown in Fig.I.1.5-1. The estimated n_e increase of the second scrape off layer is shown in Fig.I.1.5-2. This improvement is clear for long pulses. Another idea such as "control

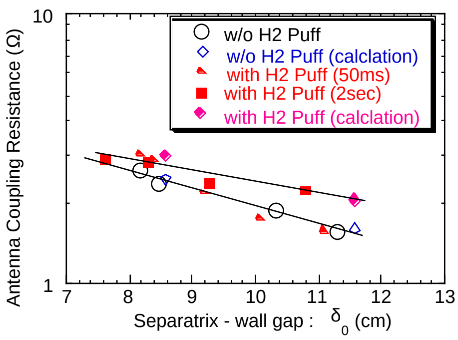

Fig. I.1.5-1 Coupling was improved with gas-puff near antenna.

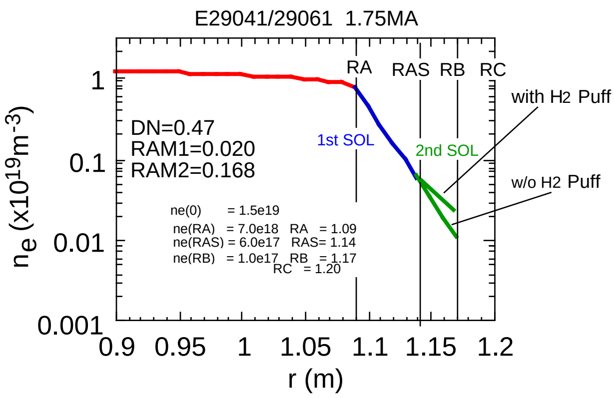

Fig. I.1.5-2 Estimated increase of ne in the 2nd SOL.

of local B_T just in front of the antenna by a magnet or an electromagnet" was checked by means of measuring the coupling resistance with various B_T and I_P. Further study in wider parameter range will be needed to clarify the relationship between R_C and B_T or safety factor.

A first test of the feedback control of the separatrix-antenna gap, δ_0, was performed. To keep δ_0 constant is quite effective to couple stable ICRF power to the plasma. It is expected that the control improve the ICRF heating of the plasma which tends to change the separatrix position, i.e., reversed magnetic shear plasma.

1.5.2 LHRF System

The lower hybrid range of frequencies (LHRF) system for JT-60 was operated for experiments focused on improvement of confinement by profile control through current drive with LHRF waves. The total plasma current was selected around 1 MA for full current drive condition with two antennas after 2-3 days conditioning shots. Heat load on the antenna was a key issue for these experiments, because fast ions bombarded antenna mouth due to banana orbit loss produced high magnetic ripple of 2 % at outside of the JT-60 vacuum vessel. This heat load led rf-breakdowns at the antenna, and then the experimental performance was limited by these breakdowns. In order to avoid excessive heat load, the temperature profile on the antenna had been measured by infra-red (IR) TV camera. But its resolution was not enough, so a telephoto lens was introduced. Plasma position and/or antenna position were regulated to suppress heat load by monitoring the increase in temperature with the improved IRTV, for example, in the experiment of quasi-steady sustainment of a reversed magnetic shear configuration with the internal transport barrier [1.5-1]. For this configuration, it is found that the coupling was good even in the case that the antenna was settled around 15 mm behind the first wall.

After modification of divertor configuration from open to W-shaped closed type in 1997, the coupling of the third LHRF antenna became worse because the gap between the antenna and the plasma was wider. To overcome this, it is considered to make the frequency higher from

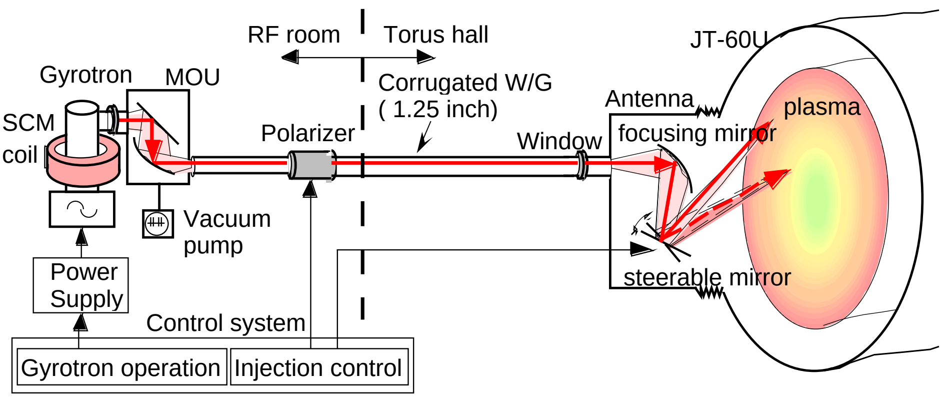

Fig.I.1.5-3 Outline of a mm-wave current drive system designed for JT-60U.

2 GHz to 110 GHz in the mm-wave frequency range. A mm-wave current drive system was designed for JT-60 as shown in Fig.I.1.5-3, which has advantages of highly controlled local current drive and heating as well as easy and high coupling. One RF line was introduced in March 1999 by using a newly developed RF source, a 1MW gyrotron and modifying the power supply and the transmission line of the existing LHRF system.

References

[1.5-1] Ide S., et al, "17th IAEA Fusion Energy Conference Yokohama, Japan, 19 – 24 October 1998", IAEA-CN-69/CD1/4, (1998).

1.6 Diagnostics System

1.6.1 Core Correlation Reflectometer

A core correlation reflectometer has been newly installed on the JT-60 tokamak [1.6-1]. The reflectometer can measure electron density fluctuations near the cut-off layer at which the launched millimeter wave is reflected. The reflectometer consists of four channels, two of which operate at a fixed frequency and the other two channels are tunable. The correlation of the fluctuations is determined from the correlation between fixed and variable frequency channels. The profile of the correlation is measured by using this reflectometer in the high performance reversed shear plasma. The correlation length in the ITB region is shorter than that in the flat density region after the formation of the clear ITB.

1.6.2 Behaviour of Divertor Neutral Pressure at the Onset of an X-point MARFE [1.6-2]

It is found for the first time that a rapid change of the asymmetry in the neutral pressure at the inner and outer divertors occurs at the onset of an X-point MARFE. The change in the pressure ratio is much clear than that in the averaged electron density, so that it is a good index of the onset of X-point MARFE. Though the mechanism of this change in asymmetry at the onset of the X-point MARFE is not clear yet, the result suggests that a detached divertor plasma could be sustained by the control of an in/out pressure ratio. Feedback control of the gas puffing rate is planned by using the pressure ratio of the outer to inner private region, for the purpose of keeping the divertor detachment without inducing the X-point MARFE.

1.6.3 Tangential Dual CO_2 Laser Polarimeter

The dual CO_2 laser polarimeter has been developed [1.6-3, 4] based on the results from the proof-of-principle experiment of tangential Faraday rotation measurement [1.6-5]. The tangential Faraday rotations of two CO_2 lasers (10.6 and 9.27 μm) were well measured along the same optical path in a tokamak. Such a two-wavelengths operation is expected to improve the accuracy of density signal by eliminating the Faraday rotation component at vacuum windows.

Here, the evaluation of window component requires that the system is fully calibrated. For this purpose, the development of appropriate calibration tools is planned in FY 1999.

1.6.4 Heterodyne Radiometer System for Electron Cyclotron Emission (ECE) Measurement

It was shown that the heterodyne radiometer can give the detailed information on the structure of the magnetic island in the steady state high β_p discharges [1.6-6]. To extend the measurement range, a new 12-channel heterodyne radiometer, whose measurable ECE frequency is 188.5 to 199.5 GHz, has been installed. The upgraded heterodyne radiometer system will also give the detailed information on electron temperature and its fluctuations near the internal transport barrier especially in the reversed shear plasmas. The new system will work from June 1999.

1.6.5 Time-of-flight Neutron Spectrometer

A 2.45 MeV neutron time-of-flight spectrometer [1.6-7] was developed for measurements of neutron energy spectra from the JT-60 tokamak. The spectrometer consists of two fast plastic scintillators (50 cm and 1800 cm thickness: 2 cm) where each detector is located on two constant time-of-flight spheres. The time-of-flight spheres have radius of 1 m which gives a neutron flight length of ~164 cm and a time-of-flight of ~92 ns for 2.45 MeV source neutrons. The performance of the spectrometer was calibrated with the 14 MeV neutron source FNS, where the energy resolution of 5.8% and the detection efficiency of 3.1×10^{-4} were obtained for 14 MeV neutrons. The energy resolution of 4.3 % (105 keV) was extrapolated for 2.5 MeV neutrons from the calibration. In December 1998, the spectrometer was installed in the basement of JT-60 with a vertical viewing cord. Preliminary measurement of the 2.4 MeV neutron spectra has been carried out since March 1999.

1.6.6 Measurement of Electron Temperature and Density in the Divertor Plasma Using Intensity Ratios of He I Lines [1.6-8]

Emission of He I lines (668 nm, 706 nm and 728 nm) has been simultaneously observed in the divertor plasma. From calculations using a collisional-radiative model, intensity ratios of these He I lines are considered to be useful to measure electron temperature and density. In order to evaluate the feasibility of the intensity ratio method for temperature and density measurements, the measured intensity ratios are compared with those calculated from the temperature and density measured with Langmuir probes. As a result, the measured intensity ratios are well reproduced by the calculations. Therefore, the emission rate coefficients for the He I lines are reliable for measurement of the temperature and density.

1.6.7 CO_2 Laser Collective Thomson Scattering [1.6-9]

A collective Thomson scattering based on pulsed CO_2 laser (λ = 10.6 μm) have been developed in collaboration with ORNL to measure ion temperature and fast ions in JT-60. A high power pulsed CO_2 laser (energy: 10 J, pulse length: 1 μs, repetition rate: 0.5 Hz) and a heterodyne receiver system with a hot CO_2 absorber cell as a stray light notch filter has been installed and tested in the diagnostic room. Neutron shield of the beam penetration optics from diagnostic room to the torus hall has been constructed. Injection of the laser to the JT-60 plasma will start in 2000.

References

[1.6-1] Shinohara K., Nazikian R., Fujita T., Yoshino, submitted to Rev. Sci. Instrum. (1999).
[1.6-2] Tamai H., Asakura N., Hosogane H., et al., J. Plasma Fusion Res. **74** 1336 (1998).
[1.6-3] Kawano Y., Chiba S., Shirai H., et. al., Rev. Sci. Instrum. **70**, 1430 (1999).
[1.6-4] Kawano Y., Chiba S., Inoue A., JAERI- Research (in press).
[1.6-5] Kawano Y., Chiba S., Shirai H., et al., Rev. Sci. Instrum. **70**, 714 (1999).
[1.6-6] Isayama A., Kamada Y., Ozeki T. and Isei N., Plasma Phys. Control. Fusion **41**, 35 (1999).
[1.6-7] Hoek M., Nishitani T., Takahashi H., et al., to be published in Fusion Eng. Design.
[1.6-8] Kubo H., Goto M., Takenaga T., et al., to be published in J. Plasma and Fusion Research.
[1.6-9] Kondoh T., and Nagashima A., to be published in JAERI-Research (1999).

1.7 Data Analysis System

1.7.1 Data Analysis Tools, Database and Computer System

Some of the data analysis tools on the JT-60 analysis server have been improved. The data illustration system (DAISY) using the X-Window has been greatly enhanced and now has the following new features: multiple plot windows, easy saving/loading of command files, producing figures in Macintosh's formats, online help, data transformation utility. The software showing a time slice profile of plasma parameters, SLICE, has been modified to produce the multi-time profile data for the time transient transport analyses. The new version of the fast plasma-boundary identification code (FBI) incorporates the optional eddy current analysis. It can also call user-supplied subroutines for extensive analysis. A special version of the MHD equilibrium analysis code SELENE has been developed which can take the data from motional Stark effects (MSE) diagnostic and reconstruct the MHD equilibrium for reverse magnetic shear plasmas. The experiment logbook system FELLOW now generates electronic logs and users can view these files online.

The JT-60 experimental database has enriched the content. Appropriately for the update of diagnostic systems, such as divertor visible spectroscopy, H_α array, these diagnostic data have been added to the experimental database. Plasma equilibrium data calculated by the new FAME, which is described in Sec. 1.7.2, and calculated data by new RTP (real time processor) have also been added to the database.

Some subsystems of JT-60 data processing system have been improved according to the demands of plasma diagnostic systems by utilizing the progress of the computer and network technology. The main computer ISP (inter-shot processor) of FACOM M-780 has been replaced with a compatible computer FACOM GS8300 using state-of-art CMOS technology, which results in lower power and space usage with nearly the same performance. A gigabit ethernet switch with FDDI ports has been introduced to cope with the increase of handling data. The switch connects the UNIX file server, which has a capacity of ~100GB RAID disks and ~900GB MO (magneto-optical disk) auto-exchangers, at the bandwidth of gigabit per second with the main computer and many data acquisition workstations, such as a VME-based fast data acquisition system, a planned new TMDS (transient mass data storage system). The new CICU, which has a function of interfacing the main computer with the CAMAC system by using a byte-serial highway driver and is composed of a workstation and a VMEbus byte serial highway driver, has been developed and has been finally in practical operation without any major problems after careful tests and fine tuning.

1.7.2 FAME System

The new system of FAME (Fast Analyzer for MHD Equilibrium), to provide about 130 MHD equilibria in time series which are enough for the non-stationary analysis of the experimental data of JT-60 within a shot interval, has been utilized since1997 with a high processing speed using IBM RS/6000 SP. The system is a MIMD type small scaled parallel computers with 7 CPUs and the maximum theoretical speed is 3.42 GFLOPS. The SELENE and FBI codes are tuned up taking the parallel processing into consideration as well as the original system. Consequently, the computational performance of the new FAME system becomes more than 3 times faster than the original system. The new system also has the file server system with the large capacity of the data storage of 50 GB.

Efforts of utility development and update have been concentrated on more effective use of the new FAME system. An equilibrium animating system has been developed on a workstation arranged in the central control room. The system can provide animations of MHD equilibrium analyzed by the FAME, incorporated with SLICE. A new workstation has been added to system to meet the increased demands of the experimental team. To see the animation earlier after the shot, the way to get raw data for the equilibrium calculation has been changed from the access of the database server to the direct data transfer from the ZENKEI control system. As a results of this improvements, the waiting time after the shot has been largely shortened from ~11 min to ~ 6 min. In order to display typical equilibrium data as functions of time with other experimental data, the new FAME system recalculates equilibria at an interval of 10 ms during off-experimental hours at night and transfers the results of over 80 variables to JT-60 database server.

1.7.3 Data Link System and Remote Participation in JT-60 Experiments

The remote participation in JT-60 experiments from PPPL has been carried out by utilizing the Data Link System and the video conferencing systems. The Data Link System provides standard JT-60 data analysis tools: DAISY, FBI, EQREAD (MHD equilibrium display code), and SLICE. Participants from both JAERI and PPPL jointly analyzed and discussed the JT-60 data together.

Seven projects have started as remote collaboration under the Cooperation among the Three Large Tokamak Facilities. The total number of participants amounts to about one hundred. These projects cover a wide range of research topics with outcomes of 2 presentations at major conferences.

Reference

[1.7-1] Hasegawa Y., Hamamatsu K., Shirai H., et al., JAERI-Tech 99-015, "Development of FAME Animation System", (1999) (in Japanese).

[1.7-2] Hasegawa Y., Nakamura Y., Shirai H., et al., "Development and Performance of High Speed Processing System of Magnetohydrodynamic Equilibria for Discharge Analyses on the JT-60 Tokamak ", J. At. Energy Soc. Japan, **41**, 48 (1999) (in Japanese).

[1.7-3] Matsuda T., Tsugita T., Oshima T., et al., "Systems for Remote Participation in JT-60 Experiments", Rev. Sci. Instrum., **70**, 502 (1999).

[1.7-4] Matsuda T., Aoyagi T., Saitoh N., et al., "Recent Developments in JT-60 Data Processing System", Fusion Eng. Des., **43**, 285 (1999).

2. Experimental Results and Analyses

2.1 Reversed Shear Experiments

2.1.1 Achievement of High Fusion Gain in W-shaped Pumped Divertor [2.1-1]

The record value of equivalent fusion multiplication factor in JT-60, Q_{DT}^{eq} = 1.25, has been achieved in a high current reversed shear discharge with an L-mode edge (B_t = 4.4 T, I_p = 2.6 MA and q_{95} = 3.2) in the campaign after the installation of W-shaped pumped divertor. The DD neutron emission rate was 3.6×10^{16} /s with neutral beam power of 12 MW. To obtain high performance, it is essential to form a large radius internal transport barrier (ITB) in low q regime (q_{min} ~ 2). This was accomplished by plasma current ramp-up with the persistent ITB. The control of pressure and current profiles by changing the plasma volume and the feed-back control of beam power using the neutron emission rate were found effective to suppress a collapse before reaching high current regime.

Reduction of impurity (Z_{eff} ~ 3.5 to ~3.2) was obtained in the W-shaped pumped divertor, which resulted in 20% increase of Q_{DT}^{eq}, the record value of which had been 1.05 at 2.8 MA in the previous open divertor [2.1-2], though the plasma current was restricted below 2.6 MA due to smaller plasma volume.

2.1.2 Sustainment of Internal Transport Barrier in ELMy H-mode Edge Discharges [2.1-1]

The performance in L-mode edge discharges was limited by disruptive beta collapses with β_N ~ 2 at q_{min} ~ 2. An H-mode transition was obtained by use of enhanced heat pulse with degradation of ITB, which was caused by toroidal rotation control. The stability in the low-q_{min} region was successfully improved in the H-mode edge discharges, and a high β_N value of 2.3 has been achieved at q_{min} = 1.5. Long sustainment (5.5 s) of ITB and improved confinement was realized in an ELMy H reversed shear discharge (B_t = 3.5 T, I_p = 1.5 MA, q_{95} = 4.3, triangularity ~ 0.26); H factor of 1.5-2.0 and β_N of 1.0-1.4 were sustained. The q_{min} continued to decrease to ~1.8 during the ITB sustainment period. The density and temperature profiles were changed according to the time evolution of q profile, which indicated the importance of current profile control for sustainment of ITB.

2.1.3 Stationary Sustainment of Internal Transport Barrier by LHCD [2.1-3]

A reversed shear configuration that was accompanied by ITBs was successfully maintained in a quasi-steady state almost entirely non-inductively by the lower hybrid (LH) driven current (~77 %) and the bootstrap current (~23 %). The LH waves were injected after the formation of reversed shear configuration and ITB by neutral beam heating during plasma current ramp-up. The q_{min} was kept near 2 and the normalized beta was kept near 1 with B_t = 2.0 T and I_p = 0.85 MA. The neutron emission rate was nearly steady as well indicating no accumulation of impurities into the plasma. Diagnostics showed that all the profiles of the electron and ion temperatures, the electron density and the current profile were almost unchanged during the LH current drive phase.

2.1.4 MHD Stability Analysis Associated with ITBs

Localized MHD activity observed in JT-60 and TFTR near ITBs with their associated large pressure gradients is investigated [2.1-4]. Stability analysis of equilibria modeling the experiments supports an identification of this MHD as being due to an ideal MHD n=1 instability. The appearance of the instability depends on the local pressure gradient, local magnetic shear in the q profile and the proximity of rational surfaces where q~m/n and m and n are the poloidal and toroidal mode numbers respectively. The mode width is shown to depend on the local value of q, and is larger when q is smaller. In addition the role of the edge current density in coupling the internal mode to the plasma edge and of the energetic particles which can drive fishbone like modes is investigated.

2.1.5 Studies on ITB Formation

Onset conditions of ITB in reversed shear discharges were investigated [2.1-5]. Local values of electron density, electron temperature, and the ion temperature seem not to be essential for the ITB onset. Remarkable correlation between electron temperature gradient and magnetic shear was observed at the onset. In addition, ITB well outside the q-minimum position was found. Its onset condition seems to be continuous with that observed in negative shear region.

The radial correlation lengths of density fluctuations in reversed shear plasmas with ITBs were firstly measured using a correlation reflectometer operating the upper X-mode, which was developed and installed under collaboration between JAERI and PPPL [2.1-6]. The correlation length in the ITB layer (r/a~0.55) was shorter than that at r/a~0.35 before the ITB foramtion. This suggests that there is a decorrelation of long scale turbulence in the ITB layer and it would contribute to the reduction of particle and thermal transport there.

References

[2.1-1] Fujita T., Kamada Y., Ishida S., et al., to be published in Proc. 17th IAEA Fusion Energy Conf., Yokohama, 1998, IAEA-F1-CN-69/EX1-2.

[2.1-2] Ishida S., Fujita T., Akasaka H., et al., Phys. Rev. Lett. 79, 3917 (1997).

[2.1-3] Ide S., Naito O., Oikawa T., et al., to be published in Nucl. Fusion.

[2.1-4] Manickam J., Fujita T., Gorelenkov N., et al., to be published in Proc. 17th IAEA Fusion Energy Conf., Yokohama, 1998, IAEA-F1-CN-69/EX8-4.

[2.1-5] Koide Y., Fujita T., Takizuka T., et al., to be published in Proc. 17th IAEA Fusion Energy Conf., Yokohama, 1998, IAEA-F1-CN-69/EX5-2.

[2.1-6] Nazikian R., Shinohara K., Yoshino R., et al., to be published in Proc. 17th IAEA Fusion Energy Conf., Yokohama, 1998, IAEA-F1-CN-69/PD2.

2.2 High β_p and High Triangularity Discharges

This section summarizes development of quasi-steady ELMy high-β_p H-mode discharges with enhanced confinement and high-β stability, where i) long sustainment time, ii) increase in absolute fusion performance and iii) extension of the discharge regime toward low-q_{95} (~3) are the main objectives. For these purposes, the current and pressure profile control is essential and high triangularity is beneficial. In particular, optimization of the pressure profile characterized by the double transport barriers (the internal and the edge transport barriers) with a high triangularity δ enabled us to extend the performances in long pulses.

The DT equivalent fusion gain Q_{DT}^{eq} ~0.1 (δ =0.16) was sustained for ~9 sec (~$50\tau_E$, ~$10\tau_p$*) and Q_{DT}^{eq} ~0.16 (δ = 0.3) for 4.5 s at I_p=1.5 MA. In the latter case with higher δ, H-factor (=$\tau_E/\tau_E^{ITER89PL}$)~2.2, β_N~1.9 and β_p~1.6 were sustained with 60-70 % of noninductive driven current. In the low q_{95} (~3) region, the β-limit was improved by the high δ (~ 0.46) shape where β_N~2.5-2.7 was sustained for ~3.5 s with the collisionality close to that of ITER-FDR plasmas [2.2-1]

The product of β_N x H-factor sustainable for >$5\tau_E$ (> τ_p* : effective particle confinement time) increases with δ and reaches ~6 at δ~0.46. This is mainly because the pedestal βN increases with δ because the edge p increases with δ [2.2-1]. The sustainable β_N-values are limited by appearance of resistive modes with low toroidal numbers such as m/n=3/2 and/or 2/1.

The measured island width was consistent with the predicted width of the neoclassical tearing mode. Values of β_N at onset of m/n=3/2 and 2/1 modes showed positive dependence on electron density [2.2-2].

As for high confinement at high density, the density range with H-factor >2 was extended from ~$0.5n_eGW$ to ~$0.6n_eGW$ by increasing triangularity δ from 0.2 to 0.4. However, strong gas puffing is required for a further increase in density, and the H-factor decreases with density. This situation has not been improved by the W-shaped pumped divertor [2.2-1].

In JT-60 ELMy H-mode plasmas, dependence of the width of the edge pedestal Δ_{ped} on the edge parameters has been extensively studied [2.2-3]. The width Δ_{ped} in the ELMy phase is 2-3 times larger than that in the ELM-free phase. At high triangularity, Δ_{ped} reaches 8-15cm (9-16 % of the minor radius) at Ip=1 MA and the pedestal T_i and Δ_{ped} can increase gradually with a time constant of ~2 s, which is ~10 times longer than τ_E. In addition, p in the pedestal layer increases simultaneously. The width Δ_{ped} scales linearly with the poloidal gyro radius of thermal ions ρ_{pi} with a weak dependence on q_{95} ; $\Delta_{ped} \sim 5\rho_{pi}\ q_{95}$- 0.3 . Shrinkage of Δ_{ped} observed at a high density can be explained by decrease in the edge ion temperature viz. decrease in ρ_{pi}. At higher q_{95} (~6), further increase in Δ_{ped} was observed after disappearance of type I ELMs. In particular, at high-δ (>0.3), high-q_{95}(>5-6) and high-β_p(>1.5-2) the type I ELMs disappear and minute grassy ELMs appear. The stability calculation including the edge bootstrap current suggests the access to the second stability regime of the high n ballooning mode.

References

[2.2-1] Kamada Y., et al., Proc. 17th Int. Conf. on Fusion Energy (Yokohama, 1998)) CD2/EX9/2; Nucl. Fusion to be published.

[2.2-2] Isayama A., Kamada Y., Ozeki T., et al, Plasma Phys. Control. Fusion **41** 35 (1999).

[2.2-3] Kamada Y., et al., ‘Growth of the edge pedestal in JT-60U ELMy H-mode” submitted to Plasma Phys. Control. Fusion.

2.3 H-mode Study

Although the L-H transition threshold power is generally described in terms of the global quantities, such as the averaged density and magnetic field, the significance of the edge plasma quantities was also intensively investigated hitherto in various tokamaks. Above all, influence of the edge magnetic shear on the H-mode threshold power has long been an issue of controversy. The theoretical predictions conceived so far are either that an increased edge shear may suppress the edge micro-turbulence or the locally reversed edge magnetic shear might stabilize the drift-resistive ballooning modes. The possible role of the edge current density was first pointed out at ASDEX. In 1990, reduction of the H-mode threshold power by a rapid rampdown in plasma current during the auxiliary heating was first demonstrated in the JIPP T-IIU experiment, where nearly a factor of two decrease was reported at the ramping rate of 1.8 MA/s. However, no such clear results have been thereafter obtained, except that a small reduction of 20% was recently found in ASDEX Upgrade for dI_p / dt = 1.0 MA/s. In an effort to reduce the additional heating power required for RTO/RC-ITER to acquire the H-mode as much as possible, the ITER physics R&D expert group has coordinated the current rampdown experiment in various tokamaks, as an urgent Physics R&D issues. In addition, it has been known that edge region of the reversed shear plasmas with strong internal transport barriers in JT-60 stays in L-mode under the intensive NB heating, where the plasma current is continuously ramped up. The reduction of heat flow to the edge, due to the internal barrier formation, may herein be the cause. However, a reduction of the edge magnetic shear can also play a substantial role. Accordingly, a dedicated runs to elucidate the influence of the edge magnetic shear was performed at JT-60.

In the initial experiment, the plasma current was ramped down in 0.75 s from 1.6 MA to 1.2, which provides the ramp rate of 0.53 MA/s. Right after the end of the current ramp down, the heating power was stepped up in a stairway fashion. The evaluated L-H threshold power was compared with a reference pulse with a fixed current of 1.2 MA. The density was set in the range, where the L-H threshold is the minimum in JT-60, in order to eliminate the contribution of the density dependence. The malign MHD activities were not observed as a result of the rampdown. Here, edge magnetic shear was evaluated at 95% poloidal flux, using the FBEQU equilibrium solver. Similar to the changes of the plasma internal inductance, which varied from 1.1 to 1.6, edge magnetic shear increased monotonously after the start of the rampdown, and it gradually decreased during the auxiliary heating. However, reduction of the L-H threshold power was not obvious, whereas the H-factor increased by 15 to 20%. The comparison of pressure profiles with and without the rampdown indicates that an increase of H-factor is mainly produced at $\rho \leq 0.6$. The rampdown results follow the previous JT-60 L-H threshold power scaling, which does not corroborate the rampdown effect found in JIPP T-IIU tokamak. Even though the plasma current was ramped down from 1.6 to 1.0 MA, the result was the same.

The followings have been conceived:

(1) The time derivative of number of trapped ions lost from the orbit might be important for the L-H transition,

(2) The magnetic flux diffusion in the boundary of a plasma will diminish the shear in the edge region during this heat diffusion period, while the edge shear effects are at their maximum towards the end of the rampdown period, and it takes an energy confinement time for the heating power to diffuse out of the core and contribute to power-though-the-separatrix, and

(3) The amount of rampdown may not have been adequate, the rampdown was performed during the NB heating, of which power is right below the threshold, in the second campaign. In addition, the rampdown rate was increased up to 3.0 MA/s.

In prior, the heating power was stepped up in a stairway fashion with a fixed current to determine the threshold. The normalized heating power was reduced to 89% during the rampdown, and the hitpoints on the divertor target plates were also deliberately adjusted. The values of internal inductance and edge magnetic shear respectively increased up to 7.5 and 2.7 toward the end of the current rampdown. However, no clear signs of the L-H transition were observed in the divertor recycling or stored energy signals. Nevertheless, the edge temperatures as well as averaged density increased during the rampdown, seemingly due to an increase of the edge magnetic shear. Instead, an increase of the edge toroidal flow velocity, which is often observed as a result of the formation of the radial electric field in the negative direction, was not observed. The evaluated edge ion collisionality was 1.1 and 1.2 in the middle and end of the rampdown. Recent progress in theory indicates that even 3.0 MA/s is not adequate to induce the L-H transition, and the formation of large bootstrap current at the edge, which produces the strong edge magnetic shear further in the edge, may prove efficient.

2.4 Current Drive Experiments by N-NBI

The current drive capability of Negative Ion Based NBI (N-NBI), which is expected to realize MeV class beam energy required on the reactor, has been assessed. In view of adopting N-NB on the fusion reactor, the predictability of current drive and heating characteristics is quite important for its design and the extrapolation to the reactor regime. Current drive study has been accelerated by Motional Stark Effect (MSE) measurement and the time-dependent equilibrium analysis technique. On JT-60, maximum value of N-NB driven current, 0.6 MA, has been achieved with the injection power of 3.7 MW at the beam energy of 360 keV in deuterium operation (both plasma and beam), where the central electron temperature of 4keV and the line-averaged density 0.9×10^{19} m^{-3}. Figure I.2.4-1 shows N-NB driven current profile. The centrally peaked profile is confirmed experimentally as expected from on-axis trajectory of N-NB. The experimental result (solid line) agrees well with the prediction (dashed line) by current drive analysis code

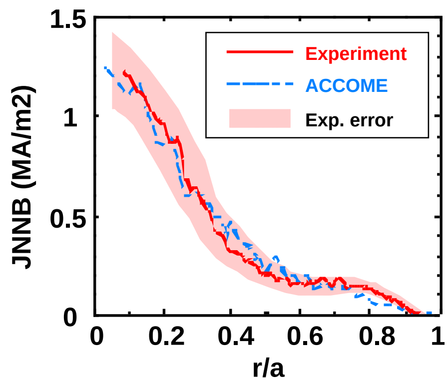

Fig.I.2.4-1 N-NB driven current density profile ($j_{N\text{-}NB}$). The experimental and theoretical results are shown.

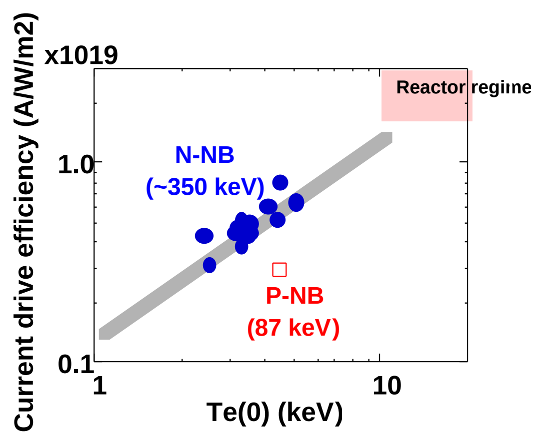

Fig.I.2.4-2 The central electron temperature Te(0) dependence of the current drive efficiency for N-NB and for P-NB.

ACCOME. Figure I.2.4-2 shows current drive efficiency as a function of central electron temperature $T_e(0)$ for N-NB (E_B=330-370 keV) and P-NB (E_B=87 keV). The electron temperature is 2-6 keV, and Z_{eff} is 2-3.5. They are obtained in the same series of N-NB current drive experiments (deuterium). The current drive efficiency for N-NB is higher than that for P-NB and increased with $T_e(0)$. Increase in current drive efficiency with higher $T_e(0)$ is due to longer slowing down time of beam ions. The central electron temperature is chosen as a representative value characterizing current drive efficiency because N-NB has central deposition. These results are consistent with the theoretical prediction that the current drive efficiency is improved with the electron temperature and the beam energy. These results indicate that current-drive capability of neutral beam can reach the value required for the fusion reactor with beam energy of 1 MeV under the typical plasma parameters on the reactor Te>10 keV and Z_{eff}~1.5.

References

[2.4-1] Oikawa T., Ushigusa K., Forest C. B., et al., “Heating and Non-inductive Current Drive by Negative-ion based NBI in JT-60U", 17th IAEA Fusion Energy Conf. (Yokohama, 1998), CD1/1.

2.5 W-shaped Divertor and SOL Plasmas

Reduction of impurity contamination in the main plasma was demonstrated in the W-shaped divertor, pumping from inner private slot (inner divertor pumping). In Nov.-Dec. 1998, outer pumping slot of the W-shaped divertor was opened to increase effective pumping speed at high density using inner and outer divertor pumping. Divertor and SOL diagnostics such as neutral pressure gauges and midplane Mach probes were implemented. Studies of SOL plasma flow along the field lines, in-out asymmetry in neutral pressure, and divertor detachment were progressed.

2.5.1 Impurity Reduction in Main Plasma with “Puff and Pump” [2.5-1]

An effect of “puff and pump” on reduction in the intrinsic carbon impurity was demonstrated using gas puffing from the plasma top and the inner divertor pumping. Experiment of the main gas puff and divertor pump (case I) has been performed in ELMy H-mode plasmas with high NB injection power of 18 MW. Results (I) were compared to cases (II) increasing inner gap (between strike point and pumping slot) to 6 cm, and (III) closing the pump shutter (stop pumping). Under the attached divertor condition, Z_{eff} was reduced to be 2.1-2.2 for the small gap case (I). The value of Z_{eff} was smaller than 2.4-2.6 for (II) and 2.6-2.8 for (III). Effect of “puff and pump” was also observed at higher n_e during the x-point MARFE. Values of Z_{eff} were maintained to be relatively small (2.2-2.4), whereas Z_{eff} increased to 2.7-2.9 for (II).

For the same n_e, brightness of CVI line at the main plasma edge was smaller than the cases (II) and (III), while brightness of CII line at the divertor chamber was similar. At the same time, large gas puff rate of 73 Pa m^3/s, which was a factor of 2 larger than case II, was required to maintain the high n_e plasma. The estimated throughput increased up to 14 % of the particle recycling in the divertor. It suggests that combination of large main gas puff and inner leg pumping with small inner gap from the pumping slot produces SOL plasma flow and improve the impurity retention in the divertor chamber.

2.5.2 Reversal of Plasma Flow with the Ion Grad-B Direction [2.5-2]

Control of the SOL plasma flow has been considered important because of its implications for helium ash exhaust and impurity retention in the divertor for long pulse operation of a tokamak reactor. SOL plasma flow was investigated at the two important locations (i.e. the outer midplane and the x-point) for the cases of normal and reversed I_p and B_t directions. For the ion grad-B drift away from the divertor (reversed B_t), the SOL plasma flew from the plasma top to the outer divertor target. On the other hand, for the ion grad-B drift towards the divertor (normal B_t), “flow reversal” occurred at the midplane, while the plasma flew from the x-point to the target plate in the divertor.

Flow reversal was also observed between ELMs in the ELMy H-mode. It disappeared in a short period of 1-2 ms just after the ELM event. Rapid formation of the flow reversal at the end of the ELM pulse was one of the evidences that the drive mechanism exists in the plasma edge.

One of the candidate mechanisms is the toroidal effect on the poloidal ion drift, which drives the parallel ion flux (“Pfirsh-Schlüter flow”) at the outer midplane. The flow direction is consistent with the measurements for three cases: (1) normal I_p and B_t directions, (2) reversal I_p and B_t directions, and (3) normal I_p and reversal B_t directions. Mach number of the “Pfirsh-Schlüter flow” was evaluated to be 0.1-0.3 using the measured T_i, E_r (= V_f+2.8T_e) and the e-folding lengths of T_i and n_e profiles. This suggests that the poloidal ion drift produces net ion flow at the main plasma edge, and the “flow reversal” at the midplane SOL would be found in toroidal plasma.

Effect of the outer divertor pumping on the SOL plasma flow at the outer midplane and divertor is investigated in the both side divertor pumping experiments in 1999.

2.5.3 In-out Asymmetry in Neutral Pressure at Private Region [2.5-3, 2.5-4]

Fast-response ionization gauges developed by the ASDEX team have been implemented in the divertor chamber (i.e. at inner and outer divertor targets, and inner, outer and top of the private dome). Asymmetry in neutral pressure at the inner and outer divertor chambers has been investigated at high density. Neutral pressure increased with increases in ion flux to the divertor target and particle recycling, and it saturated or decreased when the plasma detachment proceeded at the strike points. It was found, for the first time, that inner-divertor enhanced asymmetry in neutral pressure at the private dome changed to the outer-divertor enhanced one (for the ion grad-B drift towards the divertor). Similar behavior of in-out asymmetries in ion flux and particle recycling profiles was found at the same time, which was reported in the open divertor [2.5-5]. Asymmetry in neutral pressure was maintained and it was enhanced with an increase in n_e during the detachment and MARFE. This fact shows that the private dome can separate neutral transport between the inner and outer divertor chambers, while the in-out asymmetry might be produced by the SOL/divertor plasma transport related to the ion drift motion.

After starting the outer divertor pumping experiment (1999), neutral pressure at the onset of the x-point MARFE increased, in particular, at the outer divertor (by a factor of up to ~5) compared to that for the inner divertor pumping (1997-1998), whereas increment of p_0^{out} at the divertor detachment (inner and outer) was small (1–3). It was observed in particular for the low x-point height cases (i.e. small gap between the pumping slot and strike point). It suggests that if in-out neutral pressure ratio, p_0^{out}/p_0^{in}, is kept in wide range of 0.4–1.3 (it was larger than 0.6–0.8 for the inner divertor pumping), plasma detachment at both side divertor chambers could be sustained in a steady state operation without an appearance of the x-point MARFE. The demonstration of feedback control with an actuator of the pressure ratio in order to maintain the divertor detachment is prepared.

References

[2.5-1] Hosogane N., et al., to be published in Nucl. Fusion (1999).

[2.5-2] Asakura N., et al., to be published in Nucl. Fusion (1999).

[2.5-3] Tamai H., et al., J. Plasma Fusion Res. 74, 1336 (1999).

[2.5-4] Tamai H., et al., to be published in Eur. Phys. Soc. Conf. (1999).

[2.5-5] Asakura N., et al., Nucl. Fusion 36, 795 (1996).

2.6 Particle Transport and Control with the W-shaped Divertor

2.6.1 Particle Confinement and Density Controllability [2.6-1, 2]

A new scaling law for the ion number in the main plasmas was proposed for ELMy H-mode discharges. We assumed two particle confinement times; one was for the particles supplied by NBI (center fuelling) and the other was for those supplied by recycling and gas-puffing (edge fuelling). The confinement time for the center fuelling increased and that for the edge fuelling decreased, as the electron density increased. The both confinement times increased with plasma current and toroidal magnetic field. They decreased rapidly, as the input power increased. The scaling was compared with data obtained in high β_p ELMy H-mode and reversed shear plasmas. In some reversed shear plasmas, the particle confinement seemed to be enhanced by a factor of two compared with the scaling. Density controllability was discussed based on the scaling, and it was found that additional fuelling with a confinement time of 0.1-0.4 s was necessary for the density control in the ELMy H-mode plasmas.

2.6.2 Helium Removal from Reversed Shear Plasmas [2.6-3]

Helium exhaust characteristics in reversed shear plasmas has been studied using a short-pulsed helium gas puff. The residence time of helium particles inside the ITB (Internal Transport Barrier) was 1.9 times as long as that outside the ITB. Assuming that the local τ^*_{He} equals the decay time of the helium density inside the ITB, we estimated that τ^*_{He}/τ_E was 8 - 10 and it was within the range expected for future fusion reactors. However, the helium exhaust efficiency depended on strength of the ITB. In the case the ITB was strong, the central electron density increased with time and then partial or major collapse occurred because of MHD instability. In such cases, pressure gradient at the ITB position was steep and the helium particle confinement was enhanced. Then, helium removal from the inside of the ITB was difficult.

2.6.3 Dome Effect on Carbon Impurity Transport [2.6-4, 5]

From simulation using an impurity transport code (IMPMC) [2.6-6], it was predicted that the dome in the private flux region prevents the upstream transport of hydrocarbon impurity produced by chemical sputtering. Intensity profile of a CD-band in the divertor region was observed and analyzed in order to investigate the dome effect on the carbon impurity transport. Profiles of the CD-band intensity in the new W-shaped and previous open divertor are shown in Fig.I.2.6-1. The intensity around the X-point in the W-shaped divertor is obviously lower than that in the open divertor. The observed profile was reproduced using the impurity transport code. The results suggest that the dome works to prevent hydrocarbon impurity invading the upstream as predicted.

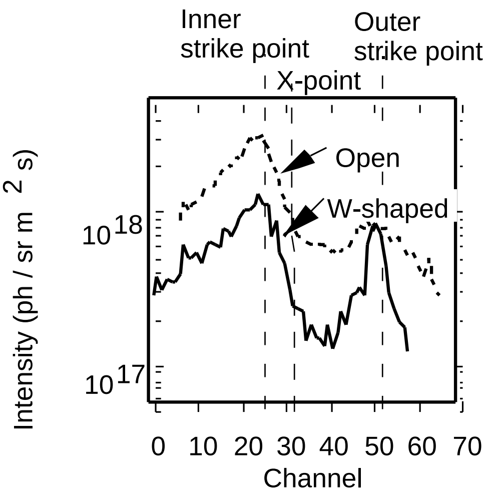

Fig. I.2.6-1. Profiles of the CD-band intensity in the W-shaped and open divertors

2.6.4 Impurity Transport in Reversed Shear and ELMy H-mode Plasmas [2.6-7]

Particle transport was investigated for several impurity species in reversed shear and ELMy H-mode plasmas. In the reversed shear plasmas, the particle diffusivity was significantly reduced in the internal transport barrier. It was almost the same level for helium, carbon and neon. In contrast, the inward pinch velocity seemed to be large for high-Z species in the internal transport barrier. On the other hand, in the ELMy H-mode plasmas, the particle diffusivity was also the same for helium and neon, and an increase in the inward pinch velocity for high-Z species was not observed.

References
[2.6-1] Takenaga H., Nagashima K., Sakasai A., et al., 17th IAEA Fusion Energy Conference, Yokohama 1998.
[2.6-2] Takenaga H., Nagashima K., Sakasai A., et al., to be published in Nuclear Fusion.
[2.6-3] Sakasai A., Takenaga H., Hosogane N., et al., 17th IAEA Fusion Energy Conference, Yokohama 1998.
[2.6-4] Hosogane N., Kubo H., Higashijima S., et al., 17th IAEA Fusion Energy Conference, Yokohama 1998.
[2.6-5] Higashjima S., Kubo H., Sugie T., et al., J. Nucl. Mater. **266-269**, 1078 (1999).
[2.6-6] Shimizu K., Takizuka T., Sakasai A., J. Nucl. Mater. **241-243**, 167 (1997).
[2.6-7] Takenaga H., Sakasai A., Koide Y., et al., submitted in Journal of Plasma and Fusion Research.

2. 7 Fast Ions and Alfvén Eigenmodes

The Alfvén eigenmodes (AEs) were studied with the negative-ion-based neutral beam (NNB) injection into weak or reversed magnetic shear plasmas. The Toroidicity-induced Alfvén eigenmodes (TAEs) were observed in weak shear plasmas with $<\beta_h> \geq 0.1$ % and $0.4 \leq v_{b||}/v_A \leq 1$. Here, $<\beta_h>$ is the volume-averaged beta value of energetic ions, $v_{b||}$ is the beam speed in the toroidal direction and v_A is the Alfvén speed. The excitation and stabilization of TAEs is consistent with predictions by the NOVA-K code (PPPL). New burst modes and chirping modes were observed at higher beta of $<\beta_h> \geq 0.2$ %. A few percent drop in the neutron emission rate was observed correlating with the burst modes. In the strongly-reversed shear plasma with the ITB, AEs were suppressed due to the misalignment of the AE gap and/or the low pressure gradient and low fast ion beta in the low shear region [2.7-1, 2]. The TAEs and high frequency modes observed in ICRF-heated low-q discharges were analyzed in detail using the NOVA-K code. The TAE frequency change being called "chirping" observed before the sawtooth crash during the ion cyclotron range of frequency ($2\omega_{CH}$ ICRF) heating of low-q plasmas has been simulated well. The frequency chirping is caused by a small change in the safety factor profile in the core region of the plasma. The NOVA-K code simulation suggests that frequency chirping occurs mixing of the global and core localized TAE [2.7-3]. It was shown that high frequency modes observed after the sawtooth crash were the Ellipticity-induced Alfvén Eigenmodes (EAEs) excited at the q=1 surface. The EAEs were stabilized with the NNB. The stability analysis using the NOVA-K code suggested that the stabilization mechanism was beam ion Landau damping [2.7-4].

Ripple loss of energetic alpha particles and neutral beam ions was calculated for reversed shear (R/S) discharges in ITER-FDR (Final Design Report) using the orbit following Monte-Carlo code (OFMC code). The result indicates that, compared with the normal operation with positive shear (P/S), the R/S operation drastically enhances the ripple loss. The ripple loss can reach 25 % for alpha particles and 20 % for neutral beam ions. The calculation also suggests that the toroidal field ripple in a fusion reactor should be designed to be less than 0.6 % at the plasma surface. Ferritic steel insert to the vacuum vessel is a probable solution to reduce the ripple to an allowable level in the ITER-FDR design [2.7-5]. Characteristics of energetic ion tail formation and confinement of tail ions in ICRF-heated R/S plasmas on JT-60 were investigated with the

OFMC code. Because of the enhanced banana diffusion and large orbit side in the R/S plasma, a scale length of pressure profile in the R/S plasma is large enough to compensates lower density of tail ions than that in the positive shear plasma, which enables to contain the stored energy comparable to that in the P/S plasmas [2.7-6].

References

[2.7-1] Kusama Y. and the JT-60 Team, Phys. Plasma, **6**, 1935 (1999).

[2.7-2] Kusama Y., Kramer G. J., Kimura H., et al., "Characteristics of NNB-driven Alfvén eigenmodes, burst modes and chirping modes in the Alfvén frequency range in JT-60U", to be published in Nucl. Fusion.

[2.7-3] Kramer G. J., Cheng C. Z., Fu G. Y., et al., "Frequency chirping of core localized Toroidicity induced Alfvén eigenmodes and their coupling to global Alfvén eigenmodes", submitted to Phys. Rev. Lett.

[2.7-4] Kusama Y., Fu G. Y., Kramer G. J., et al., "Destabilization of ellipticity-induced Alfvén eigenmodes during ICRF heating and stabilization by negative-ion-based neutral beam injection in JT-60U", submitted to Plasma Phys. Control. Fusion.

[2.7-5] Tobita K., Hamamatsu K., Takizuka T., et al., J. Plasma and Fusion Research, Phys. Plasma, **75**, 582 (1999) (in Japanese).

[2.7-6] Kusama Y., Kimura H., Nemoto M., et al., "Production and confinement characteristics of ICRF-accelerated energetic ions in JT-60U negative-shear plasmas", to be published in Plasma Phys. Control. Fusion.

2.8 Plasma Control and Disruption

2.8.1 Active Feedback Control for Steady State Improved Confinement [2.8-1]

Real-time feedback control of line integrated electron density was routinely employed for the reliable production of the internal transport barrier (ITB) in reversed magnetic shear plasmas. As to the MHD stability control, feedback technique of the DD neutron emission rate was adopted. In accordance, the equivalent DT fusion gain of 1.25 was achieved. In order to extend the period of improved fusion performance in reversed magnetic shear plasmas, feedback control of the DD neutron emission rate was first performed. The sustainment of ITB was hereupon achieved for 4.3 s with the H-factor of 1.7 and β_N of 1.5. Investigations on the simultaneous feedback control of three parameters were undertaken in ELMy H-mode discharges. They were (1) the line integrated electron density, (2) the DD neutron emission rate and (3) the divertor radiation power fraction compared with the NB heating power. The contributions of individual actuators to each control variable were resolved in a quantitative manner.

2.8.2 Generation and Termination of Runaway Electrons [2.8.2]

Disrupted discharges in JT-60 have been investigated in order to clarify necessary conditions for avoiding runaway electrons generation. It has been found that runaway electrons are not observed for low B_T (<2.2 T) or low plasma current quench rate (I_γ=-($dI_p/dt)/I_p$) of < 50 s^{-1} and low effective safety factor at the plasma edge of < 2.5. On the other hand, in controlled disruptions with small plasma shifts (stationary shutdown), q_{eff} easily increases above 8, and runaway electrons are observed even for low current quench rates of 50-100 s^{-1}. Furthermore, it has been found that in these controlled disruptions the runaway current tail can gradually decay even for zero or weakly positive plasma surface voltages. These observations of the avoidance and termination of runaway electrons suggest some anomalous loss mechanisms for runaway electrons.

2.8.3 Characteristics of Halo Currents [2.8-3]

Halo currents and their toroidal peaking factor (TPF) have been measured in JT-60 by Rogowski coil type halo current sensors. The maximum TPF*Ih/Ip0 was 0.52 in the operational range of I_p = 0.7 ~ 1.8 MA, B_T = 2.2 ~ 3.5 T, including ITER-EDA design parameters of $\kappa > 1.6$ and $q_{95} = 3$, which was lower than that of the maximum value of ITER database (0.75). The magnitude of halo currents tended to decrease with the increase in stored energy just before the energy quench and with the line integrated electron density at the time of the maximum halo current. A discharge termination technique without a shift of a plasma current channel was useful to avoid halo current generation.

References

[2.8-1] Fukuda T. and the JT-60 team, Fusion Eng. Des. **38** (1999), in print.
[2.8-2] Yoshino R., Tokuda S., Kawano Y., Nucl. Fusion, **39**, 151 (1999).
[2.8-3] Neyatani Y., Yoshino R., Nakamura Y., et al., Nucl. Fusion, **39**, 559 (1999).

3. Design Progress of the JT-60SU

3.1 Basic Design for Compact Type of JT-60SU

In the fiscal year of 1998, the design study of a superconducting tokamak machine JT-60SU (Super Upgrade) was continued. The device size was changed to a compact type compared to the last five fiscal years. The major radius R_p is 3.9 m, the minor radius a is 0.98 m, the toroidal field B_T is 5.8 T and the maximum plasma current I_p is 8 MA. The objective of the compact design was to enhance the technical design margin and to reduce the production cost. An option of DT operation with Q_{DT}~5 was excluded for the cost reduction. An advanced operation scenario of a reversed shear mode was involved and the technical assessment was conducted.

JT-60SU compact has 18 toroidal field (TF) coils and the superconductor was planned to be $(NbTi)_3Sn$. However, Nb_3Al conductor could be adopted, if the manufacturing cost was reduced to that of $(NbTi)_3Sn$. The up-down symmetric vacuum vessel with 18 horizontal, 18 oblique and 18 vertical ports was employed for JT-60SU compact. As the material of the vacuum vessel, low Co concentration (0.05 %) 316SS with tungsten coating was a first candidate, but the usage of Ti-6Al-4Vi and Ti-Al alloy were also studied. For all cases, it was indicated that the nuclear heating in the TF coils and the radiation dose rate were less than the design guideline values. In these analyses, the conditions to reduce the radiation dose rate were as follows: (a) the TF coils are connected with shear panel each other, and (b) cooling water containing boron (several %) is filled up or (c) high Mn steel plates are inserted in the vacuum vessel boards. The poloidal field (PF) coils consists of 6 central solenoid pieces (CS) and 6 outer equilibrium field (EF) coils, and the superconductors for CS and EF coils are of $(NbTi)_3Sn$ and NbTi, respectively. The PF coil system was designed to excite independently for each coil and produce a wide variety of plasma shaping (elongation κ_X up to 2.0 and triangularity δ_X up to 0.8) in order to improve the β-limit in the steady state operation scenario. To obtain high triangularity, the double-null divertor configuration with the up-down symmetry exhaust ports, total 8 oblique ports, was employed. The schematic drawing of JT-60SU compact device is shown in Fig.I.3.1-1, where the inner diameter and the height of the cryostat is 21.5 m and 12 m, respectively.

As an advanced operation scenario, the reversed shear operation was considered in addition to the ordinaly high li and hot ion mode operation, which was considered in the last fiscal years. To realize the stable steady-state reversed shear operation, however, it was necessary to make the reversed shear configuration from the plasma initiation phase, and the raising time (t = 0.02 ~ 0.2 s) of the plasma current just after break down of the plasma should be shorter than the current penetration time. If the equilibrium of circular plasma cross section was applied to small plasma at the initiation phase, the high voltage above the limited value was required for the divertor coil system. To avoid the high voltage limit, it was suggested that the equilibrium with an elliptic cross section of the reversed shear operation should be applied. To confirm the vertical positional stability, the up-down symmetry baffle plate was adopted. The values of growth rate and stability margin were improved from 45 Hz to 22 Hz and 0.68 to 1.46, respectively, with two baffle plates of 20 mm thickness SUS316. These improved values satisfied the conditions of the JT-60SU design guideline.

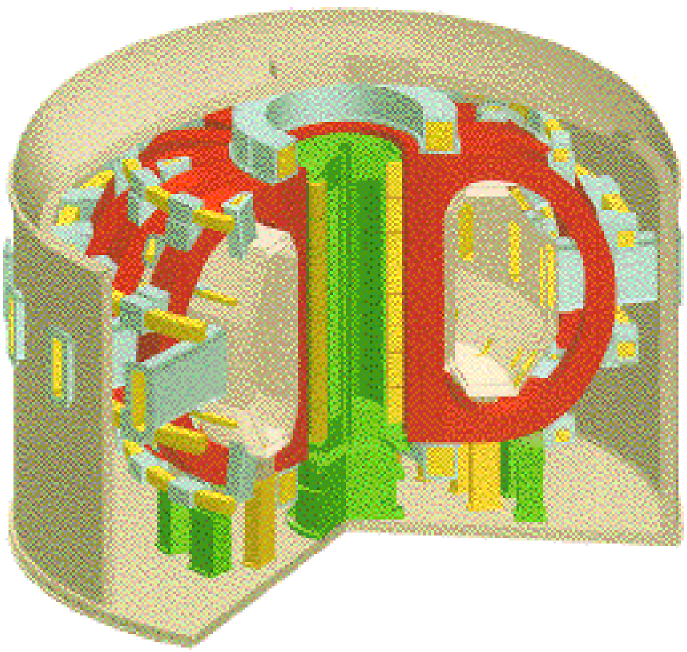

Fig.I.3.1-1 Schematic drawing of JT-60SU Compact

3.2 JT-60SU Divertor and ECH Transmission System Conceptual Design

An up/down symmetric double-null divertor for highly triangular elongated double-null plasma operation on JT-60SU (R_p = 5.0 m, a = 1.5 m, I_P = 10 MA, BT = 6.25 T, κ = 2.0, δ = 0.63) was conceptually designed. A tightly baffled arrangement was produced using contoured plasma facing surfaces. The divertor shape was designed to fit equilibrium produced using the EFIT code. A simplified component-mounting scheme was adopted to the new double-null JT-60SU divertor geometry and halo current loads. The simulations showed that JT-60SU could produce a peak axisymmetric halo current fraction $I_{h(pol)}/I_{p0}$ ~ 0.47 in the case of post-thermal quench core and the halo temperature of 25 eV for an equilibrium with initial growth rate of γZ = 50 rad/s. Stress analyses of support concepts for the divertor were performed for the calculated halo current loads. The peak heat flux was significantly reduced (~2 times) in both standard single-null and double-null options, as compared with an original “flat” divertor option in the previous design. A thermal analysis of the JT-60SU divertor was performed. The power flow and heat fluxes were based on the assumption that input power is 80 MW and 50 % of this power is radiated. A slantblock design with a block width of 30 mm and a flow channel diameter of 15 mm was used in this analysis. Based on the heat fluxes and geometry, a cooling water flow velocity of 7 m/s was found to be sufficient to keep the surface temperature of the CFC below 1000 °C and to provide a safety factor of 2 for the critical heat flux. The total flow required was 1500 l/s.

The previously designed ECH transmission system of JT-60SU (the waveguide transmission system and the antenna design) was reviewed. The performance and cooling of waveguide components with an inner diameter of 31.75 mm were adequate for 1000 s operation. A small increase of the waveguide diameter would achieve a greater safety margin for cooling. Certain guidelines for an alignment of the waveguides were provided that most of the waveguide supports should not be rigidly tied to the waveguides and miter bends and adjacent waveguides should not be rigidly tied to supports. For the antennas, the beam spreading by local shaping of a secondary mirror (M2) was reduced with a moderate mirror curvature for focusing the centers of all the beams. Steering by rotating M2 instead of a primary mirror (M1) to reduce maintenance and improve reliability was suggested.

References

[3.2-1] Baxi C.B., Doane J.L., Friend M.E. et al., GA Report GA-C23110 (1999).

II. JFT-2M PROGRAM

JFT-2M carries out advanced and basic research for the development of high-performance plasmas for nuclear fusion, making use of the mobility of a medium-sized device. Both domestic and international cooperations are intensively utilized. In FY 1998, following subjects were mainly pursued. For the core plasma research, the confinement study with a heavy ion beam probe (HIBP) in collaboration with National Institute for Fusion Science (NIFS) and the electron cyclotron current drive experiment were carried out. For the peripheral plasma research, the closed divertor and the compact toroid injection for the development of advanced fuelling were investigated. The latter was done in collaboration with the Himeji Institute of Technology and NIFS. Design and preparation for the Advanced Material Tokamak EXperiment (AMTEX) were also carried out. Main results are as follows: (1) A fast change of the electric potential distribution at the L/H transition was measured directly for the first time with the HIBP. (2) Electron cyclotron current drive was confirmed. It appeared that no difference on the suppression of the tearing mode by the co-direction and the counter direction current drive. (3) Low temperature and high density divertor plasma, and high confinement performance were maintained by the closed divertor. (4) Fuelling by the compact toroid injection to a central part of the high power NBI-heated plasma (H-mode) was demonstrated for the first time. (5) Optimized design for the ripple reduction by the ferritic board installation outside the vacuum vessel was established.

The operation in FY 1998 started from April 1998. In October 1998, the baffle plates for the closed divertor were removed according to the AMTEX plan. Operation was resumed in December and continued to January 1999, producing 1730 plasma discharges. During February and March 1999, ferritic boards were installed outside the vacuum vessel. Check and maintenance work in the heating and power supply systems were also completed in that period.

1. Core Plasma Research

1.1 H-mode Study with Heavy Ion Beam Probe Measurement [1.1-1]

It has been claimed experimentally and theoretically that the radial electric field plays key roles for causing the L/H transition. So far the highly time-resolved and direct measurement of the potential has not been performed. The heavy ion beam probe is particularly suited for fast and the local measurement of the plasma potential. In order to study the physics of L/H transition, we installed a 500 keV heavy ion beam probe on the JFT-2M under collaboration program between NIFS and JAERI. The local plasma potential can be obtained by the measurement of the change of the secondary beam energy generated at the sample volume. Figure II.1.1-1 shows the rapid change of the potential at L/H transition triggered by a sawtooth. The potential changes positively by the sawtooth heat pulse in coincidence with the fast D_α rise. After that, it shows that a very rapid drop (~100 V / 10 μsec) of the potential together with a drop of the fluctuation in the secondary beam intensity and the magnetic field of dB_θ/dt. They seem to occur simultaneously. The potential goes down further to about -300 V with its time constant of a few hundred micro-second together with the fall of D_α. We can not conclude the causality clearly, but the results suggest an important role of the change of the potential at L/H transition.

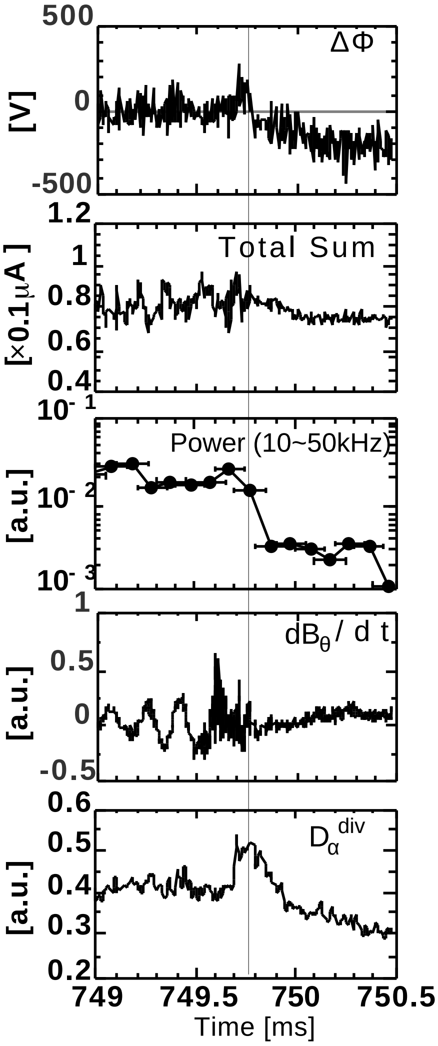

Figure II.1.1-1. Fast time behaviors at the L/H transition. The plasma potential(ΔΦ), the secondary beam intensity (Total Sum), the power of the fluctuation in the beam intensity integrated from 10 to 50kHz when the sample volume is placed around the separatrix, the magnetic probe signal of dB_θ/dt and D_α intensity.

Reference

[1.1-1] Hamada Y., Ido T., Kamiya K., et al., "Fast Potential Changes at H-mode Transition in the JFT-2M Tokamak", to be published in Proc. of 17th IAEA. Conf. on Fusion Energy (Yokohama, 1998), postdeadline paper.

1.2 Electron Cyclotron Current Drive and Disruption Control

The effect of the Electron Cyclotron Heating (ECH) or EC Current Drive (ECCD) on the m/n=2/1 tearing mode [1.2-1] was investigated using the co-injection and the counter-injection of the electron cyclotron waves by using the new variable $k_{//}$ antenna [1.2-2]. The tearing mode is the cause of the mode lock disruption. The injection angle of the rf beam (f=59.8 GHz, fundamental O-mode, 170 kW, 0.1 s) was varied toroidally shot by shot from –25˚C to +25˚C from the perpendicular direction to see the effect of the co-drive or the counter drive for suppression of the tearing mode with a single null divertor configuration of the JFT-2M tokamak. Experiments always showed a larger loop voltage drop in the co-drive case than in the counter drive case (both for the clock-wise direction and the counter-clock-wise direction of the plasma current). The estimated driven current was ~6 kA (n_e=1x10^{19} m^{-3}) in the center resonance condition (B_T=2.15 T, I_P=0.14 MA). We investigated the ECCD (at the island center) effect on the tearing mode (B_T =1.82 T, I_P=0.23 MA) and found that even the counter drive suppresses the tearing mode as well as the co-drive. The mode amplitude decreased to 1/2, and the mode frequency increased

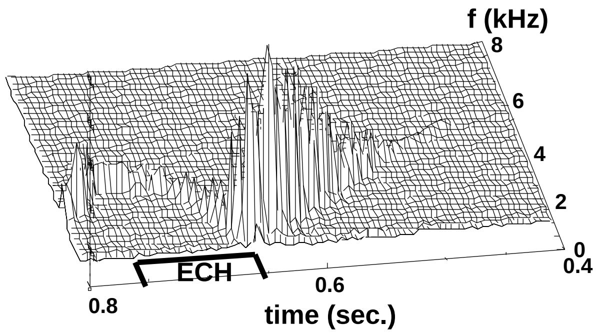

Fig.II.1.2-1 Magnetic power spectrum of the m=2 mode, B_T=1.82 T, Injection angle=25°, Counter-drive case.

from 1.2 kHz to 3.5 kHz due to the decrease of the island width as shown in Fig. II.1.2-1. No drive case (perpendicular injection) brought the same result. These facts indicate that the present effective suppression is mainly brought about by heating and not by ECCD [1.2-2].

References

[1.2-1] Hoshino K., et al., Phys. Rev. Lett. 69, 2208 (1992); Hoshino K., et al., AIP Conf. Proc. **289**, Radio Frequency Power in Plasmas (1993, Boston), 149 (1994).

[1.2-2] Hoshino K., Takahashi K., Bull. Ame. Phys. Soc. **43**, 1932 (1998).

2. Peripheral Plasma Research

2.1 Compatibility of Dense and Cold Divertor Plasma with Improved Confinement [2.1-1]

A study of the closed divertor has been carried out in JFT-2M with the aim of making a dense and cold divertor, compatible with high core confinement. Introducing a gas-puff into the divertor chamber, the baffling effect of the closed configuration is revealed by enhanced radiation loss localization and high neutral pressure in the divertor region, lower core fueling and the sustainment of energy confinement quality. The baffling effect is also enhanced significantly with the ExB flow and/or the current in the SOL by applying divertor biasing. A dense and cold divertor plasma up to n_e^{div}~$4\mathrm{x}10^{19}$ m^{-3} and T_e^{div}~4 eV together with the improved confinement modes up to $\bar{n}_e/n_e^G$~0.7 can be brought by a strong gas-puffing as shown in Fig.II.2.1-1(a) and (b). The strong gas-puffing to an ELM free H-mode plasma led to the second transition to improved L-mode (IL-mode). H-factors of the ELM free H-mode and the IL-mode (without sawtooth) only degrade at their highest densities corresponding to an abrupt increase in the radiation loss over the critical value of R_p^{crit}~0.7 in the main plasma, which was caused by impurity accumulation. However, the IL-

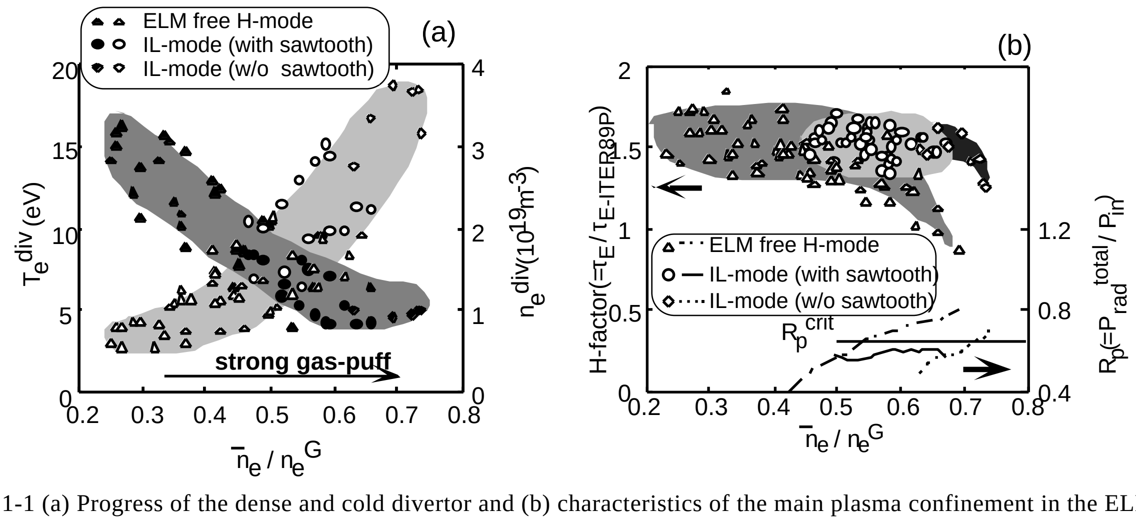

Fig.II.2.1-1 (a) Progress of the dense and cold divertor and (b) characteristics of the main plasma confinement in the ELM free H-mode, IL-mode (with sawtooth) and IL-mode (w/o sawtooth), when the main plasma density normalized by the Greenwald density limit n_e^G is increased by gas-puffing in the closed divertor chamber. Variation of R_p (ratio of P_{rad}^{total} to input power P_{in}) in a discharge which reaches the highest density of each mode is also shown as a function of $\bar{n}_e/n_e^G$ in (b).

mode (with sawtooth) keeps a low radiation loss below R_p^{crit} and has favorable features for realizing steady-state high performance at high density. The UEDA-code simulations also show that the baffle plates produce a strong neutral buildup and the dense and cold state in the divertor chamber.

Reference

[2.1-1] Kawashima H., Sengoku S., Ogawa T., et al., “Study of a Closed Divertor with Strong Gas puffing on JFT-2M”, to be published in Proc. of 17th IAEA. Conf. on Fusion Energy (Yokohama, 1998), paper IAEA-F1-CN-69/EX3/4.

2.2 Compact Toroid Injection [2.2-1]

A dense and fast compact toroid (CT) injection is expected to be a core fueling method for a fusion reactor. The CT injection experiments in NBI heated plasmas including H-mode have been carried out in the JFT-2M tokamak. It was demonstrated for the first time that the CT penetrates into the core region of the H-mode plasma heated by 1.2 MW NBI with a rapid increase in the electron density at B_T =0.8 T. Asymmetric radial profile of the soft X-ray emission indicates the CT penetration into the core plasma, while partial penetration in the peripheral region was observed at B_T=1.3T. Incremental fractions of the soft X-ray intensity of the central chord and increasing rates of the line averaged electron density due to the CT injection becomes larger with deeper penetration of CTs. We observed the largest increase of the line-averaged electron density of 0.8×10^{19} m^{-3} at a rate of 1.2×10^{22} m^{-3}/s with the CT injection in an ohmic discharge at B_T =0.8 T so far.

Reference

[2.2-1] Ogawa T., Fukumoto N., Nagata M., et al., “Compact Toroid Injection Experiment in JFT-2M”, to be published in Proc. of 17th IAEA. Conf. on Fusion Energy (Yokohama, 1998), paper IAEA-F1-CN-69/EX1/16.

3. Advanced Material Tokamak Experiment (AMTEX) Program

3.1 Preparation for Ripple Reduction Testing with Ferritic Inserts

The negative magnetic shear configuration provides a prospect toward the steady-state tokamak operation. However, negative shear experiments in JT-60U showed an enhanced loss of ripple trapped fast ions [3.1-1]. Therefore, it is one of the most important issues to reduce the loss of fast ions for the steady state operation. In ITER, it is planned to use ferritic steel to reduce the toroidal field ripple (to reduce fast ion losses) [3.1-2]. In JFT-2M, ferritic boards (FB) were inserted between the present vacuum vessel (VV) and the toroidal field coils (TFCs) for the first time in the world in order to test reduction of the toroidal field ripple and the fast ion ripple losses. In order to reduce the fast ion losses, the ripple amplitude and its toroidal mode number have to be reduced [3.1-3, 3.1-4]. The guideline of the design to reduce the fundamental and the higher toroidal mode in the case of ferritic steel insertion is as follows: wider and thicker ferritic board should be positioned far from plasma, but inside the TFCs.   A conceptual drawing of the ferritic board insertion on JFT-2M and a photograph of one of the ferritic board set is shown in Fig.II.3.1-1. Since its effect is not linear, its optimized thickness depends on the magnetic field.   It is designed to consist of elements of 8mm thickness so that its total thickness can be changed by adjusting the number of elements.   Measurements of fast ion losses without FB insertion were carried out before installation of FB.

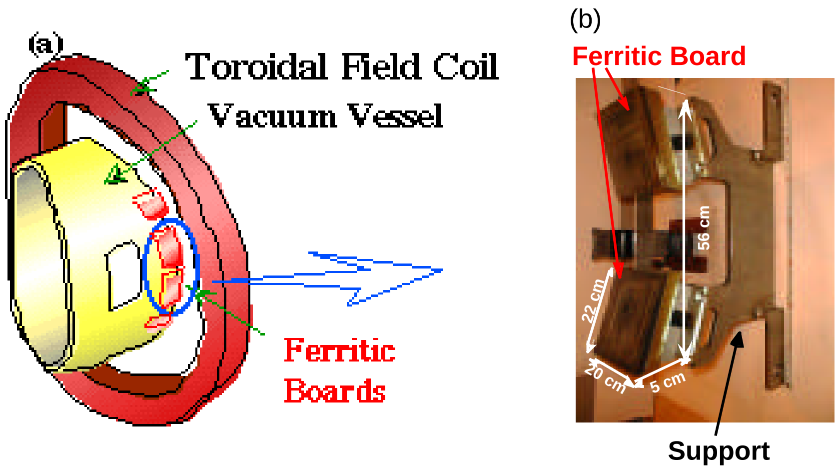

Fig.II.3.1-1   (a) Conceptual drawing of the ferritic board insertion on JFT-2M,
(b) Photograph of one of the ferritic board set.

Increments of wall temperature due to the ripple ion losses were observed between the TFCs by an infrared camera during tangential NBI heating.   Both ripple trapped ion losses and banana drift loss ions were observed at the wall of the shoulder part and the mid plane part, respectively.

References

[3.1-1] Tobita K., et. al., Proc.16th Int. Conf. on Fusion Energy, (Montreal, 1996) Vol. I, 497 (1997).
[3.1-2] Ioki K., et al., J. Nucl. Matter. **258-263**, 74 (1998).
[3.1-3] Sato M., Miura Y., Kimura H., et al., Proc. of 20th SOFT, (Marseille,1998) 545 (1998).

3.2 Design of Ferritic Vacuum Vessel [3.2-1]

The ferritic steel is proposed for the structural material of blankets in SSTR and the advanced SSTR (A-SSTR).   However, the error fields due to the ferromagnetism of the ferritic steel may affect the stability and confinement of high performance plasma.   To clarify these issues, the present VV will be replaced with a ferritic VV in the second phase of AMTEX and compatibility between plasma performance and ferritic steel will be tested.   Design study on the ferritic VV (20 mm in thickness) was carried out and following results were obtained; (i) For the plasma equilibrium, effects of a ferritic VV are small because the ferritic steel saturates easily by the toroidal magnetic field and its relative magnetic permeability is around two.   (ii) Mechanical analyses of the ferritic VV indicate that the maximum induced stress (60 MPa) with the electromagnetic force due to the disruption is much smaller than the critical stress (325 MPa).

Reference

[3.2-1] Sato M., Miura Y., Kimura H., et al., J Plasma & Fusion Research, **75**, 741 (1999).

4. Operation and Maintenance

4.1 Tokamak Machine

A drop of ground insulation resistance of the vacuum vessel at temperatures around 80˚C had been always observed during the baking of the vacuum vessel. The cause of the insulation deterioration was thoroughly inspected during the vent for the installation of diagnostic instruments in March 1999. Contact of a thermocouple wire and a cable connector of the gas-puffing system with a structure electrically connected to the ground was found, and contact between a lead wire of the baking heater and a structure electrically connected to the ground was also detected. These failures were completely fixed.

In the compact toroid (CT) injection system, a transformer was installed to reduce the noise in the low-voltage power supply and the baking system was improved. A CO_2-based fire extinguisher was newly introduced for safety. A new electrode was also introduced to improve the performance of the CT system.

An infrared TV temperature measurement system was also installed for the detecting the ripple loss of fast ions before and after the installation of the ferritic board on JFT-2M.

4.2 Neutral Beam Injection System and Radio-Frequency Heating System

The neutral beam injection (NBI) system and the electron cyclotron resonance heating (ECH) system were operated fairly smoothly and were fully utilized for the experiments. In the annual maintenance of the NBI system, the residual-gas monitoring system was serviced. The renewal was also made of the optical transmitters in the retarding power supply, the storage batteries for the control system and the water pumps in the cooling system. In the ECH system, an intensive aging was carried out to prolong the injection time after the annual maintenance of the system including the transmission system.

4.3 Power Supply System

In the operation for the magnetic field measurement before and after the installation of the ferritic steel boards (in January and March 1999), the motor generators (MGs) #2 and #1 for the toroidal field coils were halted due to the flashover of the commutator, respectively. The flashover of MG #2 occurred due to copper drags of the commutator and that of MG #1 was caused by dusts stuck on the commutator. To overcome these problems, at first, the material of the carbon brushes was changed from greasy fumes to coke, and resistance to arcs and the contact of brush were improved. Filters will be installed in the air inlet of each motor generator to reduce the dusts.

III. THEORY AND ANALYSIS

The principal objective of theoretical and analytical studies is to improve the understanding of physics of tokamak plasmas. Remarkable progress was made on the physical understanding of transport phenomena such the internal transport barrier in JT-60U in connection with radial electric field. Progress was also made on the study of stability such as the neoclassical tearing mode and the double tearing. As for divertor plasma, the importance of the thermoelectric instability was shown by using the five point model. The NEXT (Numerical EXperiment of Tokamak) project has been progressed since 1996 in order to research complex physical processes in core plasmas, such as transport and MHD, and in divertor plasma by using recently advanced computer resources.

1. Confinement and Transport

In order to understand the physical mechanism forming the discontinuity of the global drift wave structure near the minimum-q surface, a possible explanation based on the separate structure of sheared slab η_i mode near the minimum-q surface has been presented [1-1]. The discontinuity condition was approximately estimated and effects of both the poloidal rotation and the diamagnetic rotation shears were also discussed. Calculation results have a good agreement with the observations in the simulation and suggested that the discontinuous structure of the global drift wave may originate from the excitation of the sheared slab η_i mode near the minimum-q surface for the flat q-profile.

The global confinement and the local transport properties of improved core confinement plasmas in JT-60U have been studied in connection with E_r shear formation [1-2]. The improved core confinement mode with ITB, the internal transport barrier, is roughly classified into "parabolic" type ITBs and "box" type ITBs (see Fig.III.1-1). In the parabolic type ITB, the gradient of temperature and density change drastically at $r=r_{ITB}$. The temperature and density profiles in the core region $r<r_{ITB}$ are much more peaked than those of peripheral region $r>r_{ITB}$. The parabolic type ITB has the reduced thermal diffusivity, χ, in the core region; however, the E_r shear, dE_r/dr, is not so strong. In the parabolic type ITB, the thin ITB layer within which the temperature and density gradient is very large appears around $r=r_{ITB}$. The width of ITB layer is approximately several times larger than that of ion poloidal Larmor radius. The box type ITB has a very strong E_r shear at the ITB layer and the χ value decreases to the level of neoclassical transport there. The estimated ExB shearing rate, ω_{ExB}, becomes almost the same as the linear growth rate of the drift microinstability, γ_L, at the ITB layer in the box type ITB. Experiments of hot ion mode plasmas during the repetitive L-H-L transition shows that the thermal diffusivity clearly depends on the E_r shear and the strong E_r shear contributes to the reduced thermal diffusivity.

Two different transport models, CPT model (canonical profile transport model) [1-3] and SET model (semi empirical transport model), are applied to the JT-60 plasmas [1-4]. The CPT model predicts the bifurcation of the heat flux and the appearance of the ITB layer. The SET model reasonably reproduces the temperature and density profiles of the L-mode and H-mode discharges in JT-60 in a wide range of plasma parameters in the normal shear regime. In the reversed shear regime, the SET model does not describe the steep density and temperature gradient within the ITB layer.

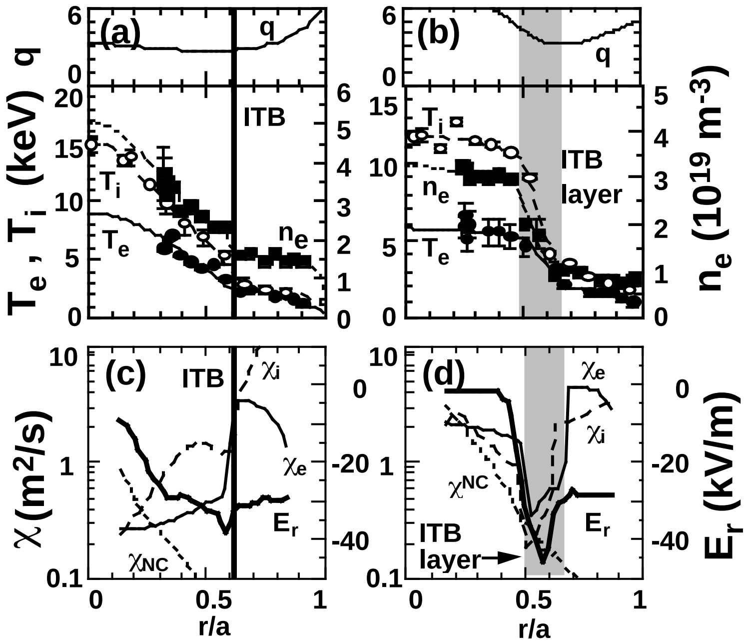

Fig.III.1-1 Profiles of safety factor, q, electron temperature, Te, ion temperature, Ti, and electron density in (a) "parabolic type ITB and (b) "box" type ITB. Profiles of experimentally evaluated electron and ion thermal diffusivity, χe and χi, neoclassical ion thermal diffusivity, χNC, and radial electric field in (c) "parabolic type ITB and (d) "box" type ITB. (c) and (d) correspond to (a) and (b), respectively (ref.[1-2]).

References

[1-1] Li J., et al., "Sheared Slab Instability in Tokamak Plasma with Negative Magnetic Shear", Phys. Plasmas **5**, 959 (1998).

[1-2] Shirai H. and JT-60 team, "Reduced Transport and Er Shearing in Improved Confinement Regimes in JT-60U", in Proc. 17th IAEA Fusion Energy Conference (Yokohama, 1998), IAEA-F1-CN-69/EX5/4: to be published in Nucl. Fusion 1999.

[1-3] Dnestrovskij Yu N., Lysenko S.E., Tarasyan K.N., "Improved Confinement Regimes within the Transport Model of Canonical Profiles", Nucl. Fusion **35**, 1047 (1995).

[1-4] Dnestrovskij Yu N., Lysenko S.E., (Polevoi A.R.), et al., "Test of Canonical Profiles and Semi Empirical Transport Models against JT-60U Plasmas", in Proc. 17th IAEA Fusion Energy Conference (Yokohama, 1998), IAEA-F1-CN-69/THP2/17: to be published in Nucl. Fusion 1999.

2. Stability

The linear and nonlinear features of a double tearing mode are investigated. The linear growth rate on resistivity η shows $\gamma \sim \eta^{1/3}$ for small Δr, a radial distance of two rational surfaces. As Δr increases, the exponent changes from 1/3 to 3/5. The nonlinear study shows that a double tearing mode grows with a linear growth rate and causes a crash when Δr is small. When Δr is large, two islands saturate in the final stage. However, in the intermediate value of Δr, a double tearing mode looks as if it becomes a saturated state once. After a long time it is destabilized nonlinearly by the interaction of two islands and causes the flattening. The phase diagrams for the double tearing mode are also obtained [2-1]. For weakly reversal case, usual tearing mode is possibly unstable and saturated with a finite island size. For strongly reversal case, a tearing mode with a resonant surface in the negative shear region or a double tearing mode becomes linearly unstable. For moderately reversal cases, a double tearing mode becomes unstable and an annular crash occurs for high q_{min} and the current profile is flatten locally. Core crash, the current profile is flattened to the magnetic axis, occurs for moderate q_{min} by magnetic reconnections. For lower q_{min}, the final state is double chains of saturated islands.

Recently, it is shown that the value of the safety factor q is equivalent to 1 at plasma surface during n=1 burst in VDE of JT-60 tokamak. The magnitude of halo current due to m/n=1 external or internal kink modes is investigated by the MHD simulation. It is shown that the vacuum bubble can be formed by m/n=1 kink mode for flat current plasma, which can cause the halo current. The estimated magnitude of halo current can be 50 % of total plasma current for the plasma with the internal inductance of 0.86 [2-2].

Ideal MHD stability of high-elongated JT60-SU plasma is investigated. It is shown that the maximum value of β_N is mainly limited by a peeling mode, when the bootstrap current near the plasma surface is enhanced in the H-mode plasma. The triangularity has stabilizing effect on the peeling modes, while the usual free-boundary modes and ideal internal modes are not affected by the triangularity [2-3].

Using the statistical theory, it is shown that the magnetic stretching term in the resistive MHD equations is responsible for the formation of the coherent structures in the 2D MHD turbulence which is related to the transport in the plasma confinement.

In a low collisionality plasma with high β_p, large bootstrap fraction and long pulse lengths, neoclassical tearing modes will play a more prominent role in limiting stored energy and degrading confinement. Especially, a weak shear and large pressure gradient enhances the growth of the neoclassical tearing mode. Therefore, effects of the pressure profile and the current profile on the neoclassical tearing mode are investigated, and stabilization by an external local current is discussed. The present stability analysis is based on the saturated island equation (dw/dt = 0), which is derived by the island evolution equation. Results of the analysis show that, for the broad-p ($dp/d\psi \quad 0.3(1-\psi)^{0.5}+0.7$) and high l_i (= 1.2) plasma, the neoclassical tearing mode has better stability where q_{min} is slightly above one or two. For the broad p and low l_i (= 0.8) plasma, the higher n mode is more stable. It is also found that a local current drive effectively stabilizes the neoclassical tearing mode. The local current of ~2 % of the total current with a width of 10 % of the minor radius reduces the island width significantly, and increases the stability boundary to the ideal MHD limit. To reduce the island width, localization of the externally driven current is effective. Ray tracing analysis of the electron cyclotron current drive (ECCD) by the fundamental resonance of the ordinary wave at 110 GHz shows localized current drive over a radial region less than 10 % of the minor radius is achievable for JT-60 like configuration with $n_{e0} = 1 \times 10^{20}$ m^{-3}, $T_{e0} = 10$ keV and $R_0 = 3.4$ m. The current drive efficiency, $\gamma = <n_e>R_0 I/P_{inp}$, is estimated as ~ 0.03 at the half minor radius and an external current of 20 kA (~2 % of 1 MA total current) can be driven by about 1 MW power of EC wave.

References

[2-1] Tuda T., Ishii Y., Kurita G., et al., "Ideal/Resistive Modes Analysis in Reversed Shear Configuration Plasmas", presented at The first general assembly of Asian Plasma and Fusion Association joint with The Third Asia Pacific Plasma Theory Conferenceep. 21-25, 1998, Beijing, China.

[2-2] Kurita G., Yochino R., Neyatani Y., et al., “Halo Current Simulation During VDE in a Tokamak”, Presented at Sherwood Theory Conference held at Atlanta USA, March 1999.

[2-3] Kurita G., Nagashima K., Kikuchi M., et al., “Triangularity Effect on Ideal MHD Stability of JT-60SU Plasma”, Plasma Phys. Control. Fusion **41**, 159 (1999).

3. Divertor

The thermoelectric instability in divertor tokamaks has been studied analytically and numerically by using the five-point model based on scrape-off layer (SOL) and divertor plasmas. To clarify the onset condition of the thermoelectric instability, the linear stability of a symmetric equilibrium of the SOL and divertor plasmas was analyzed by giving an asymmetric perturbation [3-1]. When the divertor plasma temperature T_{div} decreases below a critical temperature, the symmetric equilibrium is found to be unstable due to the thermoelectric instability. It is shown that the critical temperature of the thermoelectric instability depends on the midplane SOL plasma temperature and the divertor radiation loss. Next, the asymmetric equilibrium and its linear stability were investigated [3-2]. When the symmetric equilibrium is unstable, two asymmetric equilibria are obtained. These asymmetric equilibria are stable because the change of sheath potentials and the plasma resistivity suppresses the thermoelectric instability. In an asymmetric equilibrium, the SOL current flows from the higher-T_{div} side to the lower-T_{div} side. The heat flux flowing into the divertor plate of the higher-T_{div} side becomes larger than that of the lower-T_{div} side. The heat flux asymmetry is large for cases in high recycling and low heating power.

References

[3-1] Hayashi N., Takizuka T., et al., “Onset Condition of Thermoelectric Instability in Divertor Tokamaks”, Nucl. Fusion **38**, 1695 (1998).

[3-2] Hayashi N., Takizuka T., et al., “Numerical Analysis of Thermoelectric Instability in Tokamak Divertor”, J. Nucl. Mater. **266-269**, 526 (1999).

4. Numerical Experiment of Tokamak (NEXT)

4.1 Development of Computational Algorithm

The development of a compressible MHD code in the torus geometry has been started in order to investigate the mechanism of the collapse in high beta plasmas. The code was constructed by the finite volume method on triangular meshes in the poloidal plane and by the pseudo-spectral method in the toroidal direction. In this code, due to the adoption of the unstructured grid system, the real machine geometry in the poloidal plane will be easily realized without any singularities at the magnetic axis. On the other hand, the high resolution of the toroidal modes is achieved by the benefit of the spectral method. Up to now, the code was inspected for the propagation of linear MHD waves in a uniform plasma.

4.2 Transport and MHD Simulation

It is becoming clear that various improved modes, such as the internal transport barrier (ITB) formed in reversed magnetic shear experiments can be achieved by suppressing such semi-global structure of the toroidal mode which has been obtained in the numerical simulations. We investigate the role of plasma shear rotation and weak/reversed magnetic shear on these semi-global modes by employing our toroidal simulation code together with a non-local theory. From simulations, in addition to the overall reduction of the wave excitation in the entire negative magnetic shear region, we found that the weak or zero magnetic shear which appears near the minimum q (safety factor) surface breaks up toroidal coupling. This leads to a “discontinuity (or gap)” in wave excitation around the q-min surface, leading to the emergence of the transport barrier. The plasma shear rotation which is observed in the experiment enhances the discontinuity so that the performance of the transport barrier is increased [4-1, 4-2].

In order to clarify the nonlinear behavior of the internal collapse, the density gradient effect is studied by the gyro-kinetic nonlinear simulation in a cylindrical plasma. Even when the density gradient is not so large enough to change the process of the full reconnection, the later process is changed due to the self-generated radial electric field which is affected by the fast parallel motion of electrons. This radial field drives the E×B plasma rotation in the ion diamagnetic direction which violates the symmetry of the plasma flow. As a result, the current reconcentration which induces the secondary reconnection is restricted. Therefore, it is a delicate problem whether the minimum safety factor becomes less than unity again [4-3].

In order to investigate the availability of deep fueling in a fusion device by using the compact toroid (CT) injection method, we have carried out the MHD simulation in which the CT is injected into the target magnetized plasma region. It is revealed that magnetic reconnection between the CT magnetic field and the target magnetic field leads to supply of the CT high density plasma into the target region. Also, it is found that the injected CT is decelerated by both the magnetic pressure effect and the magnetic tension effect of the target magnetic field through the plasma pressure.

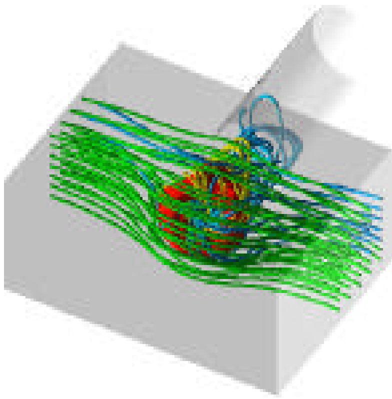

Fig.III-4-1 The spatial structure of magnetic field lines and the CT high density plasma when the CT has entered the target region (square) from the injection region (cylinder).

The boundary layer analysis of the forced magnetic reconnection due to an externally imposed boundary perturbation such as error fields is reformulated by adopting the appropriate asymptotic matching. It yields the correct reconnection process which reflects the effect of the inertia of the plasma in the inner layer exactly [4-4].

Hamilton guiding center theory has been extended to the relativistic electrons. This theory is applied to simulations on collisionless electron motion in stochastic magnetic fields in a tokamak. The simulations have demonstrated that magnetic islands having the widths expected on the major disruption cause the collisionless loss of the relativistic electrons, and that the resultant loss rate is high enough to avoid or to suppress the runaway generation. It is because, for the magnetic fluctuations in the disruption, the loss of the electron confinement due to the breakdown of the toroidal momentum conservation overwhelms the runaway electron confinement due to the phase-averaging effect of relativistic electrons. The simulation results provide a strong support for the JT-60 experiments on the fast plasma shutdown avoiding the runaway generation.

4.3 Divertor Simulation

Development of simulation codes for scrape-off layer (SOL) and divertor plasmas has been continued. The fluid codes, such as SOLDOR developed in JAERI, employ various physics models, i.e., boundary conditions at the plasma-wall boundary, heat conductivity, viscosity and so on. A particle simulation code PARASOL has been developed to validate these physics models. Magnetic field is given constant, which intersects the divertor plates obliquely. Hot particle source is given in the central region of the SOL plasma. Electron motions are approximated as their guiding-center motions, while ion motions are fully traced. The electrostatic field along the direction normal to the plate is calculated with a usual PIC method. Collisional effects are simulated by a binary collision model. The radial electric field newly introduced providing that it is proportional to the electrostatic potential. The flow pattern becomes asymmetric due to the E×B drift, and the boundary conditions are changed.

References

[4-1] Kishimoto Y., Kim J-Y., et al., “Toroidal mode structure in weak and reversed magnetic shear plasmas and its role in the internal transport barrier”, Plasma Phys. Control. Fusion **40A**, 663 (1998).

[4-2] Kishimoto Y., Kim J-Y., et al., "Discontinuity Model for Internal Transport Barrier Formation in Reversed Magnetic Shear Plasmas", 17th IAEA Fusion Energy Conference, Yokohama, IAEA-CN-69 / TH 1/2, Japan 19-24, October 1998 : to be published in Nucl. Fusion 1999.

[4-3] Matsumoto T., Tokuda S., Kishimoto Y., et al., “Complex Behavior of Internal Collapse due to Self-generated Radial Electric Field”, 9th Toki Conference, P-I-12, Toki, Japan, 7-11, December 1998 : to be published in JPFR Series Vol.2.

[4-4] Ishizawa A. and Hattori Y. "Large Coherent Structure Formation by Magnetic Stretching Term in Two-Dimensional MHD Turbulence", J. Phys. Soc. of Japan **67**, 4302 (1998).

IV. FUSION INTERNATIONAL COOPERATION

1. Multilateral Cooperation

The multilateral cooperation carried out in JAERI is summarized in Table IV.1-1.

1.1 IAEA

The 17th IAEA Fusion Energy Conference, being prepared for the prior two years and hosted by STA and JAERI, was successfully held at Yokohama from October 19th to 24th under auspice of IAEA. The most people of 824, from the most countries of 31, participated in this largest international fusion-research conference, which is ever held every two years. The most 377 papers including 120 oral presentations were presented in total, and the 35 papers including 14 oral presentations were presented by researchers of JAERI. It featured this conference that the achievements on high plasma confinements and those sustaining in JT-60, Dlll-D and JET as well as an initial experimental result on LHD, which has newly launched its helical-typed magnetic confinement experiment in NIFS, were presented. Furthermore, a computational dynamic approach for explanation of plasma theory was one of the highlights.

Technical Committee Meeting (TCM) was replaced with ITER expert meeting in this year.

ITER EDA extends its Design and R & D activities under auspice of IAEA to design the more economical experimental reactor. Please refer to the chapter V for the more details.

1.2 IEA

Fusion Power Coordinating Committee (FPCC), which is organized under IEA, coordinates the research and development programs for member nations, selects the important areas and reviews the cooperation activities.

The objective of the cooperation under the Implementing Agreement among the Three Large Tokamak facilities (JET, JT-60 and TFTR) is to enhance the effectiveness and productivity of the research and development efforts related to the development of the tokamak fusion concept by strengthening cooperation on the existing Large Tokamak Facilities. Personnel assignment is one of the main activities; 57 exchanges among the three facilities were carried out in this year, eleven of which were long-term visits exceeding 4 weeks. Operation of TFTR was terminated in 1997, however, their technologies developed on diagnostics and neutral beam injection, and theoretical codes to understand plasma instabilities have been effectively applied to JET and JT-60 plasmas through the mutual personnel exchanges. Another main activity is exchanges of data and information, which have been successfully carried out as the following Task Assignments. Originally they are (1) Research on high-β_p and related modes of operation, (2) Disruption studies, (3) Divertor plate technology, (4) Neutral beam current drive research, (5) Impurity content of radiative discharges, (6) Remote participation in experiments. Recently the seventh Task (7) Scaling of access to ITB plasmas was added.

In the Implementing Agreement on Plasma Wall Interaction in TEXTOR, plasma-wall interaction research cooperation is carried out in a form of exchanging information. This year, two scientists visited the facility of the TEXTOR tokamak in Forschungszentrum Juelich, Germany.

Cooperation under the Implementing Agreement on Fusion Materials is to perform the research and development of fusion materials. Especially, a conceptual design of IFMIF (International Fusion Material Irradiation Facility) was evaluated by the cooperation of Japan, EU, US, and Russia in order to proceed to next step.

Cooperation under the Implementing Agreement on Environment, Safety and Economics aspects of Fusion Power carried out mainly methodology development for the evaluation of environmental and safety aspects of fusion power. The cooperation on socio-economics aspects of fusion power has been initiated.

Cooperation under Implementing Agreement on Fusion Nuclear Technology carried out research cooperation and information exchange in the area of neutronics research, and the tritium breeding blanket development for the ITER test modules.

Multilateral Cooperation	
IAEA	· ITER (International Thermonuclear Experimental Reactor) /EDA Project [Japan, US, EC, Russia] · Information Exchange on Large Tokamaks · Information Exchange on Atomic and Molecular Data · International Conferences
IEA	· Three Large Tokamak Facilities [JT-60 (Japan), TFTR (US), JET (EIU)] · Plasma Wall Interaction in TEXTOR [Japan, US, EU, Canada, Switzerland, Turkey] · Fusion Materials [Japan, US, EU, Canada, Switzerland, China] · Environmental, Safety and Economic Aspects of Fusion Power [Japan, US, EU, Canada, Russia] · Nuclear Technology of Fusion Reactors [Japan, US, EU, Canada, Russia]

Table IV. 1-1. Multilateral cooperation in fusion international cooperation at JAERI

2. Bilateral Cooperation

The bilateral cooperation carried out in JAERI is summarized in Table IV.2-1. On Japan-US cooperation, the Agreement between the Government of Japan and the Government of the United States of America on Cooperation in Research and Development in Energy and Related Fields was signed in May 1979. The Coordinating Committee of Fusion Energy was established to synthetically coordinate the cooperation activities under the above agreement. The Japan-US cooperation consists of four frameworks of exchange programs, joint research project, joint research for plasma physics, and joint planning. The joint research project includes the experimental research program on tokamak plasmas with Doublet III at General Atomics, the irradiation experiment program with mixed spectrum fission reactors (HFIR/ORR) at Oak Ridge National Laboratory, the fusion-fuel processing technology program with the tritium systems test assembly (TSTA) at Los Alamos National Laboratory, and the data link program with the magnetic fusion energy computer center at Lawrence Livermore National Laboratory.

On Japan-EU cooperation, the Agreement for Cooperation between the Government of Japan and the European Atomic Energy Community in the field of controlled thermonuclear fusion was concluded in February 1989. Based on this agreement, a lower hybrid (LH) wave launcher module was fabricated at JAERI and tested in at Cadarache Institute. The test has been completed successfully in July 1998. Regarding development of negative ion source, Japanese ion source was tested at Cadarache Institute, and the properties of the negative ion source were studied at JAERI under collaboration with Cadarache Institute. Regarding development of plasma facing components, exchange programs were carried out.

With Canada, JAERI carried out information exchange and expert meeting on tritium technology and tokamak research through Atomic Energy of Canada Ltd. (AECL). Tritium was shipped from AECL to JAERI based on a contract for purchasing tritium for research and development. With Australia, information exchange and expert meeting were carried out by holding workshops mainly in the area of diagnostics, experiment, and theory for toroidal plasmas, under Agreement between the Government of Japan and the Government of Australia on cooperation in the field of Science and Technology. With Russia, collaboration through information/personal exchanges and expert meetings on plasma physics and nuclear fusion were successfully performed under Agreement between the Government of Japan and the Government of Russia in Research and Development in Science and Technology. With China, information exchange was carried out by holding workshops in the area of plasma physics and fusion under Science and Technology Cooperation Agreement between the Government of Japan and the Government of People’s Republic of China.

	Bilateral Cooperation
Japan-US	· Doublet III Project · HFIR/ORR Joint Irradiation Experiment Program · Fusion Fuel Processing Technology Development Program · Data Link Program · Cooperation in Fusion Research and Development
Japan-EU	· Cooperative Activities Concerning Lower Hybrid Antenna Module · Cooperative Activities Concerning Negative Ion Source · Cooperation in Plasma Facing Components
Japan-Canada	· Cooperation in the Field of Controlled Nuclear Fusion
Japan-Australia	· Cooperation on Diagnostics, Experiments, and Theory
Japan-Russia	· Cooperation in Fusion Research and Development
Japan-China	· Cooperation in Plasma Physics and Fusion

Table IV.2-1 Bilateral cooperation in fusion international cooperation at JAERI

3. Cooperative Program on DIII-D (Doublet III) Experiment

3.1 Highlights of FY1998 Research Results

Integration of the advanced tokamak concept, which encompasses to acquire the improved confinement in a steady-state with high normalized-beta and a large fraction of non-inductively driven current together with highly-evolved divertor functions was emphasized also in the 1998 experimental campaign. Accordingly, high performance ELMy H-mode plasmas with $\beta_N H$ of 6 was produced and sustained for 1 s. The long sustainment of core transport barriers for 5 s with the L-mode edge was also demonstrated. In addition, the off-axis electron cyclotron current drive was successfully undertaken for the first time in a tokamak, discovering efficiency above the theoretical expectations. Edge stability studies have shown that the H-mode pressure gradient is not limited by the ballooning modes and the self-consistent bootstrap provides the second regime access. From the MARFE instability criterion, the density limit was modeled, which agrees well with Hugill-Greenwald limit and which scales quite favorably to a larger device with high edge temperature. Divertor experiments have furthermore provided a new understanding of convection and recombination in radiative divertors and have produced enhanced divertor radiation with scrape off layer plasma flows and impurity enrichment.

In order to extrapolate the improved performance results to the experimental reactor such as ITER with confidence, predictive understanding of tokamak transport is necessary. Over the past several years, a number of new theoretical models of plasma transport have been developed. Averaged over a large database of plasma pulses, each of these models do about equally well in predicting quasi-steady-state equilibrium plasma profiles even though each model has a different mix of the fundamental physics. Accordingly, in order to distinguish between the models, some other methods of verification are necessary. Simulations have shown that perturbative transport experiments could provide a more critical test of transport models than the equilibrium transport analysis. Experiments have thereby been coordinated on DIII-D using the modulated ECH as the spatially localized pertubative heat source with the resonance absorption layer located off axis. The results with off-axis heating indicate the electron and ion responses to the ECH perturbation are out of phase with each other at the plasma core and at the EC resonance layer. In general, the IFS-PPPL [3.1-1] and GLF23 [3.1-2] models predict reasonably well the ion response, whereas the GLF23 and IIF [3.1-3] models are plausible more with the electron response. The GLF23 model includes the effects of both the electron and ion temperature gradient driven turbulence as well as trapped electron modes, which may be why it fits the best overall. However, GLF23 still suffers from fitting the data when the heating location was other than $r/a = 0.3$. After all, none of the developed models showed adequately good agreement with both the ion and electron perturbative responses and the equilibrium profiles, nonetheless the equilibrium profile fit of the GLF23 model was improved by including the effects of the measured average $E\times B$ shear.

References

[3.1-1] Kotschenreuther M., et al., Phys. Plasmas **2**, 2381 (1995)
[3.1-2] Waltz R., et al., Phys. Plasmas **4**, 2482 (1997).
[3.1-3] Itoh K. et al., Plasma Phys. Contr. Fusion, **36** 279 (1994).

4. Collaborative Activities Concerning Fusion Technologies

4.1 IEA Collaborative Activities on Environmental, Safety, and Economic Aspects of Fusion Power

Designated by the Government of Japan, JAERI has been participating in the IEA Implementing Agreement on a Cooperative Program on the Environmental, Safety and Economic (ESE) Aspects of Fusion Power. This collaborative activity is carried out by Canada, EURATOM, JAERI, MINATOM and USA since 1992 and extended for another five years in 1997. Review of five tasks (Tritium Safety and Environmental Effects, Transient Thermofluid Modeling and Validation Tests, Activation Products Safety and Environmental Effects, Safety System Study Methodology, Failure Rate Data Base) and plan for the future activities were performed. The scope and schedule of newly proposed tasks (Fusion Radioactive Waste Study, Socio-economic Aspects of Fusion Power) were discussed.

4.2 IEA Collaborative Activities on Research and Development of Plasma Wall Interaction in TEXTOR

An IEA implementation for a collaboration program of research and development on plasma wall interaction in TEXTOR is expected up to December 2002. TEXTOR management is under KFA (Forschungszentrum Juelich GmbH), ERM/KMS (Ecole Royale Militaire) Brussels and FOM (Stichting voor Fundamenteel Onderzok der Materie) Nieuwegein under the TEC (Trilateral Euregio Cluster). Japan is a member of the executive committee and NIFS organizing Japanese programs as a cooperation center of Japan. JAERI has been joined the program as a Japanese technical committee member. In this fiscal year, two staff members in JAERI visited TEXTOR to exchange information’s on the RI-mode physics, plasma edge diagnostics and transport, modeling of birth mechanism of runaway electrons at a plasma disruption phase, etc.

4.3 IEA Collaborative Activities on Nuclear Technology of Fusion Reactors

As for the activity in the Solid Breeder Sub Group of the Implementing Agreement, Japan has performed the Sub-Task A on Effective Thermal Conductivity Measurements of the Ceramic Breeder Pebble Beds Using the Hot Wire Method. The measurement was performed by using Alumina, as reference material, Li_2O from JAERI, Li_2ZrO_3 from CEA. The results of the measurement showed that the correlation meets the observed data by assuming the contact area fraction of 4.6×10^{-3} with accommodation factor of 0.2 for Li_2O pebble bed. With respect to Li_2TiO_3 data, the measurement was completed in the temperature range of 420 - 775 ^oC. The observed results were consistent with the correlation by SZB (Schluender, Zehner and Bauer) modified model and HM (Hall and Martin) modified model, assuming the contact area fraction and accommodation factor are the same as those of the Li_2O pebble bed. The estimation of Li_2TiO_3 bed thermal conductivity with no mechanical stress is, now, available by the result obtained in this work.

4.4 Collaborative Activities on Technology for Fusion-Fuel Processing between US-DOE and JAERI

Research and development of technology for Fusion Safety has been carried out as an US-Japan cooperative program at Tritium Systems Test Assembly (TSTA) at the Los Alamos National Laboratory since 1995. In June 1998, new phase was started to emphasize tritium safety technology R&D including new activities to understand tritium behavior in a tokamak using Tokamak Fusion Test Reactor (TFTR) at the Princeton Plasma Physics Laboratory.

In FY 1998, at TSTA, experiments using the Tritium Plasma Experiment (TPE) to evaluate tritium behavior under off-normal conditions and those on control of tritium inventory in the Isotope Separations System (ISS) were carried out. At TFTR, measurement of tritium distribution in the TFTR vacuum vessel, analysis of tritium behavior during TFTR deuterium-tritium operation, evaluation of the capabilities of advanced radioactive liquid waste treatment techniques and experiments on some technologies for decontaminating and decommissioning (D&D) of TFTR components including graphite tiles were performed.

Using TPE at TSTA, tritium permeation through a divertor simulating module with a tungsten armor tile was studied. Simulation experiment of a Loss Of Vacuum Accident (LOVA) was also performed in TPE. These were both first-of-a-kind experiments. To develop method evaluating tritium inventory in columns of ISS, a series of experiment was performed using ISS loop system at TSTA and a set of valuable systematic data was obtained.

The activity at TFTR has allowed some extremely exciting new studies of the behavior of tritium deposited in graphite tiles. There is great concern for ITER, or equivalent next-step devices, about the inventory of tritium built up by co-deposition in graphite tiles. It must be measured and a technique for its removal must be developed. The availability of the TFTR facility, which was operated extensively with tritium, has allowed some serious study on these issues. Visual observations (Figure IV.4.4-1) showed that there were considerable changes happening in the appearance of tiles. Many tiles were found to have flaking on their surfaces in the region of codeposition.

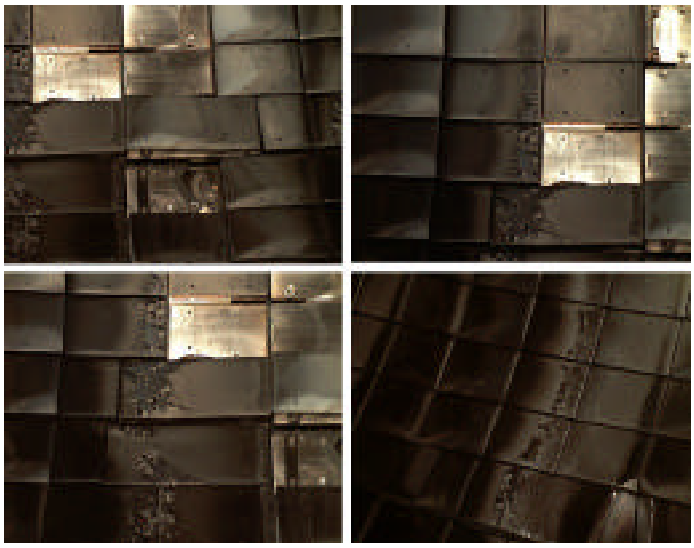

Figure IV. 4.4-1. Photograph of the inner surface of the TFTR vacuum vessel, graphite tiles. There appear flakings.

4.5 Collaborative Activities on Research and Development of Plasma Facing Components under the US-Japan Collaboration

Under the Japan and US Fusion Agreement, the workshop on Fusion High Power Density Devices and Design (FT-15) was held in the US. In this workshop, several concepts of the fusion power reactors were discussed; e.g. liquid metal cooling option, He cooling option and molten salt cooling option. From JAERI, an experimental result was reported that the large-scale divertor mock-up with CFC monoblock armor could successfully withstand the heat load conditions of the ITER divertor.

4.6 Collaboration between JAERI and CEA-Cadarache for LH Antenna Module

Cooperative activities have been started to obtain a detail outgassing database during high RF power, CW operation for a launcher design in future LHCD system since 1992. RF test was performed at CEA-Cadarache RF Test Facility, which allowed high power injection up to 0.5 MW, under quasi-continuous operation at frequency of 3.7 GHz. The aimed database was obtained and the 6 years collaboration was completed successfully in July 1998, concluding that no external pumping for the antenna is necessary. The result was applied to the ITER LHRF system design. The collaboration with CEA-Cadarache will be maintained in small scale under Annex III of EU-Japan collaboration agreement. In this frame, the first EU-Japan workshop on RF Antenna was held in Cadarache with 30 participants.

4.7 Collaborative Activities on Research and Development of Plasma Facing Components under the EU-Japan Collaboration

Under the Japan-EURATOM Fusion Agreement, three collaborative activities were carried out as follows; the JAERI-ARC (Austrian Research Center), the JAERI-FZJ and the JAERI-CEA collaborations. The non-destructive test (NDT) using an ultrasonic wave probe was conducted at ARC. It was demonstrated that joining flaws could be detected at the bond interface between CFC monoblock armor and Cu cooling tube by the probe scanning inside of the cooling tube. From this result, the ultrasonic NDT is confirmed one of the promising techniques for an inspection of soundness of the bond interface of the components.

Thermal shock test on carbon-based material before neutron irradiation was conducted at FZJ. As test materials were SiC-doped and 3D CFCs. Amounts of the erosion for test pieces are 0.3 mg for SiC-doped CFC and 1 mg for 3D CFC at a heat load of 10 MJ/m^2, which are comparable values obtained by JAERI.

A series of Critical Heat Flux (CHF) experiments were undertaken on a swirl tube manufactured by CEA Cadarache in an ion beam test facility in JAERI. CHF values of 30 to 37 MW/m^2 peak heat fluxes are determined for the highly peaked ITER transient profile.

4. 8 Cooperative Activities Concerning Negative Ion Source under the EU-Japan Collaborations

Japanese “Kamaboko” source (high confinement negative ion source) was tested at CEA-Cadarache to demonstrate continuous operation at the high current density of 20 mA/cm^2 D^-. A frame cooling type and an active cooling type plasma grids developed JAERI were also tested at Cadarache for the continuous operation. Both grids were designed to keep stable temperature of 200 – 300˚C for the efficient production of the negative ions in the cesium-seeded source. It was demonstrated that the temperature of both grids became stable at around 200 ˚ C after about 100 s of the arc discharge started [4.8-1]. Further, uniformity of the negative ion source was studied at

JAERI under a collaboration with CEA-Cadarache.

Reference

[4.8-1] Trainham R., Jaquat C., Fujiwara Y., et al, " Long pulse extraction of deuterium negative ion beams from the Kamaboko ion source", 20th SOFT Fusion Technology 367-370(1998).

4.9 Collaborative Activities on Technology for Tritium Transfer between AECL and JAERI

In October 1998, the third shipment of tritium from Chalk River Laboratory (CRL) of AECL to Tritium Process Laboratory (TPL) of JAERI was carried out safely based on the purchase contract between JAERI and Ontario Hydro Inc.. Total amount of tritium shipped from CRL was about 60 g through three shipments since 1995. All shipments were carried out securely without any technical problems by tremendous efforts of AECL and JAERI personnel.

Before the third shipment, a technical meeting was held between Ontario Hydro Inc. (including a technical stuff from CRL) and JAERI at TPL in May 1998. In this meeting, valuable discussions and information exchange were carried out which related to tritium accountancy, tritium handling technologies, future plan of tritium use, etc.

5. Collaborative Activities in Asian Area

The interactive activities including personal exchanges and meeting on fusion research among Asian countries grow significantly these days. JAERI conducted bilateral collaboration with China and Korea respectively in 1998 fiscal year.

Under the STA scientist exchange program, five Chinese scientists joined JT-60 and JFT-2M experiment in JAERI, and three JAERI scientists visited Southwestern Institute of Physics (SWIP) for two weeks. In May 1998, a new proposal for research collaboration on "plasma physics and fusion" was initiated under Science and Technology Cooperation Agreement between Japan and China. Based on this agreement, the second Japan-China workshop was successfully held at Chengdue in January 18-22th, 1999. Ten Japanese scientists including six JAERI staffs and twenty-seven Chinese scientists joined this workshop.

Two Korean scientists joined fusion research in JAERI in 1998 under the STA scientist exchange program. Two JAERI scientists participated in the Asian Plasma and Fusion Association Conference held at Beijing in September 1998.

Appendix A.1 Publication List (April 1998 - March 1999)

A.1.1 List of JAERI reports

1) Aoki I., Seki Y., et al.,"Development of Dynamic Simulation Code for Fuel Cycle of Fusion Reactor", JAERI-Data/Code 99-004 (1999).

2) Ezato K., Suzuki S., et al.,"Numerical Simulation of Runaway Electron Effect on Plasma Facing Components", JAERI-Research 98-033 (1998).

3) Fujiwara Y., Hanada M., Kawai K., et al., "Beamlet interaction in multi-aperture negative ion source", JAERI Research 99-013 (1999) (in Japanese).

4) Furuya K., Hara S., Kuroda T., et al., "Heating Facility for Blanket and Performance Test", JAERI-Tech 99-025 (1999).

5) Gilanyi A., Akiba M., Okumura Y., et al., "AC Loss Calculation of Central Solenoid Coil", JAERI-Research, 99-014 (1999).

6) Hasegawa Y., Hamamatsu K., Shirai H., et. al., "Development of FAME Animation System", JAERI-Tech 99-015 (1999) (in Japanese).

7) Isayama A., Isei N., Ishida S., et al., "Measurement of Electron Temperature Profile of ELMy H-mode Plasma by Fourier Transform Spectroscopy --Removal of Non-thermal Emission Pulses--", JAERI-Research 99-021 (1999).

8) Itou A., Nakahira M., Hamada K., et al., "ITER cryostat thermal shield detailed design", JAERI-Tech 99-027 (1999).

9) Itou A., Nakahira M., Takahashi H., et al., "ITER cryostat main chamber and vacuum vessel pressure suppression system design", JAERI-Tech 99-026 (1999).

10) Kanari M., Abe T., Enoeda M., et al., "Durability of Alumina Electrical Insulation Films by Plasma Spraying Coating Method under Repeated Impact Loads", JAERI-Research 98-029 (1998) (in Japanese).

11) Kanari M., Abe T., Tanzawa S., et al., "Geometrical Influence on Repeated Impact Durability of Alumina Insulation Film Coated by Plasma Spraying Method", JAERI-Research 99-012 (1999) (in Japanese).

12) Kikuchi S., Kuroda T., Enoeda M., "Preliminary Thermo-mechanical Analysis of ITER Breeding Blanket", JAERI-Tech 98-059 (1999).

13) Kodama K., Masaki K., Sasajima T., et al., "Design and Installation of W-shaped Divertor in JT-60U", JAERI-Tech 98-049 (1998) (in Japanese).

14) Kubo H., Omine T., Yoshida K., "Design of correction coil for ITER", JAERI-Tech 98-050 (1998).

15) Kurihara R., "Research on Unstable Fracture of Light Water Reactor Piping", JAERI-Research 98-043 (1998) (in Japanese).

16) Kuroda T., Enoeda M., Kikuchi S., et al., "ITER Breeding Blanket Module Design & Analysis", JAERI-Tech 98-051 (1998).

17) Miura, Y. M., Kawamata, K., Fukuda, T., Kurihara, K., "A New Function Parameterization Formula for the JT-60U X-point Position Control ", in "Review of JT-60U Plasma Experimental Results in 1997", JAERI-Research 98-039 (1998).

18) Miyata H., Arai T., "Study on Usage of Fluorocarbon for Toroidal Field Coil Cooling", JAERI-Tech 98-038 (1998) (in Japanese).

19) Nakano T., Kubo H., Sugie T., et al., "Visible Spectra in JT-60U Divertor Plasma (Wavelength Range between 300 nm - 780 nm)", JAERI-Research 99-003 (1999) (in Japanese).

20) Nishitani T., Johnson L.C., et al., “Design of ITER Neutron Monitor using Micro Fission Chambers”, JAERI-Research 98-049 (1998).

21) Nishitani T., Iida T., et al., “Irradiation Effects on Plasma Diagnostics Components”, JAERI-Research 98-053 (1998).

22) Obara K., Kakudate S., Itou A., et al., “Design and development of in-vessel viewing periscope for ITER (International Thermonuclear Experimental Reactor)”, JAERI-Tech 99-009 (1999).

23) Obara K., Kakudate S., Oka K., et al., “High γ-ray irradiation test of critical components for ITER (International Thermonuclear Experimental Reactor) in-vessel remote handling system”, JAERI-Tech 99-003 (1999).

24) Shiina T., Yamauchi T., Ishige Y., et al., “Technical Development of TV Thomson Scattering System on JFT-2M”, JAERI-Tech 98-048 (1998) (in Japanese).

25) Sugie T., Ogawa H., Katsunuma A., et al., "Design of Divertor Impurity Monitoring System for ITER (II)", JAERI-Tech 98-047 (1998).

26) Sugie T., Toriya T., Kasai S., "Development of Multi-channel Optical-fiber Feed Through for ITER", JAERI-Tech 98-036 (1998).

27) Tsuchiya Y., Kikuchi K.,Mstsui K., “Non-destructive measurement of residual stress for a superconductor jacket applied to the fusion deffiraction method”, JAERI-Tech 98-050 (1998).

A.1.2 List of papers published in journals

1) Akiba M., Suzuki S., “Overview of the Japanese Mock-up Tests for ITER High Heat Flux Components,” Fusion Eng. Des. **39-40**, 219 (1998).

2) Ando T., Hiyama T., Takahashi Y., et al., “Fabrication of ITER central solenoid model coil; Outer module”, IEEE Trans. Appl. Superconductivity **7**, (1998).

3) Arai T., Masaki K., Miyachi K., “Baking Technique of JT-60”, J. Vac. Soc. Jpn. **41**, 841 (1998) (in Japanese).

4) Araki M., Kitamura K., Suzuki S., “Analyses of Divertor High-Heat-Flux Components on Thermal and Electromagnetic Loads”, Fusion Eng. Des. **42**, 381 (1998).

5) Asakura N. and JT-60 Team, “Role of divertor geometry on detachment and core plasma performance in JT-60U”, J. Nucl. Mater. **266-269**, 182 (1999).

6) Bandourko V., Jimbou R., Nakamura K., et. al., “Tungsten Selfsputtering Yield with Different Incidence Angles and Target Temperatures”, J. Nucl. Mater. **258-263**, 917 (1998).

7) Barabash V., Akiba M., Bonal J.P., et al., “Carbon Fiber Composites Application in ITER Plasma Facing Materials”, J. Nucl. Mater. **258-263**, 149 (1998).

8) Boscary J., Araki M., Schlosser J., et al., “Dimensional Analysis of Critical Heat Flux in Subcooled Water Flow under One-Side Heating Conditions For fusion Application”, Fusion Eng. Des. **43**, 147 (1998).

9) Boscary J., Suzuki S., Nakamura K., et al., “Thermal Fatigue Tests on CVD-W/Cu Divertor Mock-ups”, Fusion Eng. Des. **39-40**, 537 (1998).

10) Cardella A., Chiocchio S., Ioki K., et al., "Design of ITER EDA plasma facing components", Fusion Eng. Des. **39-40**, 377 (1998).

11) Cardella A., Ioki K., Yamada M., et al., "The ITER port limiter design", Fusion Eng. Des. **39-40**, 377 (1998).

12) Costley A. E., Ebisawa K., Edmonds P., et al., "Overview of the ITER Disagnostic System", Diagnostics for Experimental Thermonuclear Fusion Reactors 2, edited by Stott P.E., Gorini G., Pradoni P., and Sindoni E. (Plenum Press, New York, 1998), p.41, May (1997).

13) deKock L. , Ando T., Ebisawa K., et al., "Diagnostic Requirements for the ITER Divertor", Diagnostics for Experimental Thermonuclear Fusion Reactors 2, edited by Stott P.E., Gorini G., Pradoni P., and Sindoni E. (Plenum Press, New York, 1998), p.67, May (1997).

14) Dnestrovskij Yu. N., Lysenko S.E., (Polevoi A.R.), et al., "Test of Canonical Profiles and Semi Empirical Transport Models against JT-60U Plasmas", to be published in Nucl. Fusion.

15) Ebisawa K., Ando T., Sugie T., et al., "VUV Divertor Impurity Monitor for ITER", Diagnostics for Experimental Thermonuclear Fusion Reactors 2, edited by Stott P.E., Gorini G., Pradoni P., and Sindoni E. (Plenum Press, New York, 1998), p.337, May (1997).

16) Enoeda M., Furuya K., Takatsu H., et al., “Effective thermal conductivity measurements of the binary pebble beds by hot wire method for the breeding blanket”, Fusion Technol. **34**, 877 (1998).

17) Ezato K. and Kunugi T., “Molecular Dynamics Simulation of Energetic Cluster Impact to Metallic Thin Film,” J. Nucl. Mater. **258-263**, 618 (1998).

18) Fukuda T., "Hidden variables affecting the L-H transition", Plasma Phys. Control. Fusion **40**, 543 (1998).

19) Fukuda T., Takizuka T., et al., “Nondimensional threshold scaling of edge plasma quantities in JT-60U”, Plasma Phys. Control. Fusion **40**, 827 (1998).

20) Fukuda T., Takizuka T., et al., "Scaling of the H-mode Power Threshold for ITER", Plasma Phys. Control. Fusion **40**, 857 (1998).

21) Fukuda T. and JT-60 Team, "Active Feedback Control of Steady-state Improved Confinement Discharges in JT-60U", Fusion Eng. Des. **38**, (1999), (in press).

22) Furuya. K., et al., “Application of HIP Bonding to First Wall Panel Fabrication made from Reduced Activation Ferritic Steel F82H”, J. Nucl. Mater. **258-263** 2023 (1998).

23) Gotoh Y., Okamura H., Kajiura S., et al., “Development And Material Testing of OF-Cu/DS-Cu Duplex Tube and Trial Fabrication of Vertical Target Mock-ups for ITER Divertor”, J. Nucl. Mater. **258-263**, 271 (1998).

24) Hanada M., Akino N., Ebisawa N., et al., “Development of Multi-Mega watt negative ion sources and accelerators for neutral beam injectors,” IAEA-CN-69-FTP/20.

25) Hasegawa Y., Nakamura Y., Shirai H., et. al., “Development and Performance of High Speed Processing System of Magnetohydrodynamic Equilibria for Discharge Analysis on the JT-60 Tokamak”, J. Nucl. Sci. Technol. **41**, 48 (1999), (in Japanese).

26) Hatae T., Kamada Y., Ishida S., et al., “Characteristics of edge pedestal width in JT-60U ELM-free H-mode plasmas”, Plasma Phys. Control. Fusion, **40**, 1073 (1998).

27) Hatae T., Nagashima A., Kondoh T., et al., “YAG laser Thomson scattering diagnostic on the JT-60U”, Rev. Sci. Instrum., **70**, 772 (1999).

28) Hatano T., Kanari M., Sato S., et al., “Fracture strengths of HIPed DS-Cu/SS joints for ITER shielding blanket/first wall”, J. Nucl. Mater. **258-263** 950 (1998).

29) Hatano T., Sato S., Kuroda T., et al., “Low Cycle Fatigue Lifetime of HIPed Bonded Bi-metallic First Wall Structures of Fusion Reactor”, J. Nucl. Sci. Technol. **35**, 705 (1998).

30) Hatano T., Suzuki S., Yokoyama K., et al., “Fabrication and Thermal Cycle Testing of a First Wall Mock-up for ITER Baffle Blanket Module”, Fusion Technol. **34**, 908 (1998).

31) Hatano T., Suzuki S., Yokoyama K. et al., “High heat flux testing of a HIP bonded first wall panel with built-in circular cooling tubes”, Fusion Eng. Des. **39-40**, 363 (1998).

32) Hayashi N., Takizuka T., et al., “Onset Condition of Thermoelectric Instability in Divertor Tokamaks”, Nucl. Fusion **38**, 1695 (1998).

33) Hayashi N., Takizuka T., et al., “Numerical Analysis of Thermoelectric Instability in Tokamak Divertor”, J. Nucl. Mater. **266-269**, 526 (1999).

34) Hayashi T., Okuno K., Ishida T., et al., “Effective Tritium Processing using Polyimide Films”, Fusion Eng. Des. **39-40**, 901 (1998).

35) Hayashi T., Carlson R..V., Kobayashi K., et al., “Tritium Behavior Intentionally Released in the Radiological Controlled Room under the US-Japan Collaboration at TSTA/LANL”, Fusion Technol., to be published.

36) Hayashi T., Suzuki T., Yamada M., et al., “Long-term Tritium Accountability Demonstration of ZrCo

Storage Bed by "In-bed" Gas Flowing Calorimetry”, Fusion Technol., to be published.

37) Higashijima S., Kubo H., Sugie T., et al., “Carbon Impurity Behavior in W-shaped Pumped Divertor of JT-60U”, J. Nucl. Mater. **266-269**, 1078 (1999).

38) Ide S., Naito O., Oikawa T., et al., "LHCD Current Profile Control Experiments towards Steady State Improved Confinement on JT-60U", to be published in Nucl. Fusion.

39) Ido T., Hamada Y., Nishizawa A., et al., “Heavy Ion Beam Probe Diagnostic System on JFT-2M”, Rev. Sci. Instrum. **70**, 955 (1999).

40) Idomura Y., Tokuda S., Wakatani M., “Gyrokinetic particle simulation using the orbit averaged electron drift-kinetic equation”, J. Plasma and Fusion Res. **75**, 131 (1999).

41) Igitkhanov Y., Janeschitz G., Sugihara M., et al., "Edge Parameter Operational Space and Trajectories for ITER", Plasma Phys. Control. Fusion **40**, 837 (1998).

42) Imai T. and Sakamoto K., “High Power Millimeter Wave Generator- Gyrotron”, Electro Magnetic Conpatibility **11**, 27 (1998).

43) Imai T. and Sakamoto K., “Diamond Window for High Power Millimeter Wave”, New Diamond **15**, 26 (1999).

44) Inabe T., Seki M., Tsunematsu T., "Fusion reactor safety - Issues and perspective", Fusion Eng. Des. **42** (1998).

45) Ioki K., Barabaschi P., Bruno L., et al., "ITER first wall/shield blanket", Fusion Eng. Des. **39-40**, 585 (1998).

46) Ioki K., Barabash V., Cardella A., et al., "Design and Material selection for ITER first wall/blanket, divertor and vacuum vessel", J. Nucl. Mater. **258-263**, 74 (1998).

2) Isayama A., Kamada Y., Ozeki. T., et al., "Measurement of magnetic island width in long-pulse, high-_ discharges in JT-60U", Plasma Phys. Control. Fusion **41**, 35 (1999).

48) Ise H., Sato S., Yamazaki S., et al., “Development of Fabrication Technologies for the ITER Divertor,” Fusion Eng. Des. **39-40**, 513 (1998).

49) Ishizawa A. and Hattori Y., "Large Coherent Structure Formation by Magnetic Stretching Term in Two-Dimensional MHD Turbulence", J. Phys. Soc. of Japan **67**, 4302(1998).

50) Isobe K., Hatano Y., Sugisaki M., et al., “Observation of Spatial Distribution of Tritium in Zrconium Alloy with Microautoradiography”, J. Nucl. Mater. **271-272**, 326 (1999).

51) Isono T., Hamada K., Ando T., et al., “Test results of high temperature superconductor current lead at 14.5kA operation”, IEEE Trans. Appl. Superconductivity **7**, (1998).

52) Itami K., Hosogane N., Konoshima S., et al., “Radiative Plasma by Impurity Seeding in W-shaped Pumped Divertor Experiment of JT-60U”, J. Nucl. Mater. **266-269**, 1097 (1999).

53) Itoh T., Akino N., Aoyagi T., et al., “Beamline Performance of 500 keV negative ion-based NBI system for JT-60U”, Fusion Eng. Des. **39-40**, 123 (1998).

54) Iwai Y., Yamanishi T. and Nishi M., “A Steady-state Simulation Model of Gas Separation by Hollow-filament Type Membrane Module”, J. Nucl. Sci. Technol., **36**, 95 (1999).

55) Jimbou R., Nakamura K., Bandourko V. et al., “Temperature Dependence of Sputtering Yield of Carbon

Fiber-Reinforced Carbon Composites with Low Energy and High Flux Deuterium Ions," J. Nucl. Mater. **258-263**, 724 (1998).

56) Johnson L. C., Barnes C.W., Ebisawa K., et al., "Overview of Fusion Product Diagnostics for ITER", Diagnostics for Experimental Thermonuclear Fusion Reactors 2, edited by Stott P.E., Gorini G., Pradoni P., and Sindoni E. (Plenum Press, New York, 1998), p.409, May (1997).

57) Kakudate S., Nakahira M., Oka K., et al., "Development of Blanket Remote Maintenance System", J. Robotics Mech. **10**, 78 (1998).

58) Kaminaga A., Arai T., Kodama K., et al., "Vacuum Leak Test Technique of JT-60", J. Vac. Soc. Jpn. **41**, 846 (1998) (in Japanese).

59) Kanari M., Hatano T., Sato S., et al., "High Heat Flux Testing and Post-Mortem Observation of Small-Scale ITER First Wall Mock-Up Made by HIP Joining", Fusion Technol. **34**, 882 (1998).

60) Kasugai A., Sakamoto K., Takahashi K., et al., Rev. Sci. Instrum. **69**, 2160 (1998).

61) Kawamura Y., Enoeda M. and Okuno K., "Isotope Exchange Reaction in Li2ZrO3 Packed Bed", Fusion Eng. Des. **39-40**, 713 (1998).

62) Kawano Y., Chiba S., Shirai H., et al., "Dual CO laser polarimeter for Faraday rotation measurement in tokamak plasmas", Rev. Sci. Instrum. **70**, 714 (1999).

63) Kawano Y., Chiba S., Shirai H., et al., "First measurement of tangen Faraday rotation of COtial laser wave in a tokamak plasma", Rev. Sci. Instrum. **70**, 1430 (1999).

64) Kimura T., Matsukawa M., Miura Y. M., et al., "Analysis Method of Current Distortion Factor of 3-Phase 3-Wire System" (in Japanese), Trans. IEE Jpn. **119-A**, 279 (1999).

65) Kishimoto Y., Kim J-Y., et al., "Discontinuity Model for Internal Transport Barrier Formation in Reversed Magnetic Shear Plasmas", to be published in Nucl. Fusion.

66) Kishimoto Y., Kim J-Y., et al., "Toroidal mode structure in weak and reversed magnetic shear plasmas and its role in the internal transport barrier", Plasma Phys. Control. Fusion **40A**, 663 (1998).

67) Kitamura K., Nagata K., Shibui M., et al., "Effects of interface edge configuration on residual stress in the bonded structures for a divertor application", J. Nucl. Mater. **258-263**, 275 (1998).

68) Koide Y., "Characteristics of Internal Transport Barriers in Tokamaks", Journal of Plasma and Fusion Res. **74**, 987 (1998).

69) Koide Y., Burrell K.H., Rice B.W., et al., "Comparison of internal transport barriers in JT-60U and DIII-D NCS discharges", Plasma Phys. Control. Fusion **40**, 97 (1998).

70) Koide Y., Mori M., Fujita T., et al., "Study of internal transport barriers by comparison of reversed shear and high$-\beta$ discharges in JT-60U", Plasma Phys. Control. Fusion **40**, 641 (1998).

71) Koizumi N., Ando T., Sugimoto M., et al., "Development of a 13-T and 40-kA Nb3Al conductor for toroidal coils of fusion reactors", Fusion Eng. Des. **41**, 277 (1998).

72) Konishi S., Maruyama T., Okuno K., et al., "Development of Electrolytic Reactor for Processing of Gaseous Tritiated Conpounds", Fusion Eng. and Des. **39-40**, 1033 (1998).

73) Koog J. S., Sakasai A., Koide Y., et al., "High time resolution ion temperature and rotation velocity measurements by charge exchange spectroscopy using three interference filters", Rev. Sci. Instrum. **70**, 372

(1999).

74) Kubo H., Sawada K., "Volume Recombination in Divertor Plasmas", J. Plasma and Fusion Res. **74**, 562 (1998) (in Japanese).

75) Kubo H., Takenaga H., Kumagai A., et al., “The spectral profile of the He I singlet line (667.82 nm) emitted from the divertor region of JT-60U”, Plasma Phys. Control. Fusion **41**, 747 (1999).

76) Kubo H., Takenaga H., Sugie T., et al., “The spectral profile of the Da line emitted from the divertor region of JT-60U”, Plasma Phys. Control. Fusion **40**, 1115 (1998).

77) Kunugi T., Takase K., Shibata M., “Thermofluid experiments on ingress of coolant event”, Fusion Eng. Des. **42**, 67 (1998).

78) Kurihara, K., “Current Profile Reproduction Study on the Basis of a New Expansion Method with the Eigenfunctions Defined in the Tokamak Plasma Interior,” Fusion Technol. **34**, 548 (1998).

79) Kurihara R., Ajima T., Kunugi T., et al., “Analysis and experimental results on ingress of coolant event in vacuum vessel”, Fusion Eng. Des. **42**, 61 (1998).

80) Kurita G., Nagashima K., Kikuchi M., et al., “Triangularity Effect on Ideal MHD Stability of JT-60SU Plasma”, Plasma Phys. Control. Fusion **41**, 159 (1999).

81) Kuriyama M., Akino N., Ebisawa N., et al., “Development of negative -ion based NBI system for JT-60”, J. Nucl. Sci. Technol. **35**, 739 (1998).

82) Kuriyama M., Akino N., Ebisawa N., et al., “Operation of the negative-ion based NBI for JT-60U”, Fusion Eng. Des. **39-40**, 115 (1998).

83) Kuroda T., Hatano T., Enoeda M., et al., “Development of joining technology for Be/Cu-alloy and Be/SS by HIP”, J. Nucl. Mater. **258-263**, 258 (1998).

84) Kusama Y., Kimura H., Ozeki T., et al., "Toroidal Alfvén eigenmodes driven with ICRF accelerated protons in JT-60U negative shear discharges", Nucl. Fusion, **38**, 1215 (1998).

85) Kusama Y. and JT-60 Team, "Recent Progress in High Performance and Steady-state Experiments on JT-60U with W-shaped Divertor", Phys. Plasma, **6**, 1935 (1999).

86) Kusama Y., Kimura H., Nemoto M., et al., "Production and confinement characteristics of ICRF-accelerated energetic ions in JT-60U negative-shear plasmas", Plasma Phys. Control. Fusion (in press).

87) Kusama Y., Kramer G. J., Kimura H., et al., "Characteristics of NNB-driven Alfvén eigenmodes, burst modes and chirping modes in the Alfvén frequency range in JT-60U", Nucl. Fusion (in press).

88) Li J., et al., "Sheared Slab Instability in Tokamak Plasma with Negative Magnetic Shear", Phys. Plasmas **5**, 959 (1998).

89) Loarte A., Asakura N., Bosch S., et al., “Comparison of B2-EIRENE calculations with multi-machine experimental measurements”, J. Nucl. Mater. **241-243**, 1123 (1997).

90) Maebara S., Seki M., Ikeda Y., et al. “Development of Plasma Facing Component for LHCD Antenna”, Fusion Eng. Des. **39-40**, 355 (1998).

91) Masaki K., Kodama K., Sasajima T., et al., “Inspection of JT-60 W-shaped Divertor after the Initial Operation”, J. Plasma Fusion Res. **74**, 1048 (1998) (in Japanese).

92) Matsukawa M., Miura Y. M., Kimura T., et al., “Design and Model Test of a Water-cooled VCB for Superconducting Magnet Power Supplies”, Fusion Technol. **34**, 684 (1998).

93) McCormick K., Asakura N., Bosch S., et al., “ITER Edge Database Investigations of the SOL Width”, J. Nucl. Mater. **241-243**, 99 (1997).

94) Miyamoto K., Asakura N., “An improved two points model of scrape-off-layer plasma of tokamaks with divertor”, J. Plasma and Fusion Res., **74**, 266 (1998).

95) Mondino P.L., Bayetti P., DI Pietro E., et al., “ITER Neutrak beam system”, IAEA-CN-69.

96) Moriyama S., Kimura H., Fujii T., et al., "A Mock-up Tests of a Ceramic-free Antenna Feeder of the Ion Cyclotron Heating System for Next-generation Tokamaks", JJAP **37**, 3536 (1998).

97) Moriyama S., Kimura H., Fujii T., et al., "High Power Test of the All-Metal Support for a Center Conductor of an ITER ICRF Antenna", Fusion Eng. Des. **45**, 31 (1998).

98) Moriyama S., Kimura H., Fujii T., et al., "Real Time Impedance Matching by Frequency Feedback Control on ICRF Experiments in JT-60U and Future Tokamaks", JJAP **37**, 1356 (1998).

99) Mukhovatov V.S., Kasai S., Yamamoto S., et al., "Role and Requirement for Plasma Measurements on ITER", Diagnostics for Experimental Thermonuclear Fusion Reactors 2, edited by Stott P.E., Gorini G., Pradoni P., and Sindoni E. (Plenum Press, New York, 1998), p.25, May (1997).

100) Murakami Y., Takase H., Shinya K., et al., “Power plant design study of a high aspect ratio Tokamak using a SiC composite structure”, Fusion Eng. Des. **41**, 501 (1998).

101) Nagashima A., Nishitani T., Fujisawa T., et al., “Development of Vacuum Seals for Diagnostic Windows of ITER”, Rev. Sci. Instrum. **70**, 460 (1999).

102) Nakahira M., Takahashi H., Akou K., et al., “Development of Thick Wall Welding and Cutting Tools for ITER”, J. Robotics Mech. **10**, 116 (1998).

103) Nakamura H., Ladd P., Federici G., et al., "ITER fuelling, pumping, wall conditioning systems and fuel dynamics analysis", Fusion Eng. Des. **42**, 883 (1998).

104) Nakamura H., Hayashi T., O’hira S., et al., “Implantation Driven Permeation Behavior of Deuterium through Stainless Steel type 316L”, J. Nucl. Mater. **258-263**, 1050 (1998).

105) Nakamura K., Suzuki S., Tanabe T. et al., “ Disruption Erosions of Various Kinds of Tungsten,” Fusion Eng. Des. **39-40**, 295 (1998).

106) Nakamura K., Suzuki S., Dairaku M., et al., “Disruption and Sputtering Erosions on SiC Doped CFC”, J. Nucl. Mater. **258-263**, 828 (1998).

107) Neyatani Y., Yoshino R., Nakanura Y., et al., "Characteristics of halo currents in JT-60U", Nucl. Fusion **39**, 559 (1999).

108) Nishikawa M., Baba A., Kawamura Y., et al., “Tritium Inventory Estimation in Solid Blanket System”, Fusion Eng. Des. **39-40**, 615 (1998).

109) Nishio S., Ueda S., Aoki I., et al., “Improved tokamak concept focusing on easy maintenance”, Fusion Eng. Des. **41**, 357 (1998).

110) Nishitani T., Ishitsuka E., et al., “Japanese Contribution to ITR Task of Irradiation Tests on Diagnostics Components”, Fusion Eng. Design, **42**, 443 (1998).

111) Nishitani T., Kasai S., et al., “Neutron Monitor using Micorfission Chambers for the International Thermonuclear Experimental Reactor”, Rev. Sci. Instrum. **70**, 1141 (1999).

112) Nishitani T., Ebisawa K., Kasai S., et al., "In-Vessel Neutron Monitor Using Micro Fission Chambers for ITER", Diagnostics for Experimental Thermonuclear Fusion Reactors 2, edited by Stott P.E., Gorini G., Pradoni P., and Sindoni E. (Plenum Press, New York, 1998), p.491, May (1997).

113) Obara K., Kakudate S., Nakahira M., et al., “Development of ITER In-vessel Viewing and Metrology Systems”, J. Robotics Mech. **10**, 96 (1998).

114) Obara K., Kakudate S., Oka K., et al., “Development of Radiation Hardness Components for ITER Remote Maintenance”, J Robotics Mech. **10**, 121 (1998).

115) O’hira S., Steiner A., Nakamura H., et al., “Tritium Retention Study of Tungsten using Various Hydrogen Isotope Irradiation Sources”, J. Nucl. Mater. **258-263**, 990 (1998).

116) O’hira S., Suzuki T., Hode S., et al., “Design Study of a Tritium Transport Package for Future Fusion Reactors”, Fusion Eng. Des., to be published.

117) O’hira S., Hayashi T., Nakamura H., et al., “Improvement of Tritium Acountancy Technology for the ITER Fuel Cycle Safety Enhancement”, Nucl. Fusion, to be published.

118) Oikawa T., Ushigusa K., Forest C. B., et al., "Heating and Non-inductive Current Drive by Negative-ion based NBI in JT-60U", to be published in Nucl. Fusion.

119) Oka K., Itou A., Takiguchi Y., “Development of Bore Tools for Pipe Welding/Cutting”, J. Robotics Mech. **10**, 104 (1998).

120) Oka K., Kakudate S., Takeda N., et al., “Measurement and Control System for ITER Remote Maintenance Equipment”, J. Robotics Mech. **10**, 139 (1998).

121) Oka K., Nakahira M., Taguchi K., et al., “Development of Bore Tools for Pipe Inspection”, J. Robotics Mech. **10**, 110 (1998).

122) Oomatsu K., Yamada Y., Ayai N., et al., “Development of Nb_3Al superconductors for ITER”, IEEE Trans. Appl. Superconductivity **7**, (1998).

123) Ozeki T., “Internal Tranaport Barrier in Tokamak Plasma, MHD Instabilitdy Induced by the Internal Transport Barrier”, J. Plasma and Fusion Research, **74**, 998 (1998) (in Japanese).

124) Ozeki T., Azumi M., Ishida S., et al., "Violation of the Mercier Criterion in Reversed Shear Confinement Configurations in Tokamaks", Plasma Phys. Control. Fusion **40**, 871 (1998).

125) Ozeki T., Ishii Y., Hudson S.R., et al., "Improvement of MHD Stability in Negative/Weak Shear Configurations for a Steady State Tokamak", to be published in Nucl. Fusion.

126) Raffray R., Chiocchio S., Ioki K., et al., "High heat flux thermal-hydraulic analysis of ITER divertor and blanket systems", Fusion Eng. Des. **39-40**, 323 (1998).

127) Sakamoto K., Kasugai A., Tsuneoka M., et al., “High power 170GHz gyrotron with synthetic diamond window”, Rev. Sci. Instrum. **70**, 208 (1999).

128) Sakamoto K. and Imai T., “Introduction of Gyrotron generating Electro-magnetic Wave”, Sangyo-to-Denki **557**, 7 (1999).

129) Sakamoto Y., Cho T., et al., "Characterization of a semiconductor detector and its application for ion diagnostics using a novel ion energy spectrometer", Rev. Sci. Instrum. **70**, 857 (1999).

130) Sakasai A., Takenaga H., N. Hosogane, et al., "Helium Exhaust in ELMy H-mode Plasmas with W-shaped Divertor of JT-60U", J. Nucl. Mater. **266-269**, 312 (1999).

131) Sakurai S., Hosogane N., Masaki K., et al. "Development of a compact W-shaped pumped divertor in JT-60U", Fusion Eng. Design **39-40**, 371 (1998).

132) Sakurai S., Asakura N., Hosogane N., et al, "Plasma characteristics near the X-point in W-shaped divertor of JT-60U", J. Nucl. Mater. **266-269**, 1191 (1999).

133) Sato S., Kuroda T., Hatano T., et al., “Development of first wall/blanket structure by hot isostatic pressing (HIP) in the JAERI”, Fusion Eng. Des. **39-40**, 609 (1998).

134) Sato S., Takatsu H., Utsumi T., et al., “Streaming analysis for radiation through ITER mid-plane port”, Fusion Eng. Des. **39-40**, 213 (1998).

135) Sato S., Hatano T., Kuroda T., et al., “Optimization of HIP bonding conditions for ITER shielding blanket/first wall made from austenitic stainless steel and dispersion strengthened copper alloy”, J. Nucl. Mater. **258-263** 265 (1998).

136) Sato S., Hatano T., Takatsu H., et al., “Fabrication of an ITER Shielding Blanket Prototype”, Fusion Technol. **34**, 892 (1998).

137) Sato S., Seki Y., Plenteda R., et al., “Shielding Analysis of the ITER NBI Ports”, Fusion Technol. **34**, 1002 (1998).

138) Sato S., Osaki T., Yamada H., et al., “Fabrication of an ITER middle-scaled shielding blanket module mock-up”, Fusion Eng. Des. **39-40**, 765 (1998).

139) Seki Y., Kurihara R., Nishio S., et al., “Safety scenario and integrated thermofluid test”, Fusion Eng. Des. **42**, 37 (1998).

140) Senda I., Shoji T., Tsunematsu T., et al., "Optimization of plasma initiation in the ITER tokamak", Fusion Eng. Des. **42**, 381 (1998).

141) Shimomura Y., Saji G., "ITER Safety and Operational Scenario", Fusion Eng. Des. **39-40**, 17 (1998).

142) Shinohara K., Miura Y., Hoshino K., “Density fluctuations in the JFT-2M H-mode plasma measured by using a new analysis method of microwave reflectometry”, J. Plasma and Fusion Res., **74**, 607 (1998).

143) Shirai H., JT-60 Team, "Recent Experimental and Analytic Progress in the Japan Atomic Energy Research Institute Tokamak-60 Upgrade with W-shaped Divertor Configuration", Phys. Plasmas **5**, 1712 (1998).

144) Shirai H. and JT-60 team, "Reduced Transport and Er Shearing in Improved Confinement Regimes in JT-60U", to be published in Nucl. Fusion.

145) Shu W., “General Formula of Tritium Permeation through Plasma Facing Materials”, J. Plasma Fusion Res. **75**, 409 (1999) (in Japanese).

146) Shu W., O’hira S. and Nishi M., “Hydrogen Permeation through Metals”, Trends Phys. Chem., to be published.

147) Smid I., Akiba M., Vieider G., Pluechl L, “Development of Bonding, Tungsten Armor and Copper Alloys for Plasma-Interactive Components,” J. Nucl. Mater. **258-263**, 160 (1998).

148) Sugie T., Ogawa H., Katsumuma J., et al., "Divertor Impurity Monitor for ITER", Diagnostics for Experimental Thermonuclear Fusion Reactors 2 , edited by Stott P.E., Gorini G., Pradoni P., and Sindoni E. (Plenum Press, New York, 1998), p.327, May (1997).

149) Sugie T., Ogawa H., Nishitani T., et al., "Divertor Impurity Monitor for the International Thermonuclear Experimental Reactor", Rev. Sci. Instrum. **70**, 351 (1999).

150) Sugimoto M., Isono T., Hamada K., et al., "Development and performance test results of 50kA vapor-cooled current lead for ITER", Cryogenics **33**, 549 (1998) (in Japanese).

151) Sugimoto M., Isono T., Tsuji H., et al., "An evaluation of the inlet flow reduction for a cable-in-conduit conductor inpulsed operation", Cryogenics **38**, 989 (1998).

152) Sugimoto M., Takano K., Tsuji H., et al., "Mechanical Strength of alumina ceramics in low temperature", Cryogenics **33**, 716 (1998) (in Japanese).

153) Sugimoto M.,Isono T., Koziumi N., et al., "R&D activity of SAGBO avoidance for the CS insert fabrication", IEEE Trans. Appl Superconductivity **7**, (1998).

154) Suzuki S., Shimakura N., Shirai T., et al., "Molecular-state treatment of electron capture in collisions of Be^{3+} ions with He atoms below 10keV/amu", J. Phys. **B31**, 1741 (1998).

155) Suzuki S., Shirai T., Nemoto M., et al., "Attenuation of high-energy neutral hydrogen beams in high-density plasmas", Plasma Phys. Control. Fusion **40**, 2097 (1998).

156) Suzuki S., Suzuki T., Araki M. et al., "Development of Divertor Plate with CFCs Bonded onto DSCu Cooling Tube for Fusion Reactor Application," J. Nucl. Mater. **258-263**, 318 (1998).

157) Tada E., Shibanuma K., "Remote Maintenance Development for ITER", J. Robotics Mech. **10**, 71 (1998).

158) Tadokoro T., O'hira H., Nishi M., et al., "Tritium Retention in CX-2002U and Methods to reduce Tritium Inventory", J. Nucl. Mater. **258-263**, 1092 (1998).

159) Taguchi K., Kakudate S., Nakahira M., et al., "Development of Standard Components for Remote Handling", J Robotics Mech. **10**, 133 (1998).

160) Takahashi Y., Oshikiri M., Kawano K., et al., "Superconducting performance test facility for large-current conductor of fusion machine", Cryogenics **33**, 323 (1998) (in Japanese).

161) Takeda N., Oka K., Akou K., et al., "Development of Divertor Remote Maintenance System", J. Robotics Mech. **10**, 88 (1998).

162) Takenaga H., Fukuda T., Sakurai S., et al., "Versatile millimeter-wave interferometer with two frequencies in the divertor region of JT-60U", Rev. Sci. Instrum. **69**, 3181 (1998).

163) Takenaga H. and JT-60 team, "Particle confinement and transport in JT-60U", to be published in Nucl. Fusion.

164) Takizuka T., "An Offset Non-linear Scaling for ELMy H-mode Confinement", Plasma Phys. Control. Fusion **40**, 851 (1998).

165) Takizuka T., "What can be Expected from Computer Simulations of Fusion Plasmas?", J. Plasma and Fusion Research, **74**, 309 (1998), (in Japanese).

166) Takizuka T. and the JT-60 Team, "Recent Progress in JT-60U Experiments with W-shaped Divertor", Fusion

Technology **34**, 301 (1998).

167) Tamai H., Asakura N., Hosogane N., “Behaviour of divertor neutral pressure at the onset of an X-point MARFE in JT-60U”, J. Plasma and Fusion Res. **74**, 1336 (1998).

168) Tamai H., Konoshima S., Hosogane N., et al., “Feedback control of radiation region in radiative divertor plasma on JT-60U tokamak”, Fusion Eng. Des. **39-40**, 163 (1998).

169) Tamai H., Asakura N., Takenaga H., et al., "Particle Control and Behaviour of Neutrals in the Pumped W-Shaped Divertor of JT-60U", J. Nucl. Mater. **266-269**, 1219 (1999).

170) Tanabe T., Akiba M., Ueda Y., et al., “On the Utilization of High Z Materials as Plasma Facing Component,” Fusion Eng. Des. **39-40**, 275 (1998).

171) Tobita K. and the JT-60 Team, “Latest plasma performance and experiments on JT-60U”, Plasma Phys. Control. Fusion **41**, A333-A343 (1999).

172) Tobita K., Hamamatsu K., Takizuka T., et al., “Numerical analysis of ripple loss in reversed shear tokamak operation”, J. Plasma and Fusion Research **75**, 582 (1999).

173) Tuchiya K., Fukuda T., Kamada Y., et al., ”Comparison of edge neutral effect on the condition of H-mode transition before and after modified divertor in JT-60U”, Plasma Phys. Control. Fusion **40**, 713 (1998).

174) Tsuji H., Kimura T., Ando T., “ITER central solenoid model coil test program”, 17th IAEA Fusion Energy Conf. Fusion Energy (1998).

175) Tsuneoka M., el al. “Development of high efficiency and crowbar switch-less d.c. power supply for 1MW CW CPD gyrotron”, Int. J. Electronics **86**, 245 (1999).

176) Ueda S. and DREAM Design Team, “A Fusion Power Reactor Concept Using SiC/SiC Composites”, J. Nucl. Mater. **258-263**, 1589 (1998).

177) Ueda S., Ohsaka T., and Kuwajima S., “Molecular Dynamics Evaluation of Self-Sputtering of Beryllium”, J. Nucl. Mater. **258-263**, 713 (1998).

178) Uehara K., Kawakami T., Amemiya H., et al., "Measurements of ion temperature and flow velocity using symmetric and asymmetric double probe in the boundary plasma of JFT-2M tokamak", Nucl. Fusion **38**, 1665 (1998).

179) Uehara K., Tsushima A. and Amemiya H., "Transport model of boundary plasma and estimation of transport coefficients", Proc. Edge-plasma theory and simulation workshop, Innsbruck, 1998, Czech J. Phys. **48**, 339 (1998).

180) Walker C., Ando T., Costley A.E., et al., "Diagnostic Access for ITER", Diagnostics for Experimental Thermonuclear Fusion Reactors 2, edited by Stott P.E., Gorini G., Pradoni P., and Sindoni E. (Plenum Press, New York, 1998), p.57, May (1997).

181) Watanabe K., Mizuno M., Nakajima S., “Development of a high performance core snubber for high power neutral beam injectors”, Rev. Sci. Instrum **69**, 4136 (1998).

182) Yamamoto S., deKock L., Belyakov V., et al., "Irradiation Tests on ITER Diagnostic Components", Diagnostics for Experimental Thermonuclear Fusion Reactors 2, edited by Stott P.E., Gorini G., Pradoni P., and Sindoni E. (Plenum Press, New York, 1998), p.269, May (1997).

183) Yamanishi T., Konishi S., Kawamura Y., et al., “Demonstration of the Integrated Fusion Fuel Loop at the Tritium Process Laboratory of the Japan Atomic Energy Research Institute”, Fusion Technol., to be

published.

184) Yamanishi T., Iwai Y., Nishi M., et al., "Control Methods of Cryogenic Distillation Column Processing Plasma Exhaust Gas", Fusion Technol., to be published.

185) Yamanishi T., Kawamura Y., Iwai Y., et al., "Development of Tritium Fuel Processing System using Electrolytic Reactor for ITER", Nucl. Fusion, to be published.

186) Yoshida H., Naito O., Yamashita O., et al., "Multilaser and high spatially resolved multipoint Thomson scattering system for the JT-60U tokamak", Rev. Sci. Instrum. **70**, 751 (1999).

187) Yoshida H., Naito O., Sakuma T., et al., "A compact and high repetitive photodiode array detector for the JT-60U Thomson scattering diagnostic", Rev. Sci. Instrum. **70**, 747 (1999).

188) Yoshino R., Tokuda S., Kawano Y., "Generation and Termination of Runaway Electrons at Major Disruptions in JT-60U", Nucl. Fusion, **39**, 151 (1999).

A.1.3 List of papers published in conference proceedings

1) Ando T., Isono T., Nakajima H., et al., “Consideration of high Tc superconductor application to magnets for tokamak fusion reactor”, 20th Symp. On Fusion Technology France, (1998).

2) Bartels H.W., Honda T., Inabe T., et al., "Loss of vacuum accident in ITER", 20th Symposium on Fusion Technology (SOFT-20) (Marseille), 1998.

2) Enoeda M., Sato S., Hatano T., et al., "Design and Development of Ceramic Breeder DEMO Blanket”, Proc. of 17th IAEA Fusion Energy Conference, Yokohama, Japan, 19-24 Oct. (1998).

3) Combs S.K., Gouge M.J., Nakamura H., et al., "Status of ITER Pellet Injector R&D", 20th Symposoum on Fusion Tech. (France), Fusion Technology 1998, Elsvier BV.

4) Di Pietro E., Mondino P.L., Inoue T., “The vacuum insulated beam source for the ITER neutral beam injection”, 20th SOFT Fusion Technology 407-410 (1998).

5) Ebisawa K., Ando T., Costley A.E., et al., "VUV Divertor Impurity Monitor for ITER Experimental Reactor", 12th Topical Conference on High Temperature Plasma Diagnostics, 7-11 June 1998, Princeton, USA.

6) Fujita T., "Formation and Sustainment of Internal Transport Barrier in JT-60U", 2nd International TRIAM Symposium, Kyushu university, Japan (1998), FURKU Report 98-04(60), p. 7 (1998).

7) Fujiwara Y., Kawai K., Hanada M., “Experimental study on the beamlet interaction in a large current negative ion source”, Proc. of 9th on Beam Engineering of Advanced Material Syntheses, 1998 (in Japanese).

8) Gordon C., Baker D., Holland D., et al., "International Cooperation in the Safety and Environmental Assessment for the ITER Engineering Design Activities",11th Pacific Basin Nuclear Conference, Banff (Canada), 1998

9) Goto M., Uno M., Saito M., et al., “Fracture strength of DS-Cu/316SS HIP bonded structure”, Fusion Technology 1998, 177-180 (1998).

10) Hanada M., Fujiwara Y., Watanabe K.,” Electrostatic deflector for multi-beamlet”, Proc. of 9th on Beam Engineering of Advanced Material Syntheses, pp97-100, 1998 (in Japanese).

11) Hara S., Sato S., Enoeda M., et al., “Packing behavior observed by CT scan for development of pebble bed breeding blanket”, Fusion Technology 1998, 1333-1336 (1998).

12) Hatano T., Kuroda T., Iwatachi T., et al., “Fabrication of a small-scaled first wall mock-up with beryllium armor hip bonded to DSCu/SS structure”, Fusion Technology 1998, 97-100 (1998).

13) Hoshi Y., Kataoka Y., Tanchuk V., et al., "ITER heat removal system-System and process control design-", 20th Symposoum on Fusion Tech. (France), Fusion Technology 1998, Elsvier BV.

14) Hoshino K., Takahashi K., JFT-2M Group, “ECH Experiment with Variable kAntenna in JFT-2M”, Bull. Amer. Phys. Soc. **43** (1998) 1932.

15) Hosogane N., Tamai H., Higashijima S., et al., “Operational Performance of JT-60U W-shaped Divertor”, Proc. of 13th Int. Conf. on Plasma Surface Interactions in Controlled Fusion Devices, San Diego, U.S.A. May 18-22, (1998).

16) Hosogane N., Kubo H., Higashijima S., et al., “Divertor Characteristics and Control on the W-shaped

Divertor with Pump of JT-60", Proc. of 17th IAEA Fusion Energy Conference, Yokohama, Japan, Oct. 19-24, (1998).

17) Inoue T., Shibata K., Di Pietro E., "Radiation analysis of the ITER neutral beam system", 20th SOFT Fusion Technology, 411-414 (1998).

18) Ioki K., Johnson G., Iizuka T., et al., "Design and R&D for the ITER Vacuum Vessel", 20th Symposium on Fusion Tech. (France), Fusion Technology 1998, Elsvier BV.

19) Janeschitz G., Pacher G., Sugihara M., et al., "L-H Transition in Tokamak Plasmas: 1.5-D Simulation", 13th International Conference on Plasma Surface Interaction in Controlled Fusion Devices, San Diego, USA, 1998.

20) Janeschitz G., Ebisawa K., Kasai S., et al., "Integration of Diagnostics into the ITER Machine", The 17th IAEA Fusion Energy Conference, (Yokohama), (1998).

21) Jimbou R., Nakamura K., Bandourko V., et al., "Temperature and Angular Dependencies of Sputtering Yield of B4C-Carbon Fiber Composite Irradiated with Low Energy Deuterium Ions," Proc. 13th Int. Conf. on Plasma Surface Interactions in Controlled Fusion Devices, San Diego, May 18-23, 1998.

22) Kakudate S., Nakahira M., Oka K., et al., "Remote handling demonstration of ITER blanket module replacement", to be presented in 17th IAEA Fusion Energy Conference, Oct. 1998 (Yokohama), IAEA-F1-CN-69/ITERP1/27.

23) Kanari M., Abe T., Enoeda M., et al., "Repeated Impact Load Durability of Alumina Electrical Insulation Coating Layer", Fusion Technology 1998, 1349-1352 (1998).

24) Kawai M.,Aoyagi T., et al., Computer Control and Data Acquisition System of the Negative-ion Based NBI for T-60U, Proc. of 17th IEEE/NPSS Symposium on Fusion Engineering, San Diego, U.S.A., (1997), Vol.1 (1998) p.531-534.

25) Kawano K., Kato T., Hamada K., et al., "Development of a 1000-g/s scale supercritical helium pump", 17th Int. Cryogenic Engineering Conf., P.255-258 (1998).

26) Khripunov V., Santoro R.T., Iida H., et al., "Activation of water coolant in ITER", 20th Symposium on Fusion Tech. (France), Fusion Technology 1998, Elsvier BV.

27) Kodama K., Sasajima T., Masaki K., et al., "Installation of the W-shaped Divertor in JT-60U", Proc. of 17th IEEE/NPSS Symposium on Fusion Engineering, San Diego, U.S.A., (1997), Vol.1 (1998) p.365-368.

28) Koizumi K., Nakahira M., Oka K., et al., "Fabrication and Assembly of Full-scale Sector Models for ITER Vacuum Vessel", 1998 ANS Annual Meeting and 13th Topical meeting on the Technology of Fusion Energy, June 9, Nashville, USA (1998).

29) Koizumi N., Terasawa A., Nunoya Y., et al., "Experimental results at pulse test facility (PTF) of butt joint used in ITER CS model coil outer module", Proc. of 17th Int. Cryogenic Engineering Conf., P.523-526 (1998).

30) Kondoh T., Nagashima A., Tsukahara Y., et al., "Fast Ion Diagnostics in JT-60U (_-ray and Collective Thomson Scattering Measurements)", Proc. of 1998 International Congress on Plasma Physics, Praha, Czech Republic, Europhysics conference abstracts, Vol. 22C,1478 (1998).

31) Kosaku Y., Abe T., Enoeda M., et al., "Preliminary Experiment of Hydrogen Permeation Through Stainless Steel" Proc. of Int. Workshop on Hydrogen Recycle at PFM. Tokyo 15-16 Oct. 1998.

32) Kubo H., Higashijima S., Sakasai A., et al., "Impurity Behavior in JT-60U W-shaped Divertor", The

Second China-Japan Workshop on Study of Toroidal Plasmas, Chengdu, Chaina (1999).

33) Kubo H., Higashijima S., Takenaga H., et al., "Spectroscopic Study of the W-shaped Divertor in JT-60U", Proc. of 1998 International Congress on Plasma Physics, Praha, Czech Republic, Europhysics conference abstracts, Vol. 22C, 427 (1998).

34) Kubo H. and JT-60 Team, "Impurity Behavior in JT-60U W-shaped Divertor", 2nd International TRIAM Symposium, Kyushu university, Japan (1998), FURKU Report 98-04(60), p. 20 (1998).

35) Kurihara, K., Kawamata, K., “Development of a Precise Long-time Digital Integrator for Magnetic Measurements in Tokamak,” Proceeding of 17th IEEE/NPSS Symposium on Fusion Engineering, (Sun Diego), **1**, 799 (1998).

36) Kuriyama M., Akino N., Ebisawa N., et al., “Progress of negative-ion based NBI system for JT-60U”, 20th SOFT Fusion Technology 391-394 (1998).

37) Kuriyama M., Akino N., et al., “High Power Beam Operation with the Negative-ion Based NBI for JT60U”, Proc. of 17th IEEE/NPSS Symposium on Fusion Engineering, San Diego, U.S.A., (1997), Vol.1 (1998) p.405-408.

38) Loarte A., Asakura N., Itami K., Shimada M., Sugihara M., et al., "Comparison of B2-EIRENE calculations with multi-machine experimental measurements", 13th International Conference on Plasma Surface Interaction in Controlled Fusion Devices, San Diego, USA, 1998.

39) Maebara S., Seki M., Ikeda Y., et al., " High Power Test of a CFC Antenna Module for Lower Hybrid Current Drive", Proc. 20^{th} Symp. on Fusion Technology, France (1998).

40) Martin Y. and JT-60 Team, "Prediction of the ITER H-mode Power Threshold by Means of Various Statistical Techniques", Threshold Database Working Group, 1998 ICCP (25th EPS), Prague, June 29-July 3 (1998) P3010.

41) Masaki K., Kodama K., Morimoto M., et al., “The First Inspection of JT-60U W-shaped Divertor after High Power Operation”, Proc. of 20th Inter. Symp. on Fusion Technology, Marseille, France, Sep. 7-11, (1998).

42) Massmann P., Fujiwara Y., Hanada M., Inoue T., et al., "EUROPEAN CONTRIBUTION TO THE BEAM SOURCE DESIGN AND R&D OF THE ITER NEUTRAL BEAM INJECTORS", 17th IAEA Fusion Energy Conference, Yokohama. (Proceedings, IAEA-F1-CN-69 /FT1/5), (1998).

43) Matsukawa M., Ohmori Y., Totsuka T., et al., “A new Coil Current Control System of the JT-60 Toroidal Field Coil Power Supply” (in Japanese), Proc. of Annual Conference of IEE of Japan, Vol. 3, p.103, Akita, 1998.

44) Matsumoto T., Tokuda S., Kishimoto Y., et al., “Complex Behavior of Internal Collapse due to Self-generated Radial Electric Field”, 9th Toki Conference, P-I-12, Toki, Japan, 7-11, December 1998 : to be published in JPFR Series Vol.2).

45) Miki N., Ioki K., Elio F., et al., "VDE/Disruption EM Analysis for ITER In-vessel Components", 20th Symposium on Fusion Tech. (France), Fusion Technology 1998, Elsvier BV.

46) Miura Y. M., Matsukawa M. and Kimura T., “Development of an IGBT Converter for a Magnet Power Supply”, Proc. of 20th SOFE, p.743, Marseille, France, 1998.

47) Mondino P.L., Senda I., Shoji T., et al., "Plasma Current, Position and Shape Control for ITER", 20th Symposium on Fusion Tech. (France), Fusion Technology 1998, Elsvier BV.

48) Mondino P.L., Iiida H., Inoue T., et al., "ITER NEUTRAL BEAM SYSTEM", 17th IAEA Fusion Energy Conference, Yokohama. (Proceedings, IAEA-AN-69 /ITER P1/17), (1998).

49) Moriyama S. et al, Development of All-metal Antenna for ICRF System in Next Generation Tokamaks, Proc. of18th IEEE/NPSS Symposium on Fusion Engineering.

50) Nagashima A., Fujisawa T., Sugie T., et al., "Development of New Vacuum Window Seal for ITER Optical Diagnostics", Proc. of International School of Plasma Physics "Piero Caldirola" Workshop on Diagnostics for Experimental Fusion Reactors, Varenna, Italy, Diagnostics for Experimental Thermonuclear Fusion Reactors 2, Plenum Press, New York, 257 (1998).

51) Naito O., Oikawa T., Ushigusa K., et al., "Current Drive by Negative-Ion-Based Neutral Beam Injector in JT-60U", 1998 ICCP (25th EPS), Prague, June 29-July 3 (1998) Or.26.

52) Nakahira M., Kakudate S., Oka K., et al., “Development of Blanket and Divertor Remote Maintenance for ITER”, 1998 ANS Annual Meeting and 13th Topical meeting on the Technology of Fusion Energy, June 11, Nashville, USA (1998).

53) Nakahira M., Koizumi K., Oka K., et al., “Integration test of ITER full-scale vacuum vessel sector”, to be presented in 17th IAEA Fusion Energy Conference, Oct. 1998 (Yokohama), IAEA-CN-69/ITERP1/24.

54) Ohga T, Usui K., et al., High Voltage Power Supply of Negative-ion Based NBI for JT-60U, Proc. of 17th IEEE/NPSS Symposium on Fusion Engineering, San Diego, U.S.A., (1997), vol.2 (1998) p.1091-1094.

55) Ohmori K., Usui K., et al., “Improvement of the ion source power supply for JT-60U negative ion based NBI”, Proc. of 20th Symposium on Fusion Technology, Marseille, France, (1998), p.395-398.

56) Oka K., Kakudate S., Takiguchi Y., et al., "Measurement and Control System for the ITER Remote Handling Mockup Test", 20th Symposium on Fusion Technology, Sept. 7-11, Marseille, France (1998).

57) Okumura Y., Hanada M., Miyamoto N., “Steady state operation of multi- ampere negative hydrogen ion source”, Proc. of 9th on Beam Engineering of Advanced Material Syntheses, 1998 (in Japanese).

58) Omori K., Usui K., Ohshima K., “Improvement of the ion source power supply for JT-60 negative-ion based NBI”, 20th SOFT Fusion Technology 395-398 (1998)

59) Osaki T., Yamada H., Satou S., et al., "Fabrication of The Curved Shielding Blanket Module with Inner Coolant Channels for ITER," Fusion Technology 1998, 1259-1262 (1998).

60) Porter G., Shimada M., Sugihara M., et al., "Analysis of Separatrix Plasma Parameters", 13th International Conference on Plasma Surface Interaction in Controlled Fusion Devices, San Diego, USA, 1998.

61) Raffray A. R., Akiba M., Cardella A., et al. “Effect of Runaway Electrons and VDE’s on ITER First Wall,” B. Beaumont, P. Libeyre, B. de Gentile, G. Tonon (edited), Fusion Technology 1998 (Proc. 20th Symp. on Fusion Technology, Marseille, France, Sept. 7-11, 1998), 211-214, 1998.

62) Rosenbluth M.N., Putvinski S., Yoshino R., "Physics of Runaway Formation", 40th Annual Meeting of the Division of Plasma Physics, New Orleans,USA, (1998), Bulletein of the American Physical Society (Plasma Physics), **43**, 1664, C2E 14 (1998).

63) Saito S., Fukaya K., Ishiyama S., et al. “Development of Bonding Techniques of W and Cu-alloys for Plasma Facing Components of Fusion Reactor with HIP Method,” B. Beaumont, P. Libeyre, B. de Gentile, G. Tonon (edited), Fusion Technology 1998 (Proc. 20th Symp. on Fusion Technology, Marseille, France, Sept. 7-11, 1998), 113-116, 1998.

64) Sakamoto K., Kasugai A., Tsuneoka M., et al., Conference Digest of 23rd International Conference on Infrared and Millimeter Waves, Editors T.J.Parker, S.R.P.Smith, at University of Essex, U.K., 7-11 Sept., 1998. F1.2, p363-364.

65) Sakamoto K., Kasugai A., Tsuneoka M., et al., 17th IAEA Fusion Energy Conference at Yokohama, 19-24 Oct.1998.

66) Santoro R.T., Iida H., Sato S., Inoue T., et al., "Nuclear Analysis of ITER ports", 20th Symposium on Fusion Tech. (France), Fusion Technology 1998, Elsvier BV.

67) Sato M., Miura Y., Kimura H., et al., “Reduction of Toroidal Magnetic Field Ripple in the Advanced Material Tokamak Experiment on JFT-2M”, Proceedings of 20th Symposium of Fusion Technology (Marseille, 1998), Vol.1 (1998) 545-548.

68) Sato S., Enoeda M., Kuroda T., et al., “Heat transfer tests of packed pebble bed for demo ceramic breeder blanket”, Fusion Technology 1998, 1199-1202 (1998).

69) Sato K., Suzuki S., Ezato K., et al. “Development of Plasma Facing Components for Fusion Experimental Reactors in JAERI,” B. Beaumont, P. Libeyre, B. de Gentile, G. Tonon (edited), Fusion Technology 1998 (Proc. 20th Symp. on Fusion Technology, Marseille, France, Sept. 7-11, 1998), 109-112, 1998.

70) Sengoku S., Kawashima H. and JFT-2M Group, “Geometrical Effect of a Closed Divertor”, Bull. Amer. Phys. Soc. **43** (1998) 1894.

71) Shikama T., Zinkle S. J., Yamamoto S., "Dynamic Irradiation Effects in Electrical Conductivity of Ceramic Insulators", The 17th IAEA Fusion Energy Conference (Yokohama), (1998).

72) Shikama T., Yamamoto S., "Heavy Irradiation Effects in Diagnostic Components to be used in ITER", Radiation Effects on Components and Systems 98 (Brussel), (1998).

73) Shimomura Y., Aymar R., Chuyanov V., et al., "ITER Overview", The 17th IAEA Fusion Energy Conference, OV4/1-ITERP1/00, (Yokohama), (1998).

74) Shimomura Y., "Status of the ITER Project", 11th Pacific Basin Nuclear Conference, Banff Canada; Proceedings of the 11th Pacific Basin Nuclear Conference Vol. 1 (1998) p 75-78.

75) Shimomura Y., "Engineering R&D in ITER EDA", Presented at The 2nd Joint Conference on Fusion Energy, Tokyo, Japan, (1998).

76) Sugie T., Ogawa H., Katsunuma J., et al., "Divertor Impurity Monitor for ITER", Proc. of International School of Plasma Physics "Piero Caldirola" Workshop on Diagnostics for Experimental Fusion Reactors, Varenna, Italy, Diagnostics for Experimental Thermonuclear Fusion Reactors 2, Plenum Press, New York, 327 (1998).

77) Sugihara M., Federici G., Grisolia C., et al., "Simulation of Transient Wall Pumping, Fuelling Effects and Density Control in Tokamaks", 13th International Conference on Plasma Surface Interaction in Controlled Fusion Devices, San Diego, USA, 1998.

78) Suzuki S., Suzuki T., Nakamura K., Akiba M. “Development of Divertor High Heat Flux Component at JAERI,” Proc. 17th IEEE/NPSS Symp. on Fusion Engineering, vol. 1, 385-388, San Diego, USA, Oct. 6-10, 1998.

79) Takahashi K., Sakamoto K., Kasugai A., et al., Proceedings of the 20th Symposium on Fusion Technology, Marseille, France (1998) pp.415.

80) Takase H., Senda I., Araki M., Shoji T., Tsunematsu T., "3-D ELECTROMAGNETIC TRANSIENT

CHARACTERISTICS OF IN-VESSEL COMPONENTS IN TOKAMAK REACTOR", The 17th IAEA Fusion Energy Conference, (Yokohama), (1998).

81) Takeda N., Akou K., Takiguchi Y., et al., "Performance Test of Divertor Cassette Transporters for ITER", 20th Symposium on Fusion Technology, Sept. 7-11, Marseille, France (1998).

82) Takizuka T., "Comment on H-mode Confinement in JT-60U", 9th ITER Confinement Database and Modeling Expert Group Meeting, October 25-29, 1998, Naka.

83) Tivey R., Ando T., Antipenkov A., et al., "ITER Divertor, Issues and R&D," B. Beaumont, P. Libeyre, B. de Gentile, G. Tonon (edited), Fusion Technology 1998 (Proc. 20th Symp. on Fusion Technology, Marseille, France, Sept. 7-11, 1998), 16-22, 1998.

84) Trainham R., Jacquot C., Fujiwara Y., et al., "Long pulse extraction of deuterium negative ion beams from the Kamaboko ion source", 20th SOFT Fusion Technology 367-370 1998).

85) Tuda T., Ishii Y., Kurita G., et al., "Ideal/Resistive Modes Analysis in Reversed Shear Configuration Plasmas", presented at The first general assembry of Asian Plasma and Fusion Association joint with The Third Asia Pacific Plasma Theory Conferenceep. 21-25, 1998, Beijing, China.

86) Uda M., Ishitsuka E., Sato K., et al. "Thermal Shock Test of Neutron Irradiated Carbon Fiber Reinforced Carbon Composites with OHBIS," Proc. 8th Int. Workshop on Carbon Materials, Juelich, Germany, Sept. 3-4, 1998.

87) Uda M., Sato K., Akiba M., et al. "Disruption and Erosion on Plasma Facing Materials with Oarai Hot-cell Electron Beam Irradiating System (OHBIS)," B. Beaumont, P. Libeyre, B. de Gentile, G. Tonon (edited), Fusion Technology 1998 (Proc. 20th Symp. on Fusion Technology, Marseille, France, Sept. 7-11, 1998), 161-164, 1998.

88) Uehara K., Tsushima A., Amemiya H., "Transport Model of Boundary Plasma and Estimation of Transport Coefficients", in Proc. of Edge-Plasma Theory and Simulation Workshop (Insbruck).

89) Ulrickson M., Tivey R., Akiba M., et al. "The ITER Divertor Cassette Project," Proc. 17th IAEA Fusion Energy Conference, Yokohama, Japan, Oct. 19-24, 1998.

90) Valovic M. and JT-60 team, "An Analysis of the ITER H-mode Confinement Database", ITER H-mode Confinement Database Working Group, 1998 ICCP (25th EPS), Prague, June 29-July 3 (1998) P3.012.

91) Watanabe K., Fujiwara Y., Hanada M., "Development of a 1 MeV H- beam accelerator for neutral beam injector", 20th SOFT Fusion Technology 493-496 (1998).

92) Yamada T., Uchimoto T., (Nakamura Y.), et al., "Application of HTSC Coils for Mitigation of VDE during a Major Disruption", Proc. the 20th Symposium on Fusion Technology, Vol. 1, Marseille, France, 7-11 September 1998.

93) Yonekawa I., Journeaux J.Y., Matsumoto Y., "Application of Sequential Function Chart methodology to ITER Control System", 20th Symposium on Fusion Tech. (France), Fusion Technology 1998, Elsvier BV.

94) Yoshida K., Iida F., Gallix R., et al., "Electrical Insulation Design and Monitoring of the ITER Magnet System", 20th Symposium on Fusion Tech. (France), Fusion Technology 1998, pp. 807-810.

A.1.4 List of other papers

1) Araki M., Akiba M., “Final Report on D308; Structual Assessment and Electromagnetic Calculation of the Standard and Diagonostic Cassette”, ITER/EDA Design Task report (D308, Task No. G17TD19FJ).

2) Costley A., Ebisawa K., Edmonds P. et al., “Diagonstics : Initial Implications for Measurements Requirements System Design and Costs for RC-ITER”, ITER/EDA Point Design Meeting on RTO/RC-ITER (Naka JWS, 1998).

3) Costley A., deCock L., Ebisawa K., “Outline Design Report; I.3.8 Plasma Measurements and Priorities, II.6 Plasma Diagonostic System”, ITER/EDA Point Design Meeting on RTO/RC-ITER (Garching JWS, 1999).

4) Fujisawa N., “Steady State Operation by NBI in RC-ITER”, 6th ITER Physics R&D Expert Meeting on Energetic Particles, Heating and Current Drive (1998).

5) Fujisawa N., “Constraints and Limits in Plasma Heating and Current Drive”, ITER/EDA Point Design Meeting on RTO/RC-ITER (Garching JWS, 1999).

6) Giannella R., Ebisawa K., “Progress Report of the Working Group on Spectroscopic Diagonostic for ITER”, ITER Expert Group on Diagonostics 9th Workshop and Technical Meeting, (St. Petersburg, 1998).

7) Inoue T., “Design of the NB H&CD system for RTO/RC-ITER”, ITER/EDA Point Design Meeting on RTO/RC-ITER (Garching JWS, 1999).

8) Inoue T., “Plasma Physics and NB H&CD for RTO/RC ITER”, ITER/EDA NB H&CD Review Meeting (Garching JWS, 1999).

9) Inoue T., “A Four Channel Design for the RTO/RC ITER NBI”, ITER/EDA NB H&CD Review Meeting (Garching JWS, 1999).

10) Ioki K., “(1) VV and Blanket Design for RC-ITER, (2) Cost Comparison, (3) Shielding and Neutronics”, TER/EDA Point Design Meeting on RTO/RC-ITER (Naka JWS, 1998).

11) Ioki K., “Conclusions of Vacuum Vessel and Blanket Design for RTO/RC-ITER”, ITER/EDA Point Design Meeting on RTO/RC-ITER (Garching JWS, 1999).

12) Koizumi K., Tada S., “Final Report for Vacuum Vessel Design (D306, Part 2)”, ITER/EDA Design Task report (D306, Task No. G15TD35 FJ).

13) Koizumi K., Eto M., “ Final Report for Design Standards (D327), Subtask-1, Material Properties Handbook (MPH) ”, ITER/EDA Design Task report (D327, Task No. S74TD09FJ).

14) Koizumi K., Hada K., “ Final Report for Design Standards (D327), Subtask-2, ITER Interium Structual Design Criteria (ISDC) ”, ITER/EDA Design Task report (D327, Task No. S74TD09FJ).

15) Kuriyama M., Operation experience and future prospect of both positive and negative ion based NBI system for JT-60, The Second Chine-Japan Workshop on Study of Toroidal plasmas, Cengdu, China, Jan. (1999).

16) Miura Y., “Edge Transport Barrier in Tokamak Plasma - Formation of Edge Transport Barrier”, J. Plasma and Fusion Research **74** (1998) 968-976, (in Japanese).

17) Nakamura H., “Fueling and Particle Control in ITER”, US/Japan Workshop on Fuelling and Active Particle Control”, (NIFS, 1998).

18) Ozawa Y., “ Cost Estimation for FDR”, ITER/EDA Design Task report (Task No. S93TD05FJ).

19) Sato M. and Miura Y., “Application of Ferreitic Steel to a Medium-Sized Tokamak (JFT-2M) -Present Status and Issues”, J. Plasma and Fusion Research **74** (1998) 448-454, (in Japanese).

20) Sato S., Ohmori J., Hatano T., et al., “Shield Blanket Design & Analysis”, ITER/EDA Design Task report (D307, Task No. G16TD78FJ).

21) Shoji T., Senda I., Tsunematsu T. et al., “Final Report on D324-2; Poloidal Field Scenario and Control”, ITER/EDA Design Task report (D324-2, Task No. N47TD21FJ).

22) Shoji T., Senda I., Takase H., Tsunematsu T., et al., “Final Report on D318; Coil Power Supply and Distribution System Design, - Power Supply System Design Support”, ITER/EDA Design Task report (D318, Task No. N41TD05FJ).

23) Sugihara M., “Status of Existing Edge Pedestal Database”, 9th ITER Physics R&D Expert Meeting on Divertor Physics, Divertor Modeling & Database, (Naka JWS, 1998).

24) Tsunematsu T., “Cost and Schedule Control”, ITER/EDA Design Task report (D329, Task No. S92TD11FJ).

25) Yamamoto S., “Review of the Radiation Effects Task T246, Introduction of Outstanding Issues”, ITER Expert Group on Diagonostics 9th Workshop and Technical Meeting, (St. Petersburg, 1998).

A.2 Scientific Staffs in the Naka Fusion Research Establishment (April, 1998- March, 1999)

Naka Fusion Research Establishment

OHTA Mitsuru (Director General)

SEKIGUCHI Tadashi (Scientific Consultant)
MIYAMOTO Kenro (Invited Researcher)
NISHIKAWA Kyoji (Invited Researcher)
KAWASAKI Sunao (Invited Researcher)
SHIMAMOTO Susumu (Invited Researcher)
TOMABECHI Ken (Invited Researcher)
AZUMI Masafumi
YAMAMOTO Takumi (Staff for Director General)
MIYA Naoyuki (Staff for Director General)
HONMA Takashi (Staff for Director General)

Department of Administrative Services

KOMAKI Akira (Director)
KAMBARA Yoyu (Deputy Director)
MATSUZAKI Yoshimi (Deputy Director)

Department of Fusion Plasma Research

FUNAHASHI Akimasa (Director)
SHIMADA Michiya
KAWANO Yoshikatsu (Administrative Manager)

Tokamak Program Division

NINOMIYA Hiromasa (General Manager)
HATAE Takaki, IDE Shunsuke, ISAYAMA Akihiko,
ISHIDA Shinichi, KISHIYA Kazuhiro (*15), KITAI Tatsuya (*15),
KURITA Gen-ichi, MORI Katsuharu (*15), OGURI Shigeru (*15),
OIKAWA Akira, SAKURAI Shinji, TOBITA Kenji,
USHIGUSA Kenkichi

Plasma Analysis Division

OZEKI Takahisa (General Manager)
HAMAMATSU Kiyotaka, HASEGAWA Yukihiro, HAYASHI Nobuhiko (*50)
KOIWA Motonao (*31), MATSUDA Toshiaki, NAITO Osamu
NAKAMURA Yukiharu, NEUDATCHIN Sergei V. (*23), OHSHIMA Takayuki
POLEVOI Alexei (*11), SAKATA Shinya, SATO Minoru
SHIMIZU Katsuhiro, SHIRAI Hiroshi, SUZUKI Mitsuhiro (*33)
TAKIZUKA Tomonori, TSUGITA Tomonori

Large Tokamak Experiment Division I

KIKUCHI Mitsuru (General Manager)
CHIBA Shinichi, FUKUDA Takeshi, HAMANO Takashi
ISEI Nobuyuki, INOUE Akira, IWASE Makoto (*36)

KAMADA Yutaka	KASHIWABARA Tsuneo	KAWANO Yasunori
KITAMURA Shigeru	KOIDE Yoshihiko	KOKUSEN Shigeharu
KRAMER Gerrit Jakob (*41)	KUSAMA Yoshinori	MENG Yuedong (*8)
MIRUNOV Maxim	MORIOKA Atsuhiko	NAGAYA Susumu
NEMOTO Hirofumi	NEMOTO Masahiro	NEYATANI Yuzuru
NISHITANI Takeo	OIKAWA Toshihiro	SAKUMA Takeshi
SHITOMI Morimasa	SUNAOSHI Hidenori	SAKAMOTO Nobuteru
TAKEJI Satoru	TSUCHIYA Katsuhiko	TSUKAHARA Yoshimitsu
UEHARA Kazuya	URAMOTO Yasuyuki	YOSHIDA Hidetoshi
ZHAO Junyu (*8)		

Large Tokamak Experiment Division II

YOSHINO Ryuji (General Manager)

ASAKURA Nobuyuki	BAK Paul Eric (*41)	FUJITA Takaaki
HATAE Takaki	HIGASHIJIMA Satoru	HILL Kenneth W. (*37)
ISHIJIMA Tatsuo (*51)	ITAMI Kiyoshi	KONDOH Takashi
KONOSHMA Shigeru	KOOG Joong San (*36)	KUBO Hirotaka
KUMAGAI Akira (*51)	NAJIKIAN Raffi (*37)	NAKANO Tomohide
OHSAWA Masaya (*24)	RAMAN Roger (*52)	ROMERO Jesus Antonino (*41)
SAKASAI Akira	SAKURAI Shinji	SHINOHARA Kouji
SONG Xianming (*40)	SUGIE Tatsuo	SUZUKI Shingo (*36)
TAKENAGA Hidenobu	TAMAI Hiroshi	

Plasma Theory Laboratory

KISHIMOTO Yasuaki (Head)

DETTRICK Sean (*41)	HUDSON Stuart (*41)	ISHII Yasutomo
ISHIZAWA Akihiro (*36)	LI Jiquan (*40)	MATSUMOTO Taro
MIYOSHI Takahiro (*36)	SUGAHARA Akihiro (*31)	SUZUKI Yoshio (*36)
TOKUDA Shinji	TUDA Takashi	

Experimental Plasma Physics Laboratory

KIMURA Haruyuki (Head)

HOSHINO Katsumichi	KAWAKAMI Tomohide	KAWASHIMA Hisato
MAEDA Mitsuru (*14)	MAENO Masaki	MIURA Yukitoshi
OGAWA Hiroaki	OGAWA Toshihide	OASA Kazumi
SATO Masayasu	SENGOKU Seio	SHIINA Tomio
TSUZUKI Kazuhiro	YOON Jae Sung(*21)	

Department of Fusion Facility

FUNAHASHI Akimasa (Director)

SHIMIZU Masatsugu (Deputy Director)

Fusion Facility Administration Division

KAWANO Yoshikatsu (General Manager)

JT-60 Facility Division I

KIMURA Toyoaki (General Manager)

ADACHI Hironori (*25)	AKASAKA Hiromi	ARAKAWA Kiyotsugu
FUKUDA Hiroyuki (*15)	FURUKAWA Hiroshi (*32)	KAWAMATA Youichi

KURIHARA Kenichi
MATSUKAWA Makoto
MIURA M. Yushi
NOBUSAKA Hiromichi (*15)
OKANO Jun
OMORI Shunzo
OMORI Yoshikazu
OOBA Toshio (*32)
SEIMIYA Munetaka
SHIMONO Mitsuru
TAKANO Shoji (*33)
TERAKADO Tsunehisa
TOTSUKA Toshiyuki

JT-60 Facility Division II

HOSOGANE Nobuyuki (General Manager)

ARAI Takashi
HIRATSUKA Hajime
HONDA Masao
ICHIGE Hisashi
KAMINAGA Atsushi
KODAMA Kozo
MASUI Hiroshi (*12)
MASAKI Kei
MIYATA Hiroshi (*6)
MIYO Yasuhiko
MORIMOTO Masaaki (*27)
OKABE Tomokazu
YAGYU Jun-ichi
MIYATA Katsuyuki (*6)
SASAJIMA Tadayuki
SASAKI Noboru (*6)
TAKAHASHI Shoryu (*6)

RF Facility Division

FUJII Tsuneyuki (General Manager)

ANNOU Katsuto
IKEDA Yoshitaka
ISAKA Masayoshi
ISHII Kazuhiro (*32)
HAGA Koichi (*28)
HIRANAI Shinichi
HIROI Toshikazu (*42)
KAJIYAMA Eiichi (*28)
MORIYAMA Shinichi
SEKI Masami
SHIMONO Mitsugu
SHINOZAKI Shin-ichi
TERAKADO Masayuki
YOKOKURA Kenji

NBI Facility Division

KURIYAMA Masaaki (General Manager)
ITOH Takao (Deputy General Manager)

AKINO Noboru
EBISAWA Noboru
HONDA Atsushi
GRISHAM Larry (*37)
KAWAI Mikito
KAZAWA Minoru
HU Liquen (*8)
MOGAKI Kazuhiko
OHGA Tokumichi
OHMORI Kenichiro
OHSHIMA Katsumi (*28)
OOHARA Hiroshi
SEKI Hiroshi (*32)
TANAI Yutaka (*32)
TOYOKAWA Yoshiharu (*28)
USUI Katsutomi
YAMAGUCHI Masao (*32)
YAMAZAKI Haruhiko (*6)

JFT-2M Facility Division

KOIKE Tsuneyuki (General Manager)
YAMAMOTO Masahiro (Deputy General Manager)

HASEGAWA Koichi
KASHIWA Yoshitoshi
KIKUCHI Kazuo
KOMATA Masao
OKANO Fuminori
SAWAHATA Masayuki
SHIBATA Takatoshi
SUZUKI Sadaaki
TANI Takashi
UMINO Kazumi (*32)
AKIYAMA Takashi (*15)

Department of Fusion Engineering Research

MATSUDA Shinzaburo (Director)
SEKI Yasushi (Deputy Director)
NAGASHIMA Takashi (Prime Scientist)
MURASAWA Michihiko (Administrative Manager)

Blanket Engineering Laboratory

OHARA Yoshihiro (Head)

ABE Tetsuya
ENOEDA Mikio
FURUYA Kazuyuki
HARA Shigemitsu (*6)
HATANO Toshihisa
KASAI Satoshi
KANARI Moriyasu (*36)
KIKUCHI Shigeto (*48)
KOSAKU Yasuo

KURODA Toshimasa (*19) NAKAMURA Jyun-ichi (*35) SATO Satoshi
YANO Atsushi (*35) YANAGI Yoshihiro (*6)

Superconducting Magnet Laboratory

TSUJI Hiroshi (Head)

ANDO Toshinari FU Youkin (*32) HIYAMA Tadao
ISONO Takaaki ISHIO Koutarou (*13) KATO Takashi
KAWANO Katsumi KOIZUMI Norikiyo KUBO Hiroatsu (*3)
MATSUI Kunihiro NAKAJIMA Hideo NISHIJIMA Gen (*36)
NUNOYA Yoshihiko OSHIKIRI Masayuki (*32) SAWADA Kenji (*26)
SHIMBA Toru (*10) SUGIMOTO Makoto TAKAHASHI Yoshikazu
TSUCHIYA Yoshinori (*36) WAKABAYASHI Hiroshi (*32)

NBI Heating Laboratory

OKUMURA Yoshikazu (Head)

AKIBA Masao BANDOURKO Vassi (*11) DAIRAKU Masayuki
EZATO Koichiro (*36) FUJIWARA Yukio GILANYI Attila (*36)
HANADA Masaya KITAGAWA Tadashi (*30) MIYAMOTO kenji
NAKAMURA Kazuyuki SATO Kazuyoshi SAWAHATA Osamu (*32)
SUZUKI Satoshi WATANABE Kazuhiro YOKOYAMA Kenji

RF Heating Laboratory

IMAI Tsuyoshi (Head)

IKEDA Yukiharu INOUE Yuji (*29) KASUGAI Atsushi
MAEBARA Sunao OHUCHI Hitoshi (*29) SAKAMOTO Keishi
SHIHO Makoto TAKAHASHI Koji TSUNEOKA Masaki
WATANABE Akihiko (*29) YAMAMOTO Masanori (*6) ZHENG Xaodong (*36)

Tritium Engineering Laboratory

NISHI Masataka (Head)

ARITA Tadaaki (*42) HAYASHI Takumi ISOBE Kanetsugu
IWAI Yasunori KAKUTA Toshiya (*19) KAWAMURA Yoshinori
KOBAYASHI Kazuhiro MARUYAMA Tomoyoshi (*27) NAKAMURA Hirofumi
O'HIRA Shigeru SAKAI Takuhiro (*48) SHU Wataru
SUZUKI Takumi TADOKORO Takahiro (*6) YAMADA Masayuki
YAMANISHI Toshihiko

Reactor System Laboratory

SEKI Yasushi (Head)

AOKI Isao AJIMA Toshio (*6) KURIHARA Ryoichi
NISHIO Satoshi UEDA Shuzo

Reactor Structure Laboratory

TADA Eisuke (Head)

AKOU Kentaro (*19) ITOU Akira (*10) KAKUDATE Satoshi
KOIZUMI Koichi SHIBANUMA Kiyoshi NAKAHIRA Masataka
OBARA Kenjiro OKA Kiyoshi TAGUCHI Kou (*32)
TAKAHASHI Hiroyuki (*6) TAKIGUCHI Yuji (*48) TAKEDA Nobukazu

Department of ITER Project

KITSUNEZAKI Akio (Director)
TSUNEMATSU Toshihide (Deputy Director)
SEKI Masahiro (Prime Scientist)
SHIMOMURA Yasuo (Prime Scientist)
FUJISAWA Noboru
ODAJIMA Kazuo

Administration Group

OKABE Takashi (Leader)

Project Management Group

ANDO Toshiro (Leader)
IIZUKA Takayuki

Joint Central Team Group

SHOJI Teruaki (Leader)

EBISAWA Katsuyuki (*48)	HATTORI Yukiya (*6)	HIROKI Seiji
HORIKIRI Hitoshi (*39)	HOSHI Yuichi (*10)	IIDA Fumio (*6)
IIDA Hiromasa	IOKI Kimihiro (*27)	INOUE Takashi
ITOH Kazuyoshi (*42)	ITOH Mitsuyoshi (*10)	KATAOKA Yoshiyuki (*6)
KAWAI Shigetaka (*26)	KOBAYASHI Noriyuki (*48)	KODAMA Tetsuhiko (*27)
MARUYAMA So	MATSUMOTO Hiroshi	MIZOGUCHI Tadanori (*6)
MOHRI Kensuke (*19)	MORIYAMA Kenichi (*43)	MITA Yoshiyuki (*34)
MIKI Nobuharu (*48)	NAKASHIMA Yoshitane (*10)	NAKAMURA Hiroo
OKUNO Kiyoshi	ONOZUKA Masanori (*27)	OSANO Katsuharu (*5)
OZAKI Fumio (*48)	SAJI Gen	SATO Kouichi (*1)
SHIBANUMA Kiyoshi	SUGIHARA Masayoshi	TAKIGAMI Hiroyuki (*48)
YAMADA Masao (*27)	YAMAMOTO Shin	YONEKAWA Izuru
YOSHIDA Hiroshi	YOSHIDA Kiyoshi	YOSHIMURA Kunihiro (*48)

Home Team Design Group

SHOJI Teruaki (Leader)

ARAKI Masanori	GOTO Yoshinori (*26)	ITOH Yutaka (*6)
KASHIMURA Shinji (*18)	KITAMURA Kazunori (*48)	KUCHIISHI Keiichi (*6)
MIURA Hidenori (*19)	OHMORI Jyunji (*48)	OHNO Isamu (*10)
OHKAWA Yoshinao	OZAWA Yoshihiro (*6)	SAKA Hidemasa (*22)
SAITO Keiji (*6)	SATO Shinichi (*19)	SHIRAI Tetsuo (*44)
TADO Shigeru (*26)	TAKASE Haruhiko (*48)	YAGENJI Akira (*4)

Safety Evaluation Group

INABE Teruo (Leader)

ARAKI Takao (*48)	HASHIMOTO Masayoshi (*10)	MARUO Takeshi

*1 Atomic Data Service Corp.
*2 Ecole Polytechnique (France)
*3 Fuji Electric Co., Ltd.
*4 Hazama-gumi Ltd.

*5 Hitachi Information Systems, Ltd.
*6 Hitachi Ltd.
*7 Hitachi Nuclear Engineering Co., Ltd
*8 Institute of Plasma Physics Academia Sinica (China)
*9 Ioffe Physical-Technical Institute (Russia)
*10 Ishikawajima-Harima Heavy Industries, Ltd.
*11 JAERI Fellowship
*12 Japan Expert Clone Corp.
*13 Japan Steel Works Ltd.
*14 JST Fellowship
*15 Kaihatsu Denki Co.
*16 Kajima Corporation
*17 Kaken Co.
*18 Kandenko Corp.
*19 Kawasaki Heavy Industries, Ltd.
*20 Kobe Steel Ltd.
*21 Korea Atomic Energy Research Institute (Korea)
*22 Kumagai-gumi Ltd.
*23 Kurchatov Institute (Russia)
*24 Kyushu University
*25 Mito Software Engineering Co.
*26 Mitsubishi Electric Co., Ltd.
*27 Mitsubishi Heavy Industries, Ltd.
*28 Nippon Advanced Technology Co., Ltd.
*29 Nissei Sangyo Co., Ltd.
*30 Nissin Electric Co., Ltd.
*31 Research Organization for Information Science Technology
*32 Nuclear Engineering Co., Ltd.
*33 Nuclear Information Service Co.
*34 Obayashi Corp.
*35 Osaka Vacuum Ltd.
*36 Post-Doctoral Fellow
*37 Princeton Plasma Physics Laboratory (USA)
*38 Shimizu Corparation
*39 Shinryo Corporation
*40 Southwestern Institute of Physics (China)
*41 STA Fellowship
*42 Sumitomo Heavy Industries, Ltd.
*43 Taisei Corp.
*44 Takenaka Corp.
*45 The Graduate University for Advanced Studies
*46 Troitsk Institute (Russia)
*47 Tomoe Shokai
*48 Toshiba Corp.
*49 University of Science and Technology (China)
*50 Keioh University
*51 Cooperative Graduate School System
*52 Washington University (USA)